JOURNAL OF MECHANICAL ENGINEERING

STROJNIŠKI VESTNIK

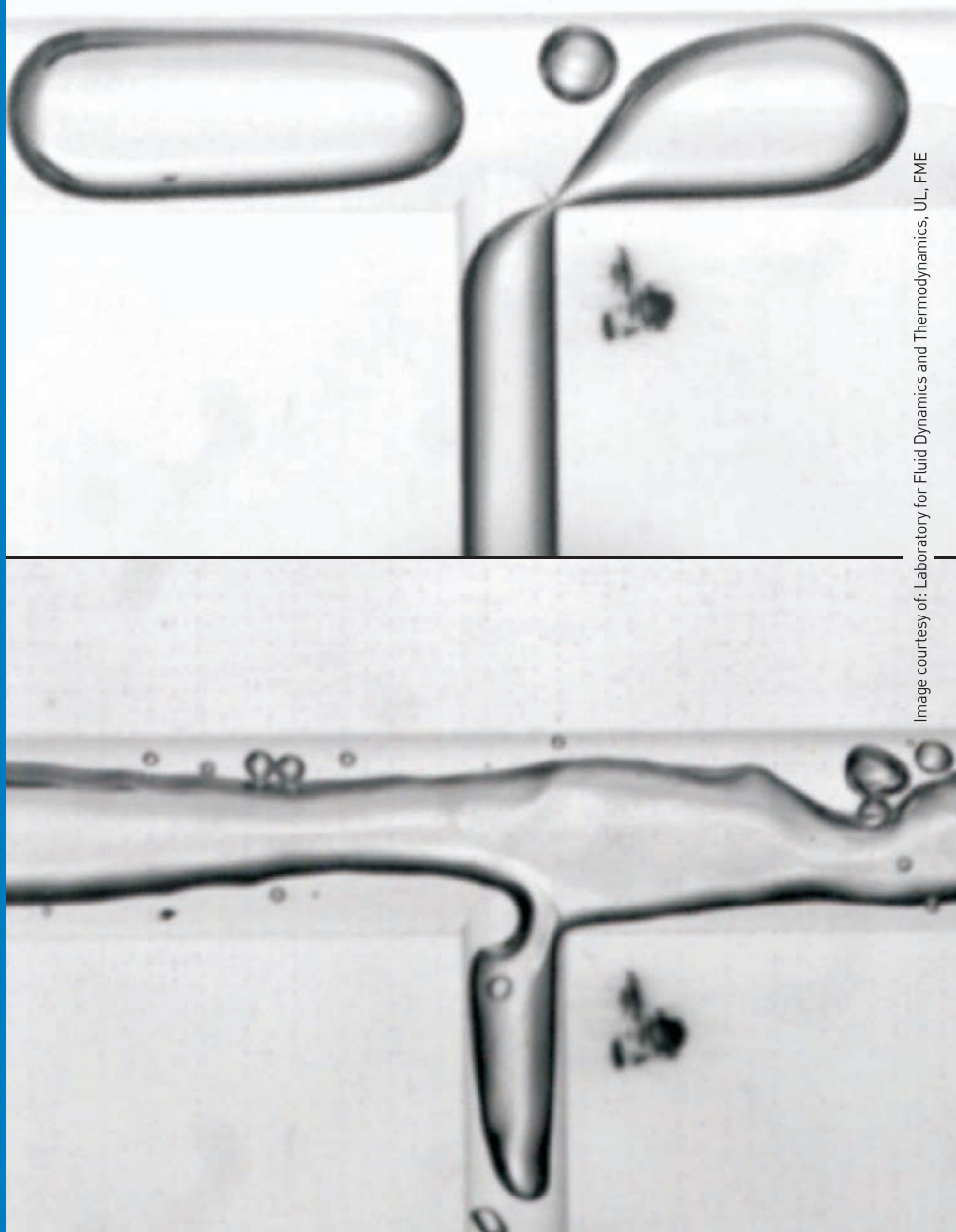

Image courtesy of: Laboratory for Fluid Dynamics and Thermodynamics, UL, FME

no. 1
year 2008
volume 54

Strojniški vestnik - Journal of Mechanical Engineering
ISSN 0039-2480

Editorial Office
University of Ljubljana
Faculty of Mechanical Engineering
Journal of Mechanical Engineering
Aškerčeva 6
SI-1000 Ljubljana, Slovenia
Phone: 386-(0)1-4771 137
Fax: 386-(0)1-2518 567
E-mail: info@sv-jme.eu
http://www.sv-jme.eu

Founders and Publishers
University of Ljubljana
- Faculty of Mechanical Engineering
University of Maribor
- Faculty of Mechanical Engineering
Association of Mechanical Engineers of Slovenia
Chamber of Commerce and Industry of Slovenia
- Metal Processing Association

Editor
Andro Alujevič
University of Maribor
Faculty of Mechanical Engineering
Smetanova 17
SI-2000 Maribor
Phone: 386-(0)2-220 7790
E-mail: andro.alujevic@uni-mb.si

Deputy Editor
Vincenc Butala
University of Ljubljana
Faculty of Mechanical Engineering
Aškerčeva 6
SI-1000 Ljubljana
Phone: +386-(0)1-4771 421
E-mail: vincenc.butala@fs.uni-lj.si

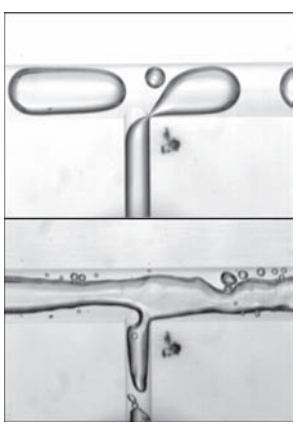

Cover plate: The flow distribution of air and water among the parallel vertical tubes of manifold system has been studied over a wide range of air and water flow rates. Examples: slug flow and semi-annular flow regimes at the first T-junction recorded at 10.000 fps, respectively. Geometry: half circle cross section, 1.22mm header hydraulic diameter, 0.61 mm side-arm hydraulic diameter. Courtesy of the Laboratory for Fluid Dynamics and Thermodynamics, Faculty of Mechanical Engineering.

Print
Littera Picta, Medvode, printed in 600 copies

Yearly subscription

companies	100,00 EUR
individuals	25,00 EUR
students	10,00 EUR
abroad	100,00 EUR
single issue	5,00 EUR

JME is indexed in *SCI-Expanded*, *Compendex* and *Inspec*.
The journal is subsidized by the Slovenian Research Agency.

Strojniški vestnik - Journal of Mechanical Engineering is also available on http://www.sv-jme.eu, where you access also to papers' supplements, such as simulations, etc.

Contents

Strojniški vestnik - Journal of Mechanical Engineering
volume 54, (2008), number 1
Ljubljana, January 2008
ISSN 0039-2480

Published monthly

Editorial

Dear readers,

at the end of 2007, the Publishing Board changed in accordance with the rules of the Strojniški vestnik – Journal of Mechanical Engineering. Both faculties of mechanical engineering aimed at including in the new Publishing Board the associates who have contributed significantly - or still do so - to the written word in the field of mechanical engineering. The invited colleagues responded to the invitation with great enthusiasm. During personal interviews, they presented their views on the development of the Journal that represents the hub of knowledge in the field of scientific papers in Slovenia. It is our goal to further open the door for knowledge exchange on the path to international recognition of the magazine, started a decade ago. The common European area now makes it possible. The Publishing Board gathered several times in order to pave the way for the Editorial Board, the chief editor and his deputy in particular. Changes of the contents and design concept are now in front of you. Judge them and write your opinion.

Changes of the contents mainly involve the absence of dividing papers into professional and scientific ones. The Journal will publish only scientific papers that will provide the highest possible level via the reviewing process. In the name of the Publishing Board, I have to thank the former editor, Prof. Alujevič, and his deputy, Prof. Karič, for taking this bold step. They have cemented the quality and influence of the magazine through enthusiastic and dedicated work. We have decided to support the integrity of mechanical engineering knowledge because it is our belief that breaking the knowledge into small pieces is less suitable for contemporary understanding of the world. Each issue will particularly focus on specific areas, which will be presented through on-going editorial policy and invited co-editors. Dear fellow scientists, we will be glad to welcome your proposals for special issue editions, ensuring prompt and far reaching presentation of the achievements of our mechanical engineering fellows. Do not hesitate to present your proposal to the chief editor, who will assess your proposal according to a special reviewing process.

Technically, the Journal has changed its cover page and the basic concept. In 2008, the Journal will be published in separate English and Slovenian editions. The main magazine has all papers in English. Then, in a separate part, abstracts of all papers will be presented as well as special news for Slovenian readers in Slovene. The entire magazine will be sent to all regular subscribers in Slovenia and foreign libraries with the national status. All other subscribers abroad will receive the English version of all papers, without the Slovenian supplement. We believe that this way, we will bring the Journal closer to all interested readers in the form, suitable for them. The website has also been changed. From now on, its new address is http://www.sv-jme.eu. Here, all papers from current issues will be available, regardless of the year. It will provide young researchers without the access to the encoded version of the Journal with a significant advantage in the access to the latest publications. The authors, waiting for publication and looking for the earliest possible confirmation of the publication, will be provided with the confirmation of the publication with all bibliographic details one month ahead.

A special new feature will include the image on the cover page, showing typical research achievements of the processes, carried out by different laboratories. On the website, each process will be presented by a video clip, which will provide the reader of the website with an insight into the recording of a specific process. It will ensure up-to-date and specific information on the processes that are otherwise not possible to present in the printed copy of the Journal. In the case of specific processes, authors are kindly asked to make use of the opportunity for the presentation on the website.

From now on, the Editorial and Advisory Board are new. Half of the members come from internationally renowned professional and scientific environment. My advance thanks go to all of you, who have accepted the responsibility of a member of the Editorial and Advisory Board, which is to take care of quality contributions and will be their first filter. With your help, the quality of the Journal will improve, which is our common obligation and a great ambition.

On behalf of the Publishing Board and my personal name, I would like to wish Prof. Andro Alujevič, the chief editor, Prof. Vincenc Butala, his deputy, and all members of the Editorial and Advisory Board successful work in the future.

Ljubljana, February 20, 2008

Prof. dr. Jože Duhovnik

Strojniški vestnik - Journal of Mechanical Engineering 54(2008)1, 3-10
UDC 627.84
Paper received: 4.10.2006
Paper accepted: 19.12.2007

Analysis of Hydraulic Characteristics of Guard-Gate for Hydropower Plant

Zlatko Rek[1,*] - Anton Bergant[2] - Miha Röthl - Primož Rodič[3] - Iztok Žun[1]
[1]University of Ljubljana, Faculty of Mechanical Engineering, Slovenia
[2]Litostroj E.I., Slovenia
[3]Institute of Hydraulic Research, Slovenia

A guard-gate can be installed at the inlet of the pressure tunnel, at the downstream end of the surge tank or in the draft tube of the water turbine. A hydraulic shape of the gate and characteristics of the hydropower plant flow-passage sytem govern the magnitude of pressure forces acting on the gate structure. Flow conditions at the downstream end of the gate may require adequate air admission. Numerical analysis of hydraulic characteristics has been performed for a vertical leaf gate at different gate openings. The analysis has been performed with Computational Fluid Dynamics (CFD) code using finite volume method. Computational results are compared with results of measurements carried out in a model test rig.

Keywords: hydropower plant, guard-gates, hydraulic characteristics, control volume methods

0 INTRODUCTION

The guard-gate can be installed at the inlet of the pressure tunnel, at the downstream end of the surge tank or in the draft tube of the water turbine [1], Figure 1. A hydraulic shape of the gate and characteristics of the flow-passage system of the power plant govern the magnitude of pressure forces during the gate closure. Early experimental investigations of the hydrodynamic behaviour of gates have been carried out in the sixties [2] and [3]. Two types of flow at the downstream end of the gate have been observed: pressurized flow and free surface flow. Flow conditions at the downstream end of the gate may induce very low pressures; there is increased danger of pipeline collapse and large pressure oscillations. Air admission at the downstream end of the gate

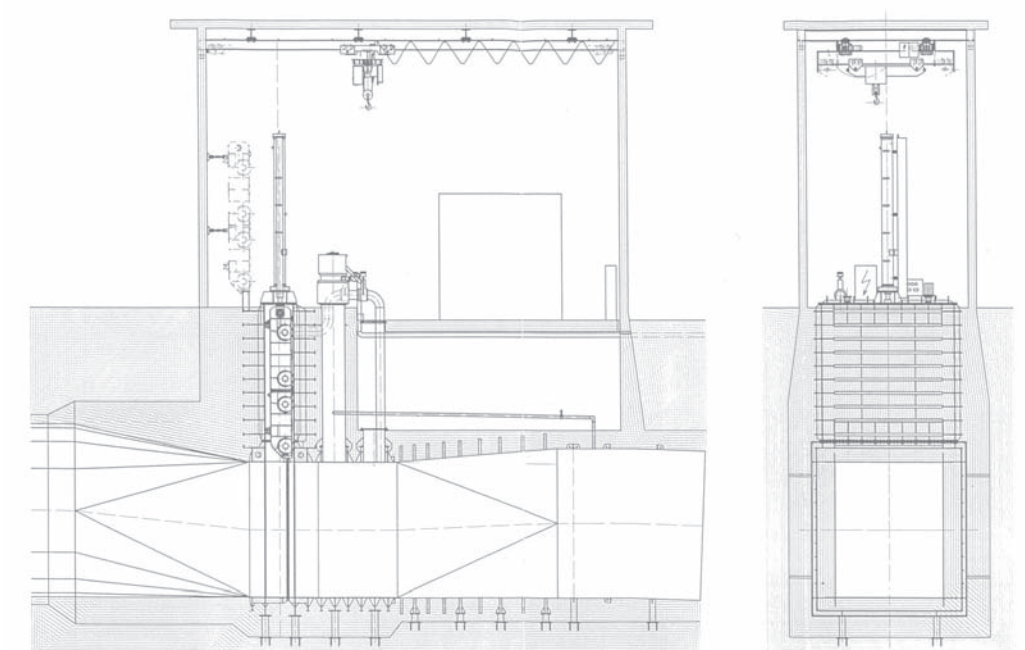

Fig. 1. Guard-gate

*Corr. Author's Address: University of Ljubljana, Faculty of Mechanical Engineering, Aškerčeva 6, SI-1000 Ljubljana, Slovenia, zlatko.rek@fs.uni-lj.si

attenuates pressure oscillations [4]. Hydraulic forces acting on the gate structure have been carefully investigated [5] and [6]. The magnitude of hydraulic forces is needed for design of the gate body and hoist mechanism.

The paper deals with numerical flow investigations of a vertical guard-gate at different gate openings. Flow computations are performed by standard numerical methods [7]. A three-dimensional finite volume method (FVM) is used [8] and [9]. The FVM is a direct method i.e. the geometry of the gate should be defined in advance. The computational results are compared with results of measurements in a hydraulically similar gate. The measurements were performed at the Institute of Hydraulic Research in Ljubljana. Validation study includes comparison of flow characteristics i.e. pressure on the gate structure. The accuracy and robustness of the numerical model (selection of appropriate turbulence model) are tested for a number of operating regimes and conclusions about industrial application of the model are drawn. This would reduce costs for future laboratory testing. Hydraulic characteristics of the gate are essential for optimum design of the gate (body, areation pipe, hoist mechanism) and prediction of operating regimes in the hydropower plant flow-passage system [6].

1 COMPUTATIONAL MODEL

Water flow through channel with guard-gate at fixed opening is cosidered as steady-state flow of viscous incompressible fluid. Flow is turbulent (Re = 174 000) due to the large volume flowrate (Q = 44.7 l/s) and pipe diameter (D = 0.32 m). RANS (Reynolds Averaged Navier-Stokes) k-ε turbulent model with wall functions [10] was used. Despite of some deficencies, this model is known to be the most applicable turbulent model for solving real engineering problems [11].

1.1 Governing equations

Water flow is governed by conservation laws [10] and [12] for:

mass

$$\frac{\partial \rho}{\partial t} + \nabla \cdot (\rho \mathbf{U}) = 0 \tag{1}$$

momentum

$$\frac{\partial}{\partial t}(\rho \mathbf{U}) + \nabla \cdot (\rho \mathbf{U} \otimes \mathbf{U}) = -\nabla p + \nabla \cdot \left(\mu_{ef} \left(\nabla \mathbf{U} + (\nabla \mathbf{U})^T\right)\right) - \rho \mathbf{g} \tag{2}$$

turbulent kinetic energy (t.k.e.)

$$\frac{\partial}{\partial t}(\rho k) + \nabla \cdot (\rho \mathbf{U} k) = \nabla \cdot \left(\left(\mu + \frac{\mu_t}{\sigma_k}\right) \nabla k\right) + \mu_{ef} \nabla \mathbf{U} \cdot \left(\nabla \mathbf{U} + (\nabla \mathbf{U})^T\right) - \rho \varepsilon \tag{3}$$

and dissipation of t.k.e.

$$\frac{\partial}{\partial t}(\rho \varepsilon) + \nabla \cdot (\rho \mathbf{U} \varepsilon) = \nabla \cdot \left(\left(\mu + \frac{\mu_t}{\sigma_\varepsilon}\right) \nabla \varepsilon\right) + C_1 \frac{\varepsilon}{k} \left(\mu_{ef} \nabla \mathbf{U} \cdot \left(\nabla \mathbf{U} + (\nabla \mathbf{U})^T\right)\right) - C_2 \rho \frac{\varepsilon^2}{k} \tag{4},$$

where: ρ – density, μ – dynamic (laminar) viscosity, $\mu_t = C_\mu \rho k^2/\varepsilon$ – turbulent viscosity, $\mu_{ef} = \mu + \mu_t$ – effective viscosity, $\boldsymbol{g}$ – gravity acceleration, $\mathbf{U}$ – time averaged velocity vector, k – turbulent kinetic energy, ε – dissipation of turbulent kinetic energy. Constants of turbulent model are represented in Table 1.

Table 1. *Constants of turbulent model*

C_μ	C_1	C_2	σ_k	σ_ε
0.09	1.44	1.92	1.00	1.22

1.2 Discrete model

Geometric model, Figure 2, was built with CFX-build pre-processor. Because CFX solver uses blok-structured grids, the model is composed by 72 blocks (solids). Three different geometries were considered: 30%, 70% and 100% openings.

Grid density is very important in the numerical solution [13]. If it is too coarse (large control volumes)

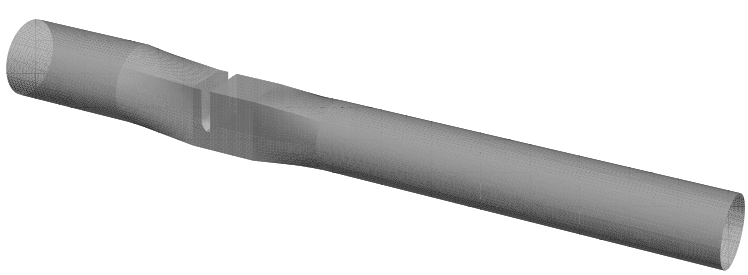

Fig. 2. *Geometric model of guard-gate at 30% opening*

the solution wil not be accurate enough or iterations will not converge at all. For very fine grid (small control volumes) there is a drastically increase in computational time, computer memory and disk space. So, the compromising grid size has to be found. In our case, the grid dependency study [9] is performed on the model with 30% opening for three grid densities:

- coarse, Figure 3,
- medium, Figure 4,
- fine, Figure 5.

The upstream end of the guard-gate was selected for analysis of pressure profile results because the flow conditions are most interesting there. We can see from Figure 6 that results for coarse grid exceedingly deviate and therefore this grid is not appropriate for numerical analysis. Much better

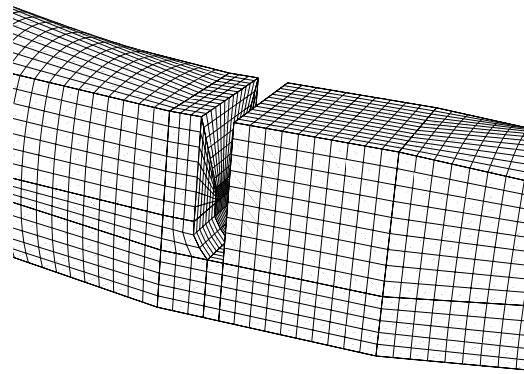

Fig. 4. *Medium grid, 86615 control volumes*

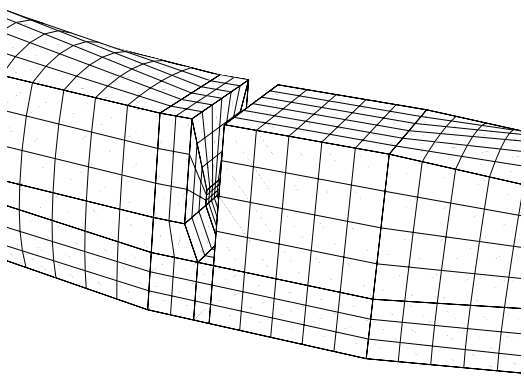

Fig. 3. *Coarse grid, 9294 control volumes*

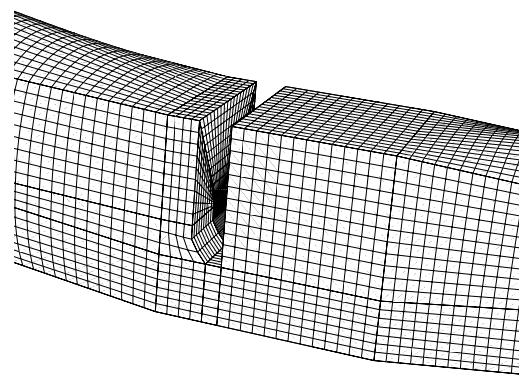

Fig. 5. *Fine grid, 197511 control volumes*

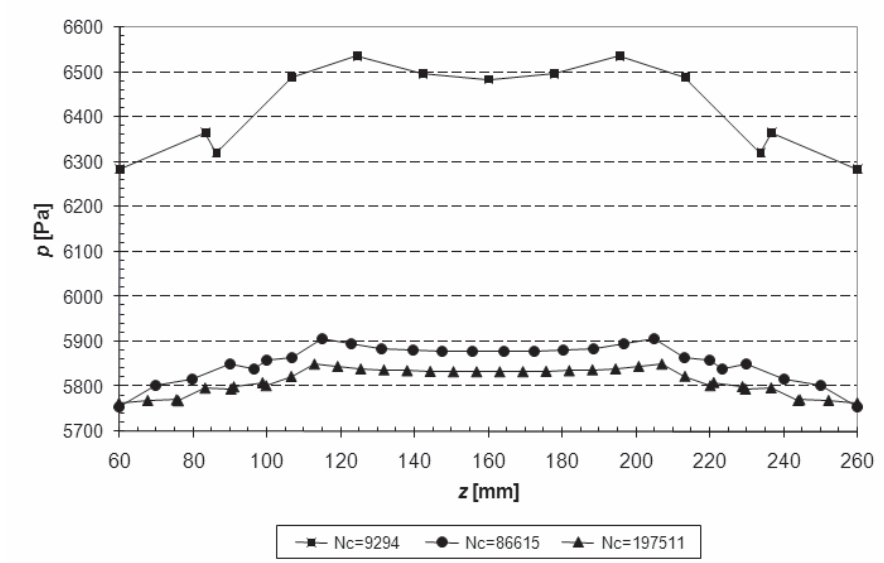

Fig. 6. *Computational grid dependency test*

agreement is with medium and fine grid. Values for pressure on the wall are practically the same. Due to the computer limitations (CPU time, available memory and disk space) and fact that we will compare values for pressure on the wall, we used the medium grid for the rest of the geometry models. We also checked criteria for grid quality, such as: Orthogonal Deviation, Grid Expansion, Skew Ratio and Twist Angle. All parameters were within recommended value intervals [10].

Velocity U = 0.56 m/s (volume flowrate Q = 44.7 l/s), 5% turbulence intensity and turbulence length scale l_{Σ} = 0.01 m were prescribed as inlet boundary condition. Numerical model doesn't include the whole geometry, because the computational domain extends to the measuring point P14; we use measured values for pressure as outlet boundary condition, Table 2.

Table 2. *Boundary conditions at outlet*

Opening [%]	p [Pa]
30	3154
70	9224
100	9221

Initial condition for velocity was **U** = (0.56 m/s, 0, 0).

1.3 Computation

The commercial CFD package CFX-4.4 from ANSYS was used for flow analysis. The discretized domain and command file with control parameters and material properties are needed to solve the system of equations. Density and dynamic viscosity at 20°C were 997.8 kg/m^3 and 0.00102 kg/ms respectively.

The code uses a segregated solver. This means that a linearized system of transport equations is solved for each variable U, V, W, k and ε. The pressure-implicite with splitting of operators (PISO) correction scheme was used for pressure computation. To solve the system of linear equations for velocity, a Block Stone (BLST) linear solver was used. For pressure, a method of Conjugate Gradients (ICCG) and for turbulence, a Line Relaxation (LRLX) method were used. Reduction factors were: 0.1 for pressure and 0.25 for velocity and turbulence. The velocity field and turbulence quantities were discretized with a upwind differencing scheme (UDS), while pressure field was discretized with a central difference scheme (CDS). Under-relaxation factors were: 0.5 for velocity, 0.8 for turbulence and 1.0 for pressure. Convergence criteria residual mass flow was 10^{-5} kg/s. Figure 7 shows the convergence history. Numerical simulation was performed on DEC AlphaPC workstation (processor Alpha 21164/ 533 MHz, 1GB memory).

The results of numerical computation are velocity and pressure fields in the nodes of discrete model. Figures 8 to 10 and 11 to 13 show streamlines and velocity vectors in vertical plane at 30%, 70% and 100% openings of the guard-gate. The re-circulation at the downstream end of the guard-gate may be seen.

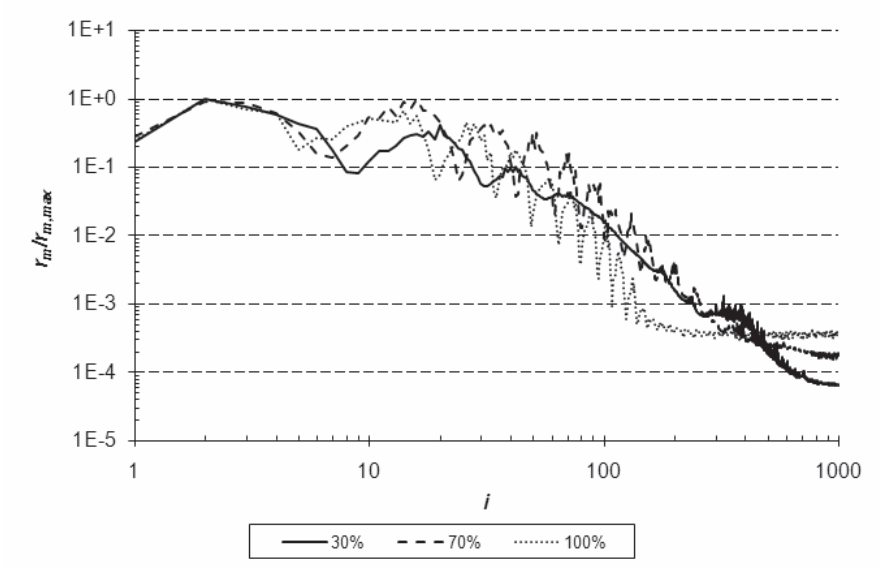

Fig. 7. *Convergence history for continuity equation residuum*

Fig. 8. *Streamlines at 30% opening of guard-gate*

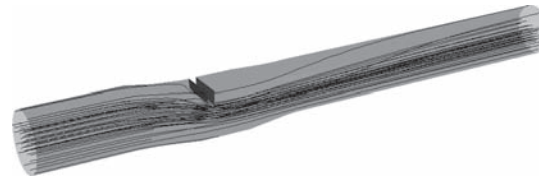

Fig. 9. *Streamlines at 70% opening of guard-gate*

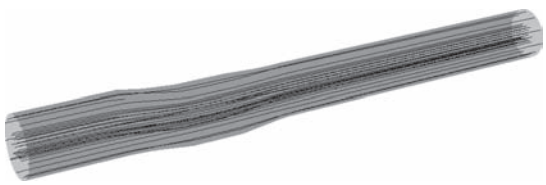

Fig. 10. *Streamlines at 100% opening of guard-gate*

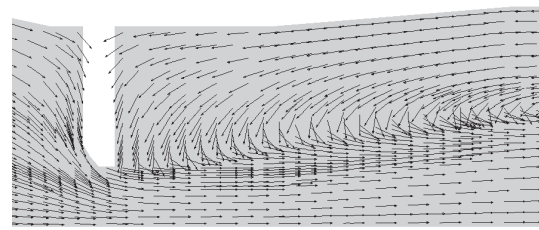

Fig. 11. *Velocity field at 30% opening of guard-gate*

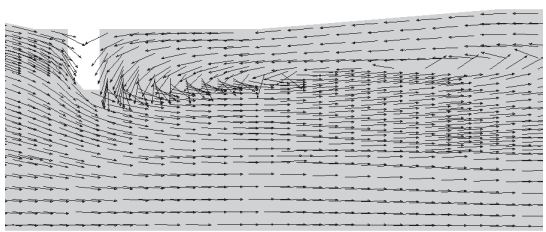

Fig. 12. *Velocity field at 70% opening of guard-gate*

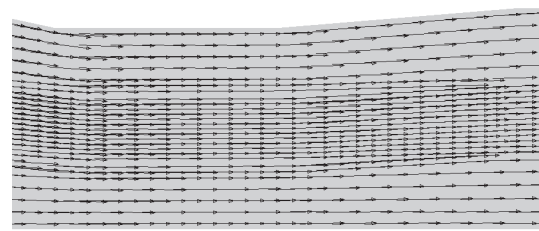

Fig. 13. *Velocity field at 100% opening of guard-gate*

2 EXPERIMENTAL APPARATUS

Experimental apparatus is installed in the High-Head Laboratory at the Institute of Hydraulic Research, Ljubljana, Figure 14. A model of Plave hydropower plant (river Soča) guard-gate was used in experiments; the scale between the model and the prototype is 1 : 20. The model apparatus includes scaled prototype gate 4 m × 5 m (width × height) with gate chamber; 105 m long, 6.5 m diameter pressure tunnel at the upstream end and 32 m long, 5.5 m diameter penstock at the downsteam end of the gate structure. The model tunnel and penstock axes are horizontal; the actual prototype penstock axis deviates 34.7° to the right and 10.2° downwards.

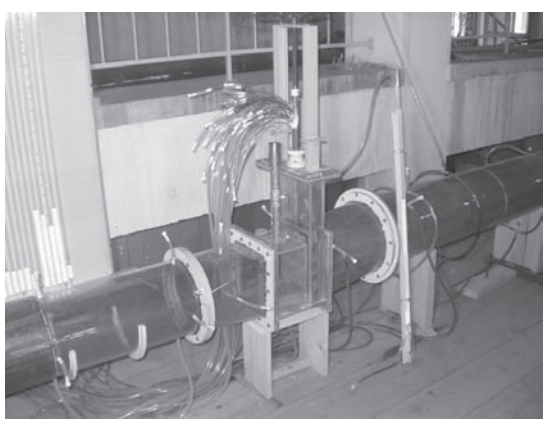

Fig. 14. *Model of the pressure tunnel; gate chamber with gate, hoist mechanism, piezometric taps and areation pipe; and penstock*

The flow rate in the model system was controlled by Thompson weir; the pressure head was adjusted by control gate valve. Pressure head measurements were performed by piezometric PVC tubes.

3 COMPARISON OF RESULTS FROM COMPUTATION AND MEASUREMENTS

Comparison of experimental and numerical results is divided into three groups. They are defined with regard to the position of pressure measuring point on the model of guard-gate, Figure 15. Upper

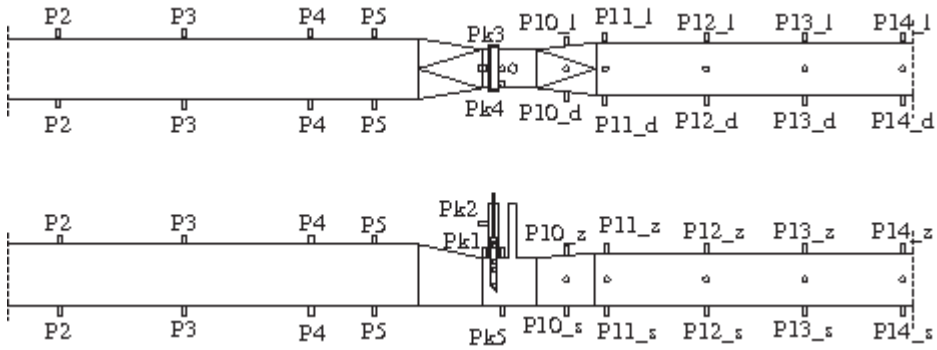

Fig. 15. *Position of piezometric taps in tunnel, gate chamber and penstock*

group is formed by experimental and numerical data which are acquired at the middle (z = 160 mm) of the upper side on the guard-gate model. Bottom group of data was acquired at the middle (z = 160 mm) of the bottom side of the model. Due to the symmetry of the guard-gate model, only the left side was considered. Measuring points with regard to:

- above: P5, PK1, PK3, P10_z, P11_z, P14_z,
- below: PK5, P10_s, P11_s,P12_s, P14_s,
- left: PQ1, PQ2, P11_l, P14_l.

Pressure measurments and corresponding numerical results are represented in Figures 16 to 18. Discrepancies of numerical results from experiment, which are given in Table 3, are normalized with regard

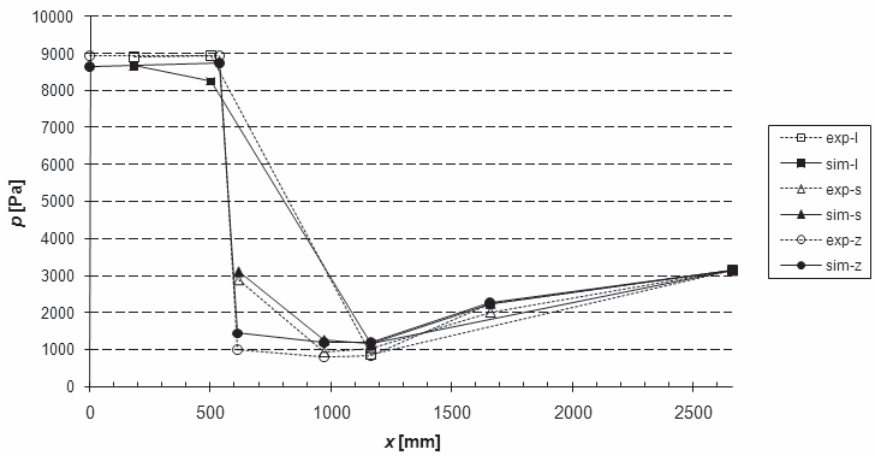

Fig. 16. *Comparison of pressures at 30% opening*

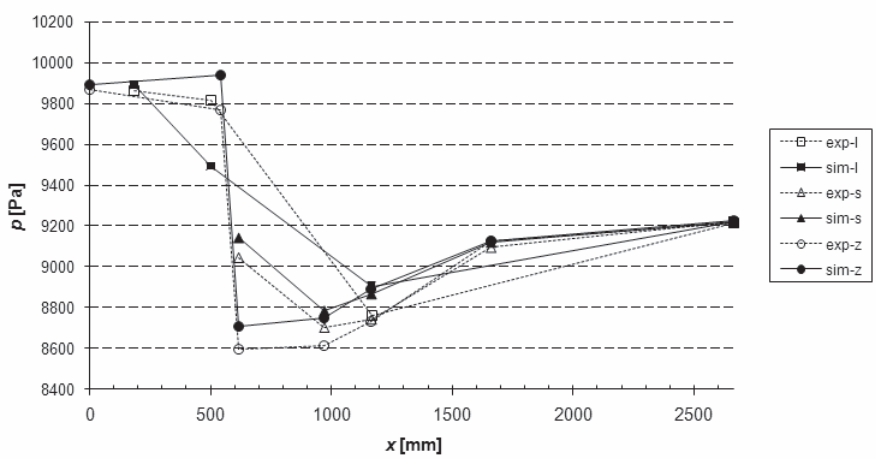

Fig. 17. *Comparison of pressures at 70% opening*

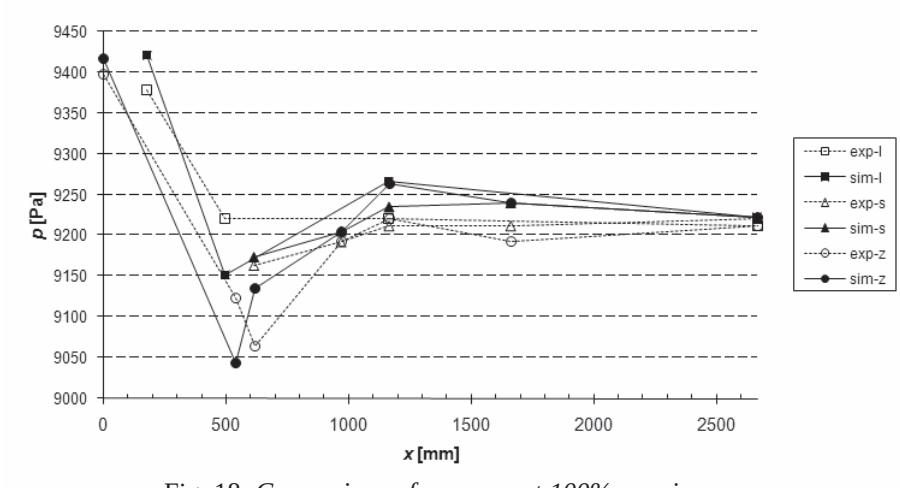

Fig. 18. *Comparison of pressure at 100% opening*

Table 3. *Descrepancies of computed pressure from measured one.*

Pa / Measuring tap	Opening [%]		
	30	70	100
P5	-3.5	1.5	5.7
PK1	-2.3	13.0	-23.8
PK3	4.9	8.9	21.2
P10_z	4.4	10.7	3.9
P11_z	4.1	12.3	12.5
P12_z	-0.1	0.3	14.4
P14_z	0.0	1.0	3.1
PK5	2.7	7.6	3.1
P10_s	3.8	6.6	3.9
P11_s	1.3	9.9	7.0
P12_s	2.7	2.1	8.5
P14_s	-0.1	0.0	0.2
PQ1	-3.2	2.5	12.8
PQ2	-8.5	-24.9	-21.1
P11_l	3.5	11.3	13.4
P14_l	0.1	0.9	3.1

to measured maximum pressure difference, which appears at particular opening of the guard-gate.

It can be observed from Figures 16 to 18 and Table 3 that the best agreement between experimental and numerical results is at 30% opening of the guard-gate. Average and maximal descrepancies at this opening reach minimum. Also the computed pressure profiles agree well with measured profiles. Comparison analysis indicates that the selected numerical model is appropriate for industrial analysis of hydraulically similar guard gates.

4 CONCLUSIONS

Analysis of gate hydraulic characteristics is essential for reliable prediction of loads acting on the guard-gate. Fluid flow characteristics were computed with the aid of the RANS k-ε turbulent model using wall functions. The system of equations is solved by the finite volume method. The results of computations were compared with the results of measurements in a guard-gate experimental apparatus. It has been found that the selected numerical model

is appropriate for industrial analysis of hydraulically similar guard gates. This would reduce a number of experimental runs in the future.

5 ACKNOWLEDGEMENT

The authors wish to thanks Litostroj Ltd. and ARRS (Slovenian Research Agency) for their generous support in the research.

6 NOMENCLATURE

C	constants of turbulence model
D	pipe diameter
$\boldsymbol{g}$	gravity acceleration
k	turbulent kinetic energy
l_{Σ}	length scale
Nc	number of cells
p	pressure
Q	volume flowrate
Re	Reynolds number
t	time
$\boldsymbol{U}$	time averaged velocity vector
U	velocity x component
V	velocity y component
W	velocity z component
x	coordinate along pipe

Greek letters:

ε	dissipation of turbulent kinetic energy
μ	laminar viscosity
μ_{ef}	effective viscosity
μ_t	turbulent viscosity
ρ	density
σ	turbulent Prandtl number

7 REFERENCES

[1] Wickert, G., Schmausser, G. *Stahlwasserbau. Theorie - Konstruktive Lösungen - Spezielle Probleme*. Berlin: Springer-Verlag, 1971.

[2] Naudascher, E. Abflussmenge und dynamische Kräfte bei Tiefschützen. *Der Bauingenieur*, 1957, 32(11), p. 428-439.

[3] Naudascher, E., Kobus, H.E., Rao, R.P.R. Hydrodynamic analysis for high head leaf gates. *Journal of the Hydraulics Division*, ASCE, 1964, 90(3), p. 155-192.

[4] Sharma, H. Air-entrainment in high head conduits. *Journal of the Hydraulics Division*, ASCE, 1976, 102(11), p. 1629-1693.

[5] Naudascher, E., Rao, R.V., Richter, A., Vargas P., Wonik, G. Prediction and control of downpull in tunnel gates. *Journal of Hydraulic Engineering*, ASCE, 1985, 112(5), p. 392-416.

[6] Naudascher, E. *Hydrodynamic forces*, IAHR Hydraulic structures manual, Vol.3, Rotterdam: A.A. Balkema, 1991.

[7] Amorin, J.C.C., de Andrade, J.L. Numerical analysis of the hydraulic downpull on vertical leaf gates. *Waterpower'99*, ASCE, Las Vegas, 1999.

[8] Patankar, S.V. *Numerical heat transfer and fluid flow*. New York: Hemisphere Publishing Corp., 1980.

[9] Ferziger, J.H., Perić, M. *Computational methods for fluid dynamics*. Berlin: Springer-Verlag, 2002.

[10] *ANSYS CFX Release 4.4 Documentation*. Harwell.

[11] Special Interest Group on "Quality and Trust in Industrial CFD". *Best parctice guidelines*. Brussels: ERCOFTAC (European Research Community On Flow, Turbulence And Combustion), 2000.

[12] Shaw, C.T. *Using computational fluid dynamics*. Englewood Cliffs: Prentice Hall Inc., 1992.

[13] Tanehill, J.C., Anderson, D.A., Pletcher, R.H. *Computational fluid mechanics and heat transfer*. Washington: Taylor & Francis, 1997.

Strojniški vestnik - Journal of Mechanical Engineering 54(2008)1, 11-24
UDC 621.83.052
Paper received: 10.7.2006
Paper accepted: 19.12.2007

Vibration Analysis to Determine the Condition of Gear Units

Aleš Belšak* - Jože Flašker
University of Maribor, Faculty of Mechanical Engineering, Slovenia

The use of the most up-to-date production technologies and a high level of production stability without any unscheduled outages are of utmost importance; they are affected primarily by monitoring the condition and by adequate maintenance of mechanical systems.
Life cycle design of machines and devices is nowadays gaining ground rather quickly; users want that machines and devices operate with a high level of accuracy and reliability and with as few outages as possible. Thus, by monitoring the condition, not only the presence of changes but also predictions related to the type and size of damage or error jeopardising the high quality of operation during the remaining life cycle of a machine is established.

Keywords: gear units, fault detection, vibration analysis, probability analysis, operation reliability

0 INTRODUCTION

Life cycle design represents a modern approach in relation to designing machine parts and structures that undergo dynamic loads. The traditional design is based on comparing the working stress with the permissible stress, whereas life cycle design is based on defining the number of loading cycles N that a mechanical part will endure at a specified loading σ.

Damages caused to machine parts and structures that are under dynamic load are referred to as fatigue failures. If compared to machine parts under static load, damages are caused to machine parts under substantially lower dynamic loads, however, only after a certain number of loading cycles N. Generally, the stages of fatigue process caused to materials of machine parts [1] are as follows:

- microcrack initiation,
- short crack propagation,
- long crack propagation,
- damage formation.

In relation to engineering analysis, the first two stages are usually dealt with as crack initiation, whereas the second two stages are dealt with as crack propagation. The life cycle of a machine part (the number of loading cycle N before the final damage is formed):

$$N = N_i + N_p \quad (1)$$

N_i is the number of loading cycles prior to crack initiation, and N_p stands for the number of loading cycles between the initial and the critical crack length, i.e. till final damage is formed.

During fatigue process, it is usually difficult to define precisely the borderline between fatigue crack initiation and propagation. The crack initiation stage represents the major part of a life cycle (usually above 90%) in relation to small loads (as a rule, substantially below proof stress) (Fig. 1). By increasing the load, the crack initiation stage decreases, whereas crack propagation stage increases.

Crack initiation is one of the most significant stages in the fatigue process of machine parts and structures. Position, size and the way of fatigue crack initiation depend primarily on material microstructure, loading type and geometry of the machine part. As a rule, cracks are initiated on the machine parts surface, where intrusions and extrusions appear due to pushing out slip planes of dislocations, which can be dealt with as microcracks (Fig. 1). In case of dynamic load, they propagate through individual crystal grains into the interior of the machine part, along the slip planes of the shearing stress (stage I). After the initial microcrack propagates through a certain number of crystal grains, crack propagation (stage II) appears. In this stage, the crack propagates along slip planes perpendicularly to the working load. At a certain critical crack length, when the remaining transverse section cannot endure the working load any longer, fracture occurs.

*Corr. Author's Address: University of Maribor, Faculty of Mechanical Engineering, Smetanova 17, SI-2000 Maribor, Slovenia, ales.belsak@uni-mb.si

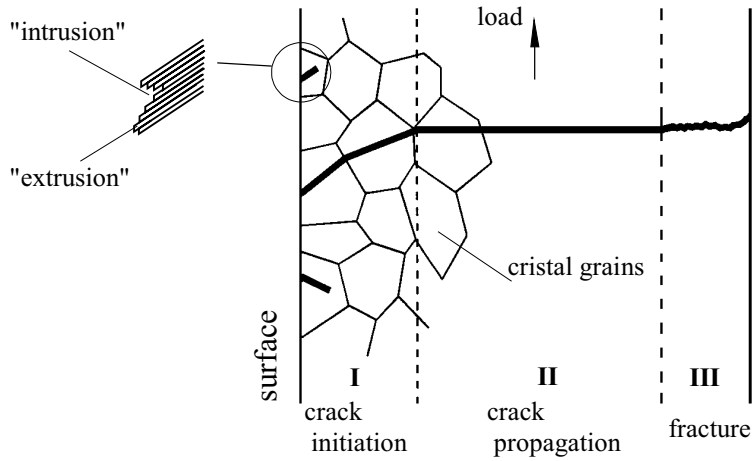

Fig. 1. *Schematic presentation of damage formation in relation to a machine part [3]*

The appearance of fracture surface (e.g. fracture of the axis in Fig. 2) is typical of a fatigue damage. Initial crack propagates from the peak of transverse section into the interior, which is clear also from a relatively smooth fracture surface (*permanent fracture*). After a certain number of loading cycles *N* when the crack length becomes critical, the remaining transverse section breaks instantaneously (*instant fracture*).

1 ESTABLISHING THE CONDITION BY MEANS OF TIME-FREQUENCY ANALYSIS OF VIBRATIONS

The objectives of maintenance are to detect, control and foresee the condition as well as to avoid and repair any damages with the purpose to maintain the characteristics of a technical system at the most favourable or still acceptable level of operation.

Maintenance is associated with assessing the condition of a technical system on the basis of collecting, analysing, comparing and processing data, acquired by means of different methods. In relation to this it is possible to reduce maintenance costs, improve operation reliability and reduce the frequency and complexity of damages. Without the capability of collecting precise data and without adequate data processing it is impossible to control mechanical systems.

Gear units are the most frequent machine parts or couplings. They are of different types and sizes, and consist of a housing, toothed wheels, bearings and a lubricating system. The majority of durable damages in gear units result from geometrical deviations or unbalanced component parts, material fatigue, caused by the engagement of a gear pair, or by damages of roller bearings.

Modern monitoring of the condition of a mechanical system is primarily associated with the

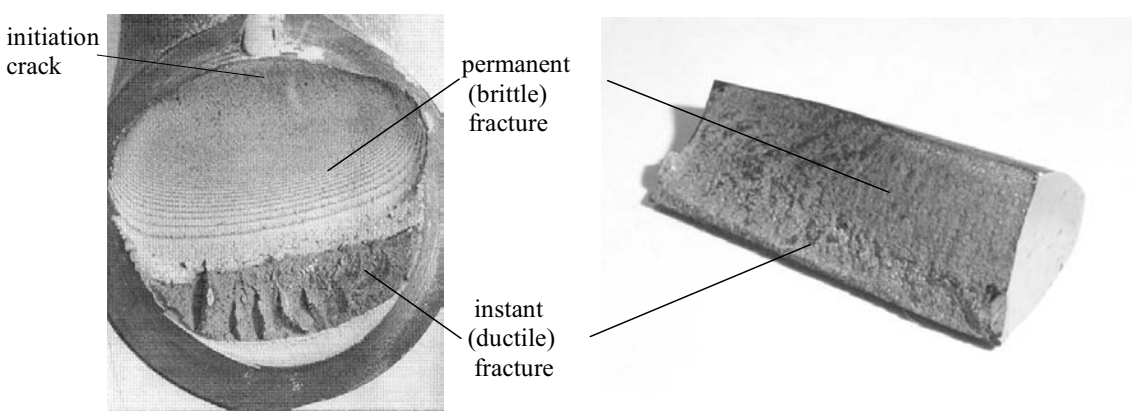

Fig. 2. *Appearance of fatigue fracture surface of an axis [4] and a gear tooth*

methods of measuring vibrations which is the most suitable way to acquire data on a gear unit. Values obtained by measurements are then additionally analysed, using adequate tools; at the same time features indicating the presence of damages and faults are defined.

A gear unit is a set of elements enabling the transmission of rotating movement; it represents a complex dynamic model. In spite of its complexity, its movement is usually periodic, and faults and damages represent a disturbing quantity or impulse. The disturbance is indicated by local and time changes in vibration signals, therefore, time-frequency changes can be expected. This idea is based on kinematics and operating characteristics.

The factor that affects reliability of operation and achievement of adequate quality of operation of gear units most negatively is the presence of cracks in gear units, this is followed by wear and tear of teeth flanks and eccentricity caused by backlash in bearings, and errors when assembling and manufacturing gear units. Monitoring the condition on the basis of measured vibrations is the most frequent method for determining the condition of a gear unit. It is usually attempted to determine deviations from reference values on the basis of a frequency spectrum. A gear unit is a complex mechanical system with changeable dynamic reactions, therefore it is impossible to establish modifications of a frequency component in time, consequently, the approach based on time-frequency methods is more appropriate.

Frequency analysis is a tool very commonly used in diagnostics, however, it may well be stated that good results are obtained only in relation to periodical processes without any local changes. As a consequence of the presence of a damage or fault, dynamic parameters of a mechanical system change, which is reflected in the frequency spectrum. Monitoring frequency reaction is one of the most common spectral methods used with the purpose to establish the condition of a gear unit. In relation to classical frequency analysis, time description of vibration is transformed into frequency description, changes within a signal are averaged within the entire time period observed. Therefore, local changes are actually lost in the average of the entire function of vibrations. As a consequence, identification of local changes is very difficult or impossible.

Time-frequency analysis represents a more thorough approach as it eliminates deficiencies mentioned above – local changes that deviate from the global periodical oscillation are namely expressed with the appearance or disappearance of individual frequency components in a spectrogram. Thus, a signal is presented simultaneously in time and frequency.

In signals related to technical diagnostics, individual frequency components often appear only occasionally. Classical frequency analysis of such signals does not indicate when certain frequencies appear in the spectrum. The purpose of time-frequency analysis is to describe in what way frequency components of transient signals change with time and to determine their intensity levels.

Fourier, adaptive and wavelet transforms, and Gabor expansion are representatives of various time-frequency algorithms. The basic idea of all linear transforms, including Fourier transform, is to carry out comparison with elementary function determined in advance. By means of various elementary functions, different signal presentations are obtained.

On the basis of previous research results [5], the applicable value of a windowed Fourier transform for evaluating the condition of gear units has been established, along with its shortcomings, which have required the use of a more advanced signal analysis method, such as adaptive transform.

2 ADAPTIVE METHOD RELATED TO VIBRATION ANALYSIS

Adaptive transform of a signal was, to a large extent, enhanced and concluded by Qian [6] although many authors had been developing algorithms without interference parts that reduce usability of individual transforms as opposed to Cohen's class. The entire presentation of the following adaptive method is based on [6].

Adaptive transform of a signal *x(t)* is expressed as follows:

$$x(t) = \sum_{p} B_p \cdot h_p(t) \qquad (2),$$

where analysis coefficients are determined by means of the following equations:

$$B_p = \langle x, h_p \rangle \qquad (3),$$

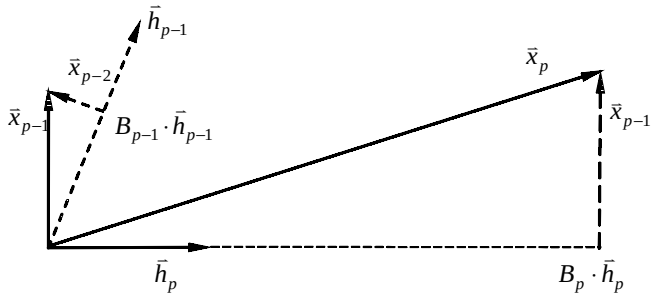

Fig. 3. *Process of adaptive signal decomposition*

expressing similarity between the measured signal $x(t)$ and elementary functions $h_p(t)$ of transform. In Figure 3, the process of adaptive signal decomposition is presented.

The original signal represents the starting point with parameter values $p=0$ and $x_0(t)=x(t)$. In the set of desired elementary functions, $h_0(t)$ is searched for that is most similar to $x_0(t)$ in the following sense:

$$\left|B_p\right|^2 = \max_{h_p} \left|\left\langle x_p(t), h_p(t)\right\rangle\right|^2 \qquad (4),$$

for $p = 0$. The next step is associated with the calculation of the remaining $x_1(t)$

$$x_{p+1}(t) = x_p(t) - B_p \cdot h_p(t) \qquad (5).$$

Without giving up the generalisation idea, $h_p(t)$ is to have a unit of energy representation of a signal. Therefore:

$$\left\|h_p(t)\right\|^2 = 1 \qquad (6).$$

The energy contained in the remaining signal:

$$\left\|x_{p+1}(t)\right\|^2 = \left\|x_p(t)\right\|^2 - \left|B_p\right|^2 \qquad (7).$$

The Equation (5) is repeated to find $h_1(t)$ that would suit best $x_1(t)$, etc. In each step one elementary function $h_p(t)$ that suits best $x_p(t)$ is found. The main objective of adaptive signal representation is to find a set of elementary functions $\{h_p(t)\}$ that are most similar to time-frequency structure of a signal, and at the same time satisfy Equations (2) and (3).

If Equation (6) is expressed as:

$$\left\|x_p(t)\right\|^2 = \left\|x_{p+1}(t)\right\|^2 + \left|B_p\right|^2 \qquad (8)$$

it indicates that the remaining energy of a signal at pth level can be determined on the basis of $p + 1$ level and the rest B_p. If this process is continued, the result is as follows:

$$\left\|x(t)\right\|^2 = \sum_{p=0}^{\infty} \left|B_p\right|^2 \qquad (9).$$

This is an equation related to energy conservation and it is similar to Parseval's relation in the Fourier transform.

The result of using Wigner-Ville distribution for both sides of the Equation (2), and organising equations into two groups is as follows:

$$P_{WV}x(t,\omega) = \sum_p B_p^2 \cdot P_{WV}h_p(t,\omega) + \sum_{p\neq q} B_p \cdot B_q * P_{WV}\left(h_p, h_q\right)(t,\omega) \qquad (10).$$

The first group represents elementary signal components, whereas the second one represents cross interference terms.

Due to the relation described in (9) and the given value of energy conservation, it is evident that:

$$\frac{1}{2\cdot\pi}\cdot\iint \sum_{p\neq q} B_p \cdot B_q * P_{WV}\left(h_p, h_q\right)(t,\omega) = 0 \qquad (11).$$

This is the reason that a new time-dependent adaptive spectrum can be defined as:

$$P_{ADT}(t,\omega) = \sum_p \left|B_p\right|^2 \cdot P_{WV}h_p(t,\omega) \qquad (12).$$

As this is an adaptive spectrum based on representations it is referred to as adaptive spectrogram. It includes no interferences and no cross terms – in this respect, it differs from Wigner-Ville distribution, and it also satisfies the condition related to energy conservation.

$$\left\|x(t)\right\|^2 = \frac{1}{2\cdot\pi}\cdot\iint P_{ADT}(t,\omega)\cdot dt\cdot d\omega \qquad (13).$$

The basic issue related to linear presentations is the selection of elementary functions. In case of Gabor expansion, a set of elementary functions comprises time-shifted and

frequency modulated prototype window function $w(t)$. In relation to wavelets, elementary functions are obtained on the basis of scaling and shifting of a mother wavelet $\psi(\tau)$. In these two examples, structures of elementary functions are determined in advance. Elementary functions related to adaptive representation are rather demanding.

Generally speaking, adaptive transform is independent from the choice of elementary functions $h_p(t)$ as it permits arbitrary elementary functions.

As a rule, elementary functions, used for adaptive representation of a signal with equation (2) are very general. In practice, however, this is not always the case. In order to stress time dependence of a signal, it is desirable that elementary functions are localised in regard to time and frequency. They also have to be able to use the presented algorithm in a relatively simple way. A Gauss type signal has very favourable features and it is considered a basic choice in relation to adaptive representation. It is expressed as follows:

$$h_p(t) = \left(\frac{\alpha_p}{\pi}\right)^{0,25} \cdot e^{-\frac{\alpha_p}{\pi}\cdot(t-T_p)^2} \cdot e^{-j\cdot\Omega_p\cdot t} \quad (14),$$

where (T_p, Ω_p) is a time-frequency centre of an elementary function, whereas α_p^{-1} stands for a variance of Gauss function at (T_p, Ω_p).

The variance, acquired by means of the ordinary Gabor transform, is stable, in (13) it is adaptive. Gauss functions, normally used in the ordinary Gabor transform, are located at fixed points $(mT, n\Omega)$ of time and frequency grid, whereas the centres of elementary functions in (13) are not fixed and can be located anywhere. The adaptation of the variance value can make elementary functions longer or shorter; the adaptation of parameters (T_p, Ω_p) changes time and frequency centres of elementary functions. Adapting both variance and time-frequency centres results in increased suitability of local time-frequency features of the signal $x(t)$.

Wigner-Ville distribution of time-frequency density of adaptive Gauss functions is expressed as:

$$P_{WV}h_p(t,\omega) = 2\cdot e^{-\left(\alpha_p\cdot(t-T_p)^2+\frac{(\omega-\Omega_p)^2}{\alpha_p}\right)} \quad (15).$$

The function of time-frequency density of the adaptive Gauss function forms an ellipse with the centre at (T_p, Ω_p). The energy concentration of Gauss functions is an optimum one. By means of Gauss functions of various variances and of a different time-frequency centre, the local behaviour of each analysed signal $x(t)$ is characterised by the Gauss function. If the signal features rapid time change, the Gauss function with a small variance value suitable for the sudden change has to be applied. If stable frequency over a longer period of time is typical of the signal, the Gauss function with greater variance value is to be used.

By entering (14) into (2), the following equation is acquired:

$$x(t) = \sum_p B_p \cdot h_p(t) = \sum_p B_p \cdot \left(\frac{\alpha_p}{\pi}\right)^{0,25} \cdot e^{-\frac{\alpha_p}{\pi}\cdot(t-T_p)^2} \cdot e^{-j\cdot\Omega_p\cdot t} \quad (16).$$

This is adaptive Gabor transform, which resembles an ordinary Gabor transform.

The adaptive transform has the same functions of analysis and synthesis, which makes it different from the Gabor transform. When the optimum function of synthesis $h_p(t)$ is achieved, it is possible to calculate adaptable coefficients B_p, on the basis of ordinary operation of internal product:

$$B_p = \int x_p(t)\cdot h_p^*(t)\cdot dt = \left(\frac{\alpha_p}{\pi}\right)^{0,25} \cdot \int x_p(t)\cdot e^{-\frac{\alpha_p}{\pi}\cdot(t-T_p)^2} \cdot e^{-j\cdot\Omega_p\cdot t}\cdot dt \quad (17),$$

which guarantees that local signal behaviour is really expressed by B_p.

By entering (15) into (12), a Gauss adaptive spectrogram, which is based on the function, the following equation is produced:

$$P_{ADT}(t,\omega) = 2\cdot\sum_p |B_p|^2 \cdot e^{-\left(\alpha_p\cdot(t-T_p)^2+\frac{(\omega-\Omega_p)^2}{\alpha_p}\right)} \quad (18).$$

As time-frequency resolutions of Gauss function are determined by one parameter α_p, it is relatively easy to calculate optimum $h_p(t)$. Thus, it is relatively easy to calculate adaptive Gabor expansion when elementary functions $\{h_p(t)\}$ are determined. There is, however, a question regarding the choice of elementary functions $\{h_p(t)\}$. As already mentioned before, $h_p(t)$ should suit $x_p(t)$ best in the sense of Equation (4), where Gabor function determined in Equations (14) and (4), represents the optimum solution in regard to $(\alpha_p, T_p, \Omega_p)$. Generally speaking, there is no analytical solution in relation to Equation (4) as, similarly to the approximation process to the final result, it is possible to obtain a numerical approximation with a corresponding deviation.

The process of calculating adaptive spectrogram begins in a wide time range of a measured signal. Then the range has to be reduced, depending on what is wanted to be achieved. As Fourier integral is included in the elementary operations of searching for a suitable elementary function, the described calculation process is very effective [7]. The accuracy of approximation depends primarily on the size of time-frequency interval. The narrower the intervals are, the better is the accuracy of representation, along with increased time of calculation. Therefore a compromise between the accuracy of approximation and the efficiency has to be found.

3 SIGNAL RESAMPLING PROCEDURE FOR LIMITED SPEED FLUCTUATION

Vibration measuring can represent measuring of a dynamic quasi periodical signal as the gear consists of rotating elements (shafts with gears and bearings). This represents complex repeated rotating movements. The information obtained by measuring the rotation speed, making it possible to follow the stability of rotation speed during the measuring, is important for the frequency analysis [8]. During measuring, rotation speed can oscilate, even more so when gears are used in machines, which are under load. This results in an unreliable frequency spectrum, which is even more expressed in case of frequency analysis of higher harmonics; additional sidebands namely appear. In relation to time-frequency analysis it is also more adequate to assess the results on the basis of stable rotation frequency [9]. By following the rotation speed signal (TTL signal), the beginning and the end of rotations are located and their length and time of duration are measured.

There are two techniques for producing synchronously sampled data; the traditional approach which uses specialised hardware to dynamically adapt the sample rate and a technique where the vibration signals and a tachometer signal are asynchronously sampled, that is, they are sampled conventionally at equal time increments (Fig. 4). From the asynchronously sampled tachometer signal re-sample times required to produce synchronous sampled data are calculated. In this paper, analysis of rotation frequency stability and, if required, suitable resampling are carried out prior to each analysis.

Recently, there has been interest in calculating synchronous sampled signals from asynchronously sampled data. Both the vibration signals and tachometer are sampled at constant time intervals, that is, asynchronously. From these signals, synchronously sampled vibration data is synthesised in a computer code.

A computed re-sampling system is generally based on two stage algorithm: the tachometer pulse trigger, with angle evaluation procedure and the signal interpolation. Tachometer determines when the edge of the pulse arrives. From these timings the angular motion of the shaft is resulting in resample times. The asynchronously sampled vibration signal is interpolated and re-sampled at these times thus producing synchronously sampled data.

To calculate re-sample times at constant angular increments, the angular motion of the shaft has to be estimated from the tachometer pulses. In the first instance constant angular speed may be assumed, which results in linear interpolation between the shaft angle at consecutive tachometer pulses.

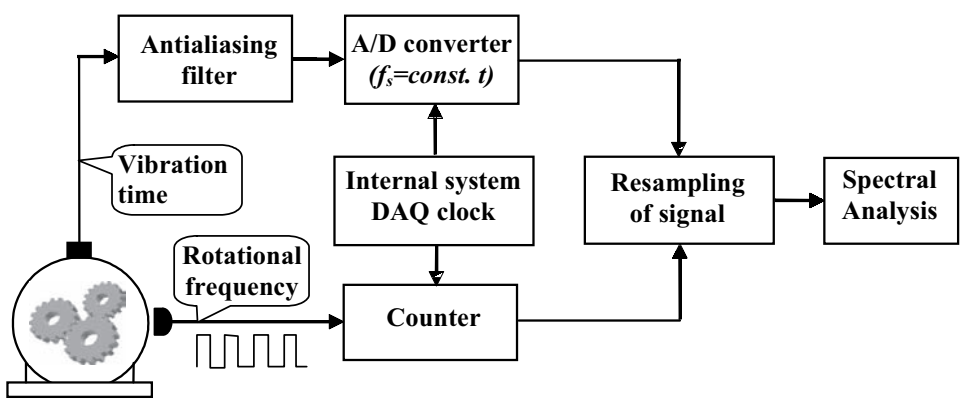

Fig. 4. *Data acquisition with fixed sampling frequency*

To produce the desired synchronously sampled signal, the value of the vibration signal must be estimated at the re-sample times.

Linear evaluation is the simplest signal interpolation method. This approach is adequate for signals with slow oscillation rotation speed.

B-spline evaluation is the most useful signal interpolation method which produces a pth-order piecewise polynomial fit to the data. The method is especially interesting because up to the (p - l)th derivative of the resulting signal is continuous. Using the weighted sum of B-spline basis functions, the signal is approximated. In the analysis cubic B-spline evaluation is used, giving good interpolation flexibility and appropriate basis functions.

A piecewise polynomial fit to the data samples is obtained through Lagrange interpolation (a spline interpolation method) [10]. A pth-order polynomial is usually used to fit (p + 1) data points; this is, however, limited with the condition that the polynomial passes through every sample. Piecewise polynomial signals are created by interpolation; the derivatives across the boundaries (at the sample points) are not constrained to be continuous, which is different from B-spline interpolation. Using the latter one (i.e. B-spline interpolation), a more original signal is actually created. The presented method is successfully applied in relation to the change in rotation frequency by 2%.

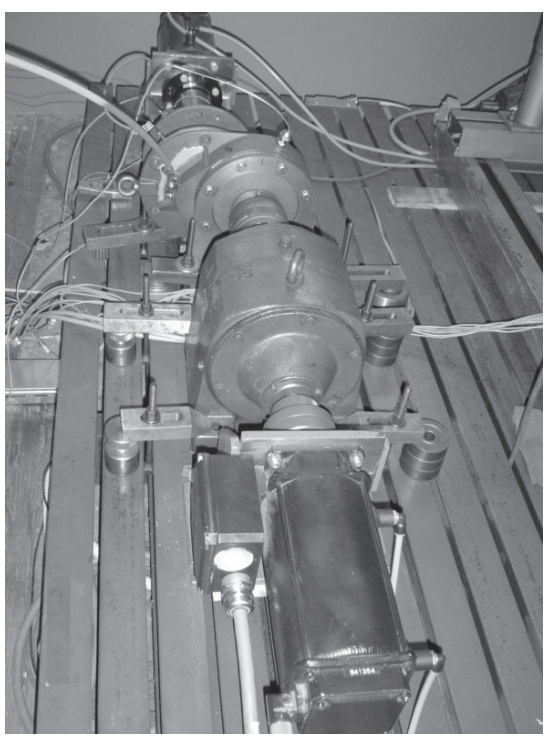

Fig. 5. *Test plant and a part of measuring equipment*

The trend of rotation speed oscillation and its stability being observed contribute to a more precise and clearer spectrogram, even to a larger extent with high harmonics and their side frequencies.

4 PRACTICAL EXAMPLE

All the measures have been carried out in the test plant of the Computer Aided Design Laboratory at the Faculty of Mechanical Engineering, University of Maribor. The test plant is presented in Figure 5, with a one-stage helical gear unit at the spot where vibration measurements have been carried out.

Some changes have been caused to a standard gear unit with the purpose to (artificially) produce faults and damages in a gear couple and to adapt some design-related features to the test plant. Simultaneously, appropriate measurements of vibration accelerations have been carried out – they serve as a tool for determining the presence of individual changes in a gear unit. As the method of determining the condition of a gear unit is based on comparing the measured signal of a faultless gear unit with the signal of a faulty gear unit, a faultless and faulty gear units were tested.

A single stage gear unit EZ5.B3.132 produced by "Strojna tovarna" in Maribor was tested. Into the gear unit, a helical gear unit with straight teeth was integrated. A more detailed description and technical documentation of the gear unit are in [5].

Measures of a gear unit with a fatigue crack in the tooth root of a pinion were carried out, under operating conditions that would be normally associated with this type of a gear unit. A ground gear pair with a crack is a standard gear pair, with the teeth quality 6, but with the presence of a crack in the tooth root of a pinion; it is presented in Figure 6.

The length of the crack in Figure 6, the presence of which can be observed on one of the teeth, is 4.8 mm. The whole measurement process and preparations for analysis are described in [5].

Own computer program for signal analysis for a family of time-frequency transformations has been developed in the LabView 7.1 program

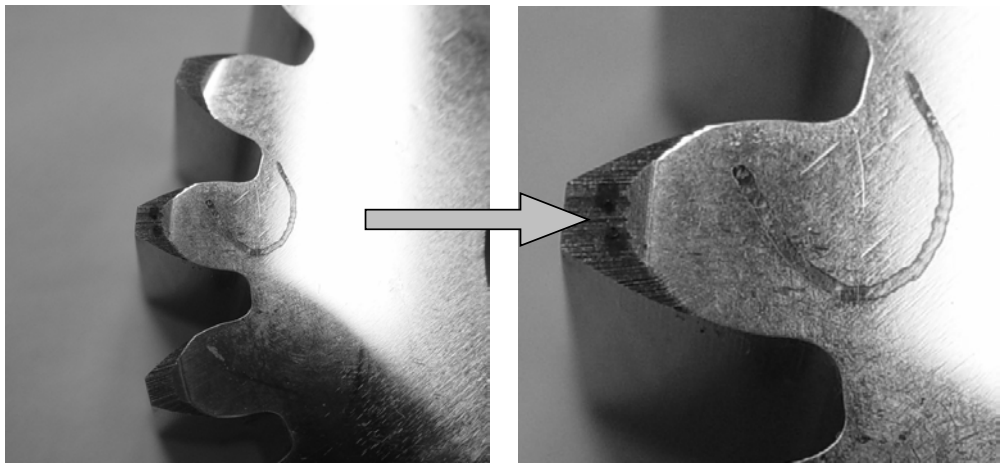

Fig. 6. *Pinion with a crack in the tooth root*

package, and tested and evaluated on the basis of a certain number of basic mathematically generated signals [11].

Adaptive transform was used to determine the presence of a crack in the tooth root. In relation to adaptive spectrogram, adaptive representation for signal decomposition, prior to Wigner-Ville distribution, was used. Additionally, only the sum of Wigner-Ville distribution of basic signal components was taken into account, whereas cross-interference terms were completely ignored.

Adaptive spectrogram has a fine adaptive time-frequency resolution because the features of elementary functions are limited. Time-frequency resolution of the transform is, therefore, adapted to signal characteristics. As an elementary function, Gauss function (impulse) and linear chirp with Gauss window can be used. If a signal is composed of linear chirps that are the consequence of a linear change in the rotation frequency of a gear unit, an adaptive spectrogram can be applied to establish in what ways a possible frequency modulation is reflected in the time-frequency domain. A possible presence of non-linear frequency modulation may represent a problem as a spectrogram may include a certain level of distortion because adaptive representation is approaching non-linear modulation in the form of a linear combination of chirps with linear frequency

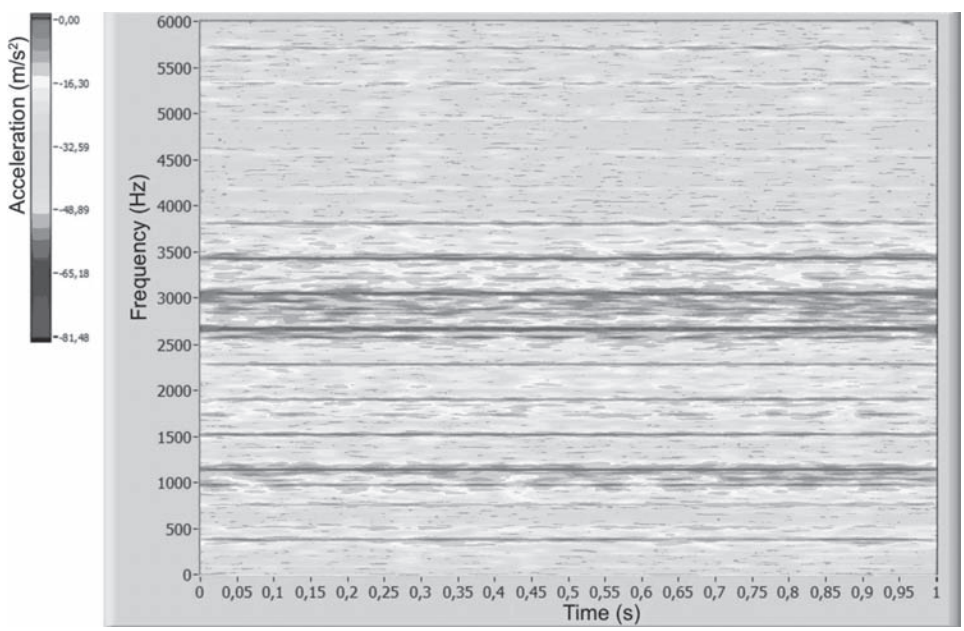

Fig. 7. *Gabor's spectrogram of a faultless gear unit*

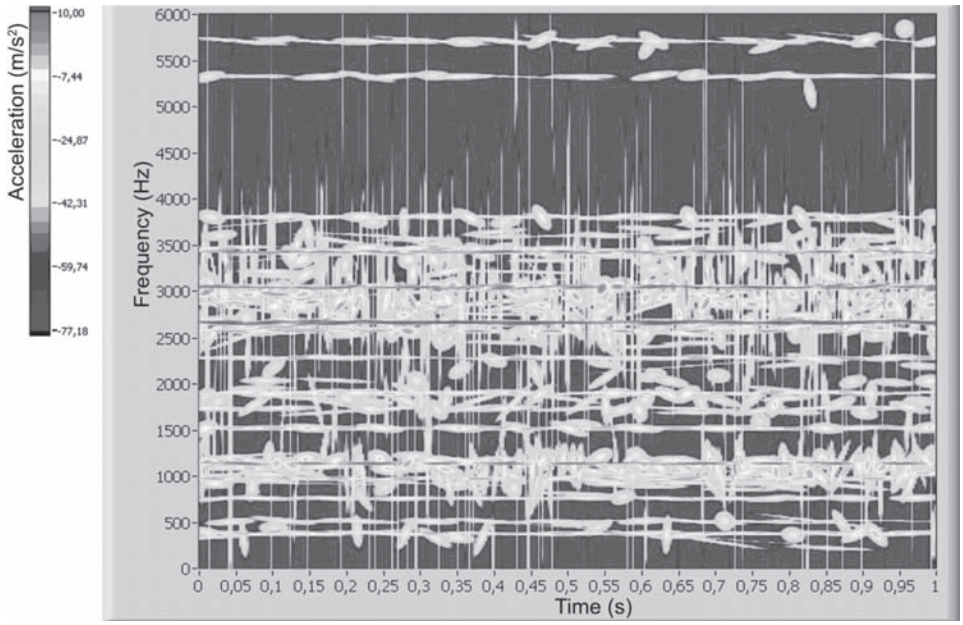

Fig. 8. *Adaptive spectrogram of a faultless gear unit*

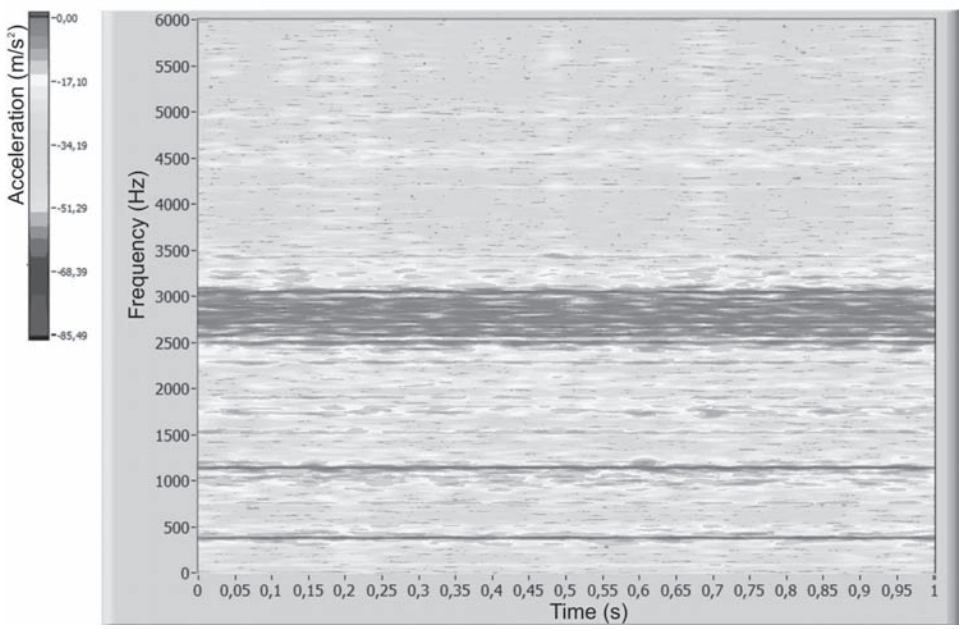

Fig. 9. *Gabor's spectrogram of a gear unit with a cracked pinion*

modulation. The time required for transform calculation increases, along with the increased amount of data and the number of cycles necessary to search for an adequate elementary function.

The signal of measured values was 1 s long and composed of, on an average, 12500 measuring points. Rotation frequency was 20 Hz at the time of measurement. The number of teeth of the pinion was 19, and of the gear unit 34. For comparison, spectrograms related to Gabor and window Fourier transforms are presented, with the length of the window being 700 points, which is 10% more that the length of the period of one rotation of a gear couple.

Calculation time required in relation to adaptive spectrogram is at least 15 times longer than the time required for the calculation associated with the Fourier transform. The resolution of the adaptive transform, however, is on an average, 1.7 times better.

In Figure 7, Gabor spectrogram is presented; no rhythmic pulsation of harmonics can be observed, with the exception of typical frequencies, determined on the basis of power spectrum. In relation to adaptive spectrogram (Fig. 8), featuring a higher level of energy accumulation in the origins, some pulsation sources are indicated but they are not very expressed. It is particularly interesting to monitor the increase or decrease (complete disappearance) in appropriate frequency components with rotation frequency of 20 Hz. This phenomenon is typical of the 3rd harmonic, 1530 Hz is expressed only in relation to the presence of a crack. The phenomenon is much more expressed in the adaptive spectrogram (Fig. 10) than in the Gabor spectrogram (Fig 9). In Figure 10, pulsation (the area, marked with a continuous line) is expressed reflecting a single engagement of a gear couple with a crack within

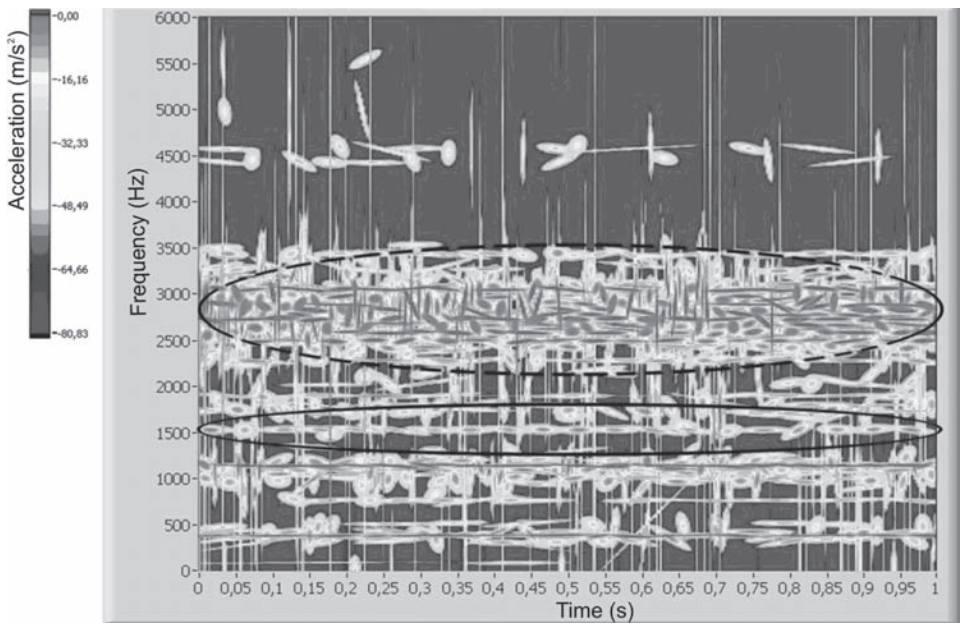

Fig. 10. *Adaptive spectrogram of a gear unit with a cracked pinion*

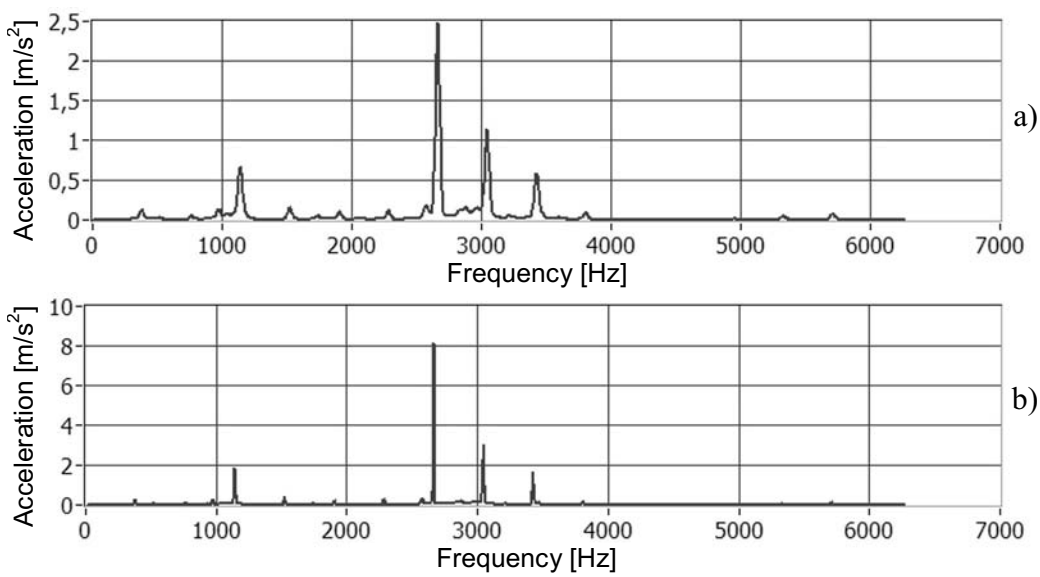

Fig. 11. *Average frequency specter of the spectrogram of vibrations produced by the faultless couple of gears with ground surface teeth: a) Gabor and b) adaptive*

one rotation of a shaft. Similarly, between the 6th and the 9th harmonics (area marked with a dashed line) rich with sources indicating pulsating portions of individual components with the frequency of 20 Hz.

The spectrogram evaluation can be based on an average spectrogram representing an amplitude spectrum of a Fourier or adaptive transform of a measured signal and by observing pulsating frequencies of individual frequency components.

In Figure 11, average frequency spectres of spectrograms of vibrations produced by the faultless gear unit are presented. It is evident that the greatest average values are achieved at the 6th, 7th, 2nd and 8th harmonics. The Figure indicates a larger width of a frequency component round individual harmonics, which is more expressed in relation to the Gabor transform, whereas in relation to the adaptive transform the concentration of frequency components is very distinguished.

Table 1. *Amplitudes and frequencies of the pulsation of harmonics in relation to the average Gabor spectrogam of vibrations of the faultless couple of gears with ground surface teeth*

h	f [Hz]	A_{pos} [m/s^2]	f_{ut1} [Hz]	f_{ut2} [Hz]	f_{ut3} [Hz]
0	379.175	0.116	1.998	4.994	10.987
1	758.350	0.044	8.989	10.987	1.998
2	1137.524	0.651	10.987	8.989	2.996
3	1516.699	0.151	10.987	0.999	7.990
4	1895.874	0.093	1.998	10.987	0.999
5	2275.049	0.103	0.999	5.993	6.992
6	2654.224	2.080	1.998	12.984	3.995
7	3033.398	0.917	1.998	0.999	12.984
8	3412.573	0.436	2.996	0.999	10.987
9	3791.748	0.068	10.987	0.999	9.988
10	4170.923	0.006	10.987	5.993	1.998
11	4550.098	0.005	2.996	8.989	6.992
12	4929.272	0.006	3.995	2.996	1.998
13	5308.447	0.027	10.987	9.988	12.984
14	5687.622	0.036	10.987	9.988	0.999
15	6066.797	0.002	6.992	3.995	4.994

Table 2. *Amplitudes and frequencies of the pulsation of harmonics in relation to the average adaptive spectrogram of vibrations of the faultless couple of gears with ground surface teeth*

h	f [Hz]	A_{pos} [m/s^2]	f_{ut1} [Hz]	f_{ut2} [Hz]	f_{ut3} [Hz]
0	379.175	0.271	11.011	14.015	1.001
1	758.350	0.088	11.011	9.009	20.021
2	1137.524	1.363	11.011	7.007	10.010
3	1516.699	0.216	11.011	8.008	20.021
4	1895.874	0.086	11.011	12.012	1.001
5	2275.049	0.082	9.009	11.011	10.010
6	2654.224	0.670	5.005	11.011	3.003
7	3033.398	0.551	11.011	2.002	9.009
8	3412.573	0.129	9.009	11.011	1.001
9	3791.748	0.053	20.021	11.011	9.009
10	4170.923	0.001	152.158	54.056	103.107
11	4550.098	0.001	131.136	128.133	132.137
12	4929.272	0.001	7.007	20.021	6.006
13	5308.447	0.007	11.011	20.021	2.002
14	5687.622	0.009	11.011	20.021	22.023
15	6066.797	0.001	25.026	154.160	129.134

In Tables 1 and 2, the amplitudes of individual harmonics along with corresponding frequencies are shown. In addition, dominating frequencies of the pulsation of individual harmonics are indicated, which makes the evaluation of changes in frequency components over a period of time easier.

In Figure 12, the vibrations of the 3rd harmonic over a period of time are shown; it has been established that it is very suitable for observing the pulsation in relation to all types of irregularities; it is evident that expressed pulsations (rhytmic changes) are not present. The frequency, which is also present, is 11 Hz and it represents rotation speed of the gear unit, whereas other parts of frequency components are much lower.

In Figure 13, average spectrograms of the vibrations of a gear unit are presented, on the basis of which it is clear that the greatest average values are associated with the 6th and 7th harmonics as well as with the 2nd harmonic and with the meshing frequency. Very expressed sideband frequencies are associated only with the 6th and 7th harmonics,

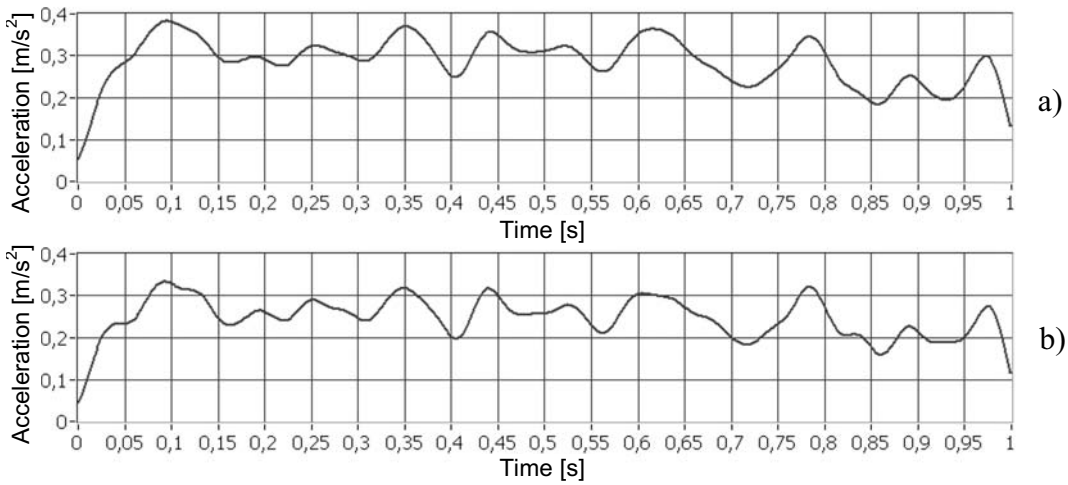

Fig. 12. *Time presentation of the 3rd harmonic (1516.7 Hz) of the spectrogram of vibrations of the faultless couple of gears with ground surface: a) Gabor and b) adaptive*

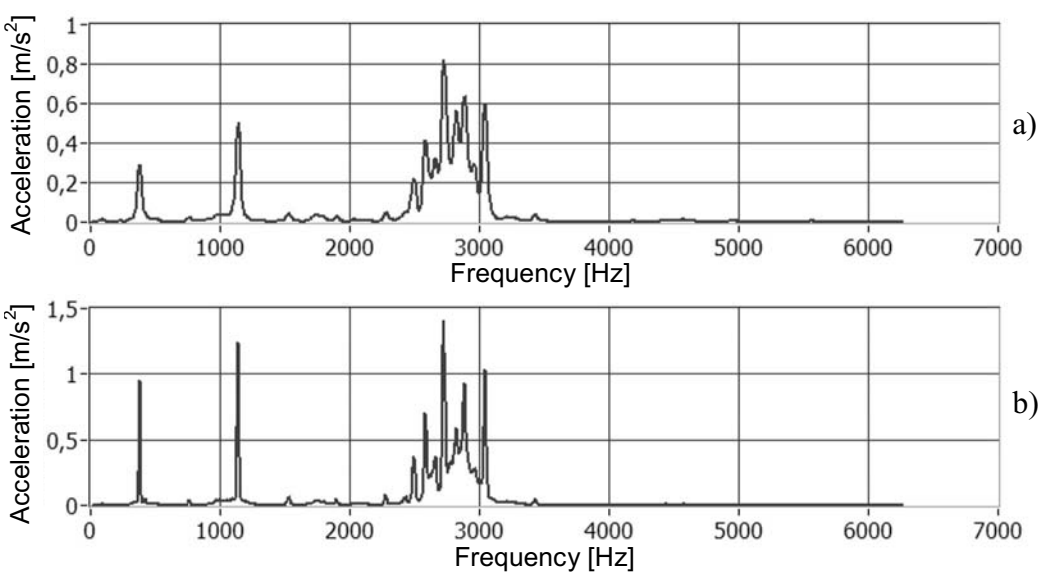

Fig. 13. *Average frequency spectrogram of vibrations of a couple of gears with a crack: a) Gabor and b) adaptive*

which is typical when a crack is present. In addition to that, the figure shows a larger width of frequency components round individual harmonics, which is particularly expressed in relation to the window Gabor transform, whereas in relation to the adaptive transform, the concentration is much larger round harmonics.

Tables 3 and 4 show amplitudes of individual harmonics with corresponding frequencies, along with dominating frequencies of the pulsation of individual harmonics. Thus, pulsating frequencies are changed and the pulsation of rotation frequencies of the shaft of the pinion (19.96 Hz) and of the gear (10.98 Hz) are dominant. Partial frequencies and higher harmonics of the rotation frequencies of both shafts appear as well. The pulsation of the 3rd harmonic (Fig. 14) is particularly interesting; it is very clear and periodic (20 Hz) and it appears only in relation to the couple of gears with a crack in the tooth root.

Table 3. *Amplitudes and frequencies of the pulsation of harmonics of an average Gabor spectrogram of the vibrations produced by a couple of gears with a crack*

h	f [Hz]	A_{pos} [m/s^2]	f_{ut1} [Hz]	f_{ut2} [Hz]	f_{ut3} [Hz]
0	378.751	0.290	10.975	5.986	19.954
1	757.502	0.023	10.975	19.954	11.972
2	1136.253	0.486	10.975	19.954	12.970
3	1515.004	0.035	19.954	1.995	18.956
4	1893.755	0.028	10.975	1.995	21.949
5	2272.506	0.041	10.975	19.954	33.921
6	2651.257	0.292	19.954	39.907	1.995
7	3030.008	0.463	10.975	19.954	2.993
8	3408.759	0.021	19.954	10.975	11.972
9	3787.510	0.002	3.991	19.954	12.970
10	4166.261	0.004	13.968	4.988	10.975
11	4545.012	0.007	10.975	19.954	7.981
12	4923.763	0.005	19.954	2.993	3.991
13	5302.514	0.002	10.975	22.947	2.993
14	5681.265	0.001	10.975	3.991	13.968
15	6060.016	0.001	3.991	1.995	10.975

Table 4. *Amplitudes and frequencies of the pulsation of harmonics of an average adaptive spectrogram of the vibrations produced by a couple of gears with a crack*

h	f [Hz]	A_{pos} [m/s^2]	f_{ut1} [Hz]	f_{ut2} [Hz]	f_{ut3} [Hz]
0	378.751	0.950	11.027	6.015	5.012
1	757.502	0.039	11.027	2.005	10.025
2	1136.253	1.238	11.027	2.005	13.032
3	1515.004	0.032	20.050	40.099	2.005
4	1893.755	0.028	11.027	5.012	2.005
5	2272.506	0.055	11.027	20.050	2.005
6	2651.257	0.289	20.050	8.020	5.012
7	3030.008	0.289	12.030	6.015	11.027
8	3408.759	0.010	20.050	11.027	2.005
9	3787.510	0.001	78.194	68.169	156.387
10	4166.261	0.001	78.194	156.387	68.169
11	4545.012	0.002	11.027	4.010	7.017
12	4923.763	0.001	9.022	10.025	23.057
13	5302.514	0.001	91.226	19.047	74.184
14	5681.265	0.001	91.226	78.194	169.420
15	6060.016	0.001	78.194	91.226	169.420

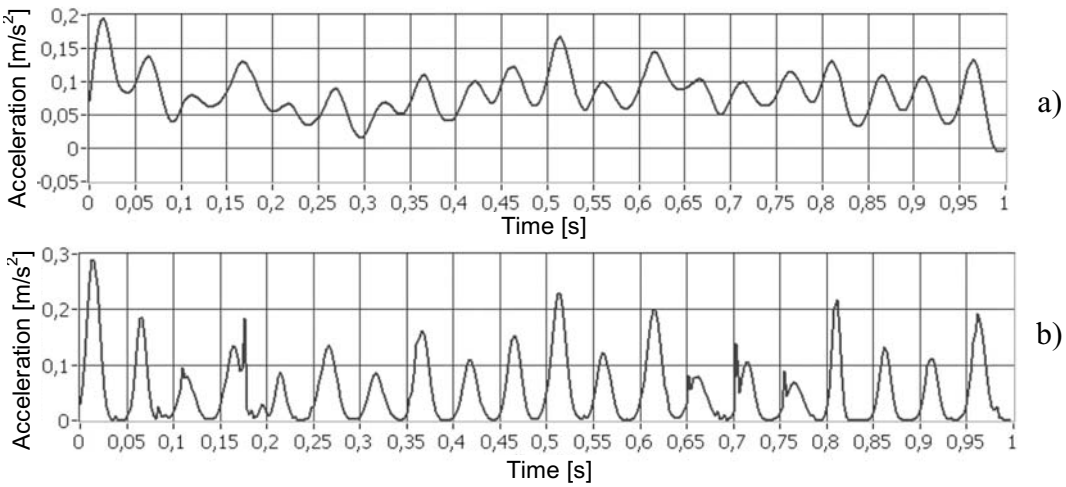

Fig. 14. *Time presentation of the 3rd harmonic (1515 Hz) of the spectrogram of vibrations of a couple of gears with a crack in the pinion: a) Gabor and b) adaptive spectrograms*

5 CONCLUSION

Fault detection, presented in this paper, in relation to industrial gear units is based on vibration analysis; it increases the safety of operation and, consequently, of monitoring operational capabilities.

Appropriate spectrogram samples and a clear presentation of the pulsation of individual frequency components that, in addition to the average spectrum, represent a criterion for assessing the condition of a gear unit make it possible to monitor life cycle of a gear unit more reliably. Adaptive time-frequency representation represents, above all, a reliable prediction as the representation is clearer, without increased dissemination of signal energy into the surroundings.

In relation to the life cycle design of machine parts and structures, it is therefore possible, by using an adequate method or criterion, to monitor the actual condition of a device and of its vital components that can affect its operational capability considerably. By detecting faults or damages, the reliability of operation is controlled to such an extent that the probability and reliability of detecting faults make a positive contribution related to the prediction of the remaining life cycle of a gear unit.

6 REFERENCES

[1] Suresh S. *Fatigue of materials*, Cambridge University Press, 1998.

[2] Buch A. *Fatigue strength calculation.* Aedermannsdorf: Trans Tech Publications, 1988. 467 p. ISBN 0-87849-536-3

[3] Stephens R.I., Fatemi A., Stephens R.R, Fuchs H.O. *Metal fatigue in engineering*, 2nd ed. New York: John Wiley & Sons Inc., 2001.472 p. ISBN 0-471-51059-9

[4] *Fe-safeWorks*, Users Manual, 2003.

[5] Belšak A. *Development of gear unit failure detection system*, Master thesis. University of Maribor, Faculty of Mechanical Engineering, 2004. (In Slovenian).

[6] Qian S., Chen D. *Joint time-frequency analysis.* New Jersey: Prentice Hall, 1996. 302 p. ISBN 0-13-254384-2.

[7] Fladrin P. *Time-frequency/Time-scale analysis*. San Diego: Academic Press, 1999. 386 p. ISBN 0-12-259870-9.

[8] Mertins A. *Signal analysis*. New York: John Wiley & Sons Inc., 1999. 317 p. ISBN 0-471-98626-7

[9] Bendar J.S., Piersol A.G. *Random data*, 3rd ed. New York: Willey, 2000. 594 p. ISBN 0-471-31733-0

[10] Rohatgi V.K., Saleh A.K. *An intruduction to propability and statistics.* John Willey & Sons, 2001.

[11] Belšak A. *Time-frequency analysis of the condition of gear units*, Doctoral thesis. University of Maribor, Faculty of Mechanical Engineering, 2006. (In Slovenian).

Strojniški vestnik - Journal of Mechanical Engineering 54(2008)1, 25-36
UDC 620.19
Paper received: 28.6.2006
Paper accepted: 19.12.2007

An Attempt to Detect Various Types of Stress-Corrosion Cracking on Austenitic Stainless Steels by Simultaneous Measurements of Acoustic Emission and Electrochemical Noise

Žiga Bajt - Mirjam Leban - Jaka Kovač* - Andraž Legat
Slovenian National Building and Civil Engineering Institute, Slovenia

This paper discusses the potential use of acoustic emission (AE) and electrochemical noise (EN) for the detection and characterization of different types of stress-corrosion cracking (SCC) in austenitic stainless steels. The discussion is based on the performance of constant load experiments. Three different measurements were performed simultaneously during the experiment: acoustic emission, electrochemical noise, and elongation of the test specimen. The stainless steel was sensitized to increase its susceptibility to SCC. Two different electrolytes and two different load levels were used to obtain different types of SCC. Intergranular stress-corrosion cracking (IGSCC) was investigated in an aqueous solution of sodium thiosulphate at a load level below the yield point, whereas transgranular stress-corrosion cracking (TGSCC) was investigated in an aqueous solution of sodium thiocyanate at a load level beyond the yield point. No simultaneous AE activity increases, EN transients or elongation discontinuities were observed in the case of IGSCC. Except for a few EN transients, the signals were smoother than in the case of TGSCC, which could reflect the more continuous nature of IGSCC processes. This is also probably the reason that no simultaneous events were observed in this case. On the other hand, a significant increase in the DC part of the measured electrochemical current, corresponding in time with increases in elongation and, to some extent, also increases in AE activity, was observed in the second part of experiment. It was assumed that the current shift in the anodic direction was caused by an increase in the dissolving surface area due to the growth of cracks. On the other hand, on the basis of the simultaneous use of the three techniques, several single TGSCC events were detected. Detection was accomplished by the observation of simultaneous increases in AE activity, EN transients, and discontinuities (jumps) in elongation. On the basis of the time resolution of the measurements, it was concluded that the detected electrochemical events were the result of corresponding mechanical events. It was also concluded that the simultaneous use of EN and AE is a promising approach for the detection and characterization of SCC, but that further research and improvements of the measuring system are needed.

Keywords: stress corrosion cracking, electrochemical noise, acoustic emission, austenitic stainless steel

0 INTRODUCTION

Stress-corrosion cracking (SCC) is one of the most dangerous degradation processes to which metals can be subjected, because it can cause unexpected failures of structural elements without any previously visible signs [1] to [4]. The most exposed groups of metals are stainless steels and other alloys that exhibit good resistance to the general corrosion.

Stress-corrosion cracking is a process which causes the initiation and propagation of cracks by the simultaneous action of mechanical stress and corrosion reactions. In general, there are three different conditions that must be satisfied for the development of SCC: a material sensitive to SCC, a corrosion solution that causes localized corrosion, and a large enough tensile load (in most cases it can be below the yield point of material). Regarding propagation, SCC processes are divided into transgranular SCC (TGSCC) and intergranular SCC (IGSCC) modes. It is known that the TGSCC process advances with bigger discontinuous steps, while researchers do not agree about the discontinuity of IGSCC. It is only certain that the individual dissolution and fracture processes (steps) are much smaller than in the case of TGSCC. In the past, several different mechanisms describing TGSCC and IGSCC processes have been proposed. All these mechanisms show relatively good agreement for some special cases, but in general the alternating processes of dissolution and fracture

*Corr. Author's Address: Slovenian National Building and Civil Engineering Institute, Dimičeva 12, SI-1000 Ljubljana, Slovenia, jaka.kovac@zag.si

have not yet been precisely explained. One important reason for the insufficient knowledge of SCC processes are the measuring techniques for their detection and monitoring. Electrochemical measuring techniques can only provide the electrochemical components of the SCC process, whereas physical measuring techniques can only provide data about the physical parameters. Also, conventional electrochemical methods for monitoring corrosion processes (different types of potentiodynamic polarization, impedance spectroscopy, etc.) are not suitable for the detection and monitoring of SCC processes, since they can only estimate the susceptibility of the investigated system metal/corrosion solution to a certain type of corrosion. For these reasons, acoustic emission and electrochemical noise are promising techniques, which have been developed for the monitoring and characterization of SCC processes.

1 ELECTROCHEMICAL NOISE AND ACOUSTIC EMISSION, AND PREVIOUS RESEARCH

Electrochemical noise (EN) is a method that measures the fluctuations of current and potential between two electrodes. Three electrodes are needed for such measurements: a working electrode and two reference electrodes. Voltage is measured between the working electrode and one of the reference electrodes, whereas potential is measured between the working electrode and the other reference electrode. In our measurements all three electrodes were made from the same material, which means that not real reference electrodes (i.e. graphite electrodes) but "pseudo" reference electrodes were used.

Corrosion events on a single electrode are reflected in the measured current and voltage. In the case of three equal electrodes no net current flows and there is zero potential between the working and the reference electrode. When local anodic corrosion damage appears at the working electrode (i.e. breakage of the passive film, the initiation of pits, the formation of new surface during SCC), it results in a shift (turn) in the so-called anodic direction of the measured current and potential. Originated electrons then travel from the working electrode to the reference electrodes. If local anodic corrosion damage occurs at the reference electrode for current measurement, it is reflected in a shift of the measured current in the opposite direction – the cathodic direction (electrons travels away from the current reference electrode), and in a shift of the measured potential in the anodic direction. In the case of local corrosion damage occurring on the reference electrode for potential measurements, this is reflected in a shift of voltage in the cathodic direction. In reality it should be taken into account that only a part of the current is measured as described, because part of electrons can be used up at the same electrode where they were produced. This is possible because anodic and cathodic areas can be present on the same electrode. Consequently, only a very small part of the current which is a result of local corrosion damage can be measured, or no current is measured in the case that all electrons are used up on the same electrode. In such situations local corrosion processes are hardly detectable.

The main advantage of the EN method in comparison with the other electrochemical methods is its ability to monitor corrosion in a freely corroding system without any external excitation signals. This feature makes it possible to measure the development of the natural corrosion process. On the basis of fast changes (transients) in the measured current and voltage, the EN technique detects the initiation and development of corrosion processes.

Over last few decades electrochemical noise measurements have become one of the most promising methods for the detection and, to some extend can be used to, characterization of local corrosion processes [5] to [29]. Positive results have been obtained in various cases of localized corrosion. The method proved to be successful in the detection of unstable pitting corrosion [7] to [10], and in the detection of the transition from unstable to stable pitting corrosion [11] and [12]. The method has also been more or less successful in the case of crevice corrosion detection [10], [13] and [14]. Numerous measurements have been performed regarding the study of passive film formation and breakage processes [15], and also regarding the study of the effect of corrosion inhibitors on these processes [12], [16] and [17].

Many more or less successful EN measurements have also been performed in the study of SCC. The beginnings of the use of EN method for the detection of SCC, the first successful detection of SCC by EN measurements, and

differentiation between the cracking non-active and the cracking active periods, go back to the 1990's [18] to [20]. Over the next period researchers [21] to [30] succeeded in recognizing single characteristic events (transients) of EN and correlated these events with crack growth. Researchers [21] found that the observed EN transients corresponded in time with sudden drops in the simultaneous measured force on the specimen during tensile tests. In the research the velocity of crack propagation calculated from the measured force drop was compared with the current transients. It was found that the crack propagation velocity is proportional to the measured current. In our previous research [24] to [27], which was performed on stainless steel in thiosulphate solutions, EN measurements were compared with simultaneous measured elongation during SCC processes. A relation between the current transients and the simultaneously generated elongation rate was found. A similar approach was used by some other researchers using pre-cracked compact tension specimens [28] and [29]. In this research periodic fluctuations were observed, and it was assumed that these fluctuations were related to the periodic propagation of the crack.

The second method used was acoustic emission (AE) analysis. This analysis is based on measured acoustic emission, which is a consequence of the fast energy relaxation that occurs at a localized source (i.e. crack development in the material). This relaxation of energy causes a development of elastic waves that propagate through the material and can be detected by piezoelectric sensors. The analysis of acoustic emission, whose purpose is to detect elastic waves, was developed in the 1960's, and since then it has developed into one of the most successful methods for the nondestructive monitoring of the initiation and progress of deformations in materials [31] to [33]. Besides use for the detection and research of mechanical defects, as well as other energy changes in materials [31] to [36], it has also been developed for the characterization and detection of chemical processes (corrosion) [33], and the monitoring of manufacturing processes [33], [37] and [38].

It is characteristic that the AE signal which is captured by the piezoelectric sensor consists of oscillating voltages, which quickly rise to the maximum level, and then drop back slowly to the previous level. Signals or AE events are caused by desired events (i.e. crack propagation) and undesired events (i.e. instrumental noise, external noise). Due to the large number of AE events, a trigger level which is a measure for the intensity of events is defined for each measurement. Only signals with an intensity above the trigger level are captured, whereas other signals are eliminated. The number of AE events is estimated on the basis of the captured signals. During such characterization various problems occur: the summation of signals from different events, and the capturing of undesired signals that are the consequence of reflected waves and noise signals from the surroundings. Not only are some undesired signals captured, but also some useful signals are lost due to the described way of measuring.

Regarding the detection and characterization of SCC, AE analysis can be used for the detection of mechanical events, as opposed to EN, which detects electrochemical events. In the SCC process mechanical and electrochemical events are related to one other, so the combination of AE and EN could be the best tool for the detection and characterization of SCC. The main idea of the combined use of AE and EN is the simultaneous monitoring of SCC using both techniques, and the search for a relation between the mechanical and electrochemical components of crack formation. The aim of the simultaneous use of both methods is also to differ between the transients caused by SCC, and the EN transients caused by other corrosion events (i.e. the initiation of corrosion pits).

Several successful investigations, which used AE for the detection and characterization of SCC, have been realized in the past [39] to [43]. One of the first investigations of SCC by means of AE was performed by Newman and Sieradzki, who are known as pioneers in the field of SCC detection. They looked for correlations between measured AE and EN signals. Experiments were performed on three different systems, and positive results were obtained in the experiment performed on brass [39]. At that time several AE experiments during SCC in different systems showed mixed results [40]. Later Jones investigated different types of cracking by using AE analysis on various materials, and TGSCC was successfully detected in this research [40]. On the other hand, results concerning IGSCC were not so successful. Jones proposed that some transgranular fracture surfaces were the result of

ligaments that fracture behind the advancing intergranular crack front, and that most of the detected AE signals were the result of the transgranular part of the fracture. In a continuation of this research it was established that the AE technique can reliably detect intergranular stress corrosion cracks of 200 to 300 μm length and at a depth of 100 to 200 μm [41]. Some other researchers have also agreed with Jones's findings. They also successfully detected TGSCC, whereas the detection of IGSCC was described as problematic. Researchers assumed that the AE signal during IGSCC comes from small individual parts of the crack that have a transgranular nature [42]. In this research it was established that pure anodic dissolution does not generate observable AE signals. Several researchers [43] have found that AE activity due to the SCC process during tensile tests is the highest immediately after the yield point is reached and during final fracture.

In our previous research [27], characteristic EN transients were compared with simultaneous measured elongation events (discontinuous jumps). In order to measure these events even more precisely, and to estimate the sequences of electrochemical and mechanical events, a combination of EN and AE was used in this research. At the same time elongation of the specimen exposed to SCC processes was also measured. Analysis of the results from all three types of measurements was performed with aim of detecting the processes in the case of transgranular and intergranular SCC, as well as to get the basic characteristic of the EN and AE signals which were generated during both types of SCC, and thus to explore the possibility of detecting and characterizing different types of SCC with EN and AE measurements. The main emphasis was on the simultaneous use of the three methods, and on the analysis of the simultaneously measured signals obtained using these methods.

2 EXPERIMENTAL

The experiments were carried out in a corrosion cell that was filled with a corrosion solution (Fig. 1 - left). Three electrodes made from the same material were sealed in the corrosion cell.

The middle electrode had the shape of a tensile specimen and was loaded during the experiment. The other two electrodes were straight, with a constant quadratic cross-section along the entire length of the electrodes. No mechanical stress was applied to them during the experiment. These two electrodes were used as pseudo reference electrodes for the EN measurements. An apparatus with a rigid frame was used for the constant load application (Fig. 1 - right). The tensile specimen was fixed between two movable jaws that were fixed to the rigid frame. An arm with weights was fixed to the bottom jaw. Weights were added or removed so

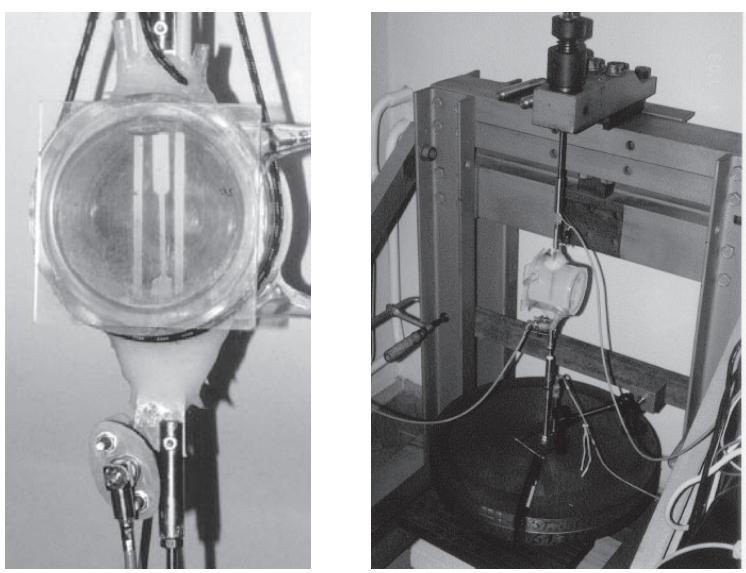

Fig. 1. *Left) The corrosion cell, inside which three electrodes can be seen. The middle electrode with the reduced cross-section is the working electrode. The AE sensor is fixed to the lower end of the working electrode. Right) The tensile testing apparatus. The elongation meter is fixed to the frame of the apparatus.*

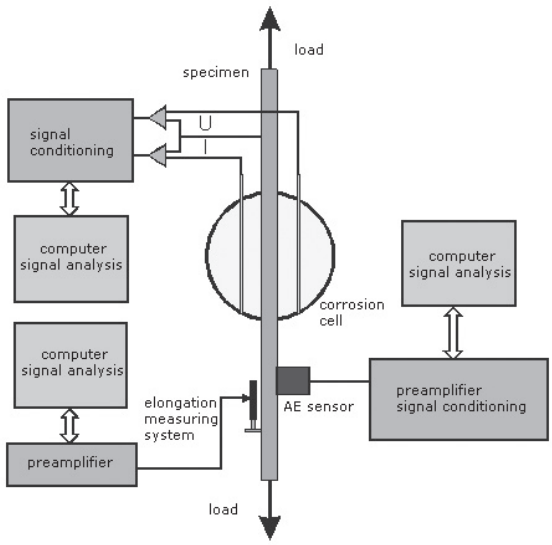

Fig. 2. *Schematic view of the experiment and of all three measuring systems*

that the desired load was achieved. The upper jaw was fixed to the top of the metallic frame. The distance between the lower and upper jaws could be adjusted by means of a spindle, which also transferred the load to the tensile specimen. The apparatus stood on a rubber support plate, which enabled electrical isolation from the neighbourhood, and also damped unwanted vibrations. The tensile specimen was additionally electrically isolated from its surroundings by means of non-conducting plugs. All the mobile elements of the apparatus were tightly screwed into the desired position, so that no unwanted oscillations could disturb the experiment.

Measurements were performed with the three different measuring systems simultaneously (Fig. 2), and the specimens were monitored up until failure. EN was measured in a freely corroding system. The current was measured between the working electrode (tensile specimen) and one of the reference electrodes with a zero resistance ammeter (ZRA), whereas voltage was measured between the working electrode and the other reference electrode with a high-impedance voltmeter. The measured current and potential were amplified and digitalized using a 16-bit A/D converter. The sampling rate for EN data collection was 10 Hz. The resolution of the measured current was 3 nA, and 30 μV for measured voltage.

A piezo-electric sensor, which was fixed to the bottom part of the working electrode outside the corrosive cell, was used for the AE measurements. Amplification of the AE measuring system was 56 dB. The maximum amplitude was 10 V. The signal was captured with a frequency of 250 kHz. In order to eliminate low-frequency disturbances, the signal was filtered by means of a high-pass filter with a cut-off frequency of 50 kHz. Since the duration of the measurements was, in many cases, several tens of hours, selection of data was performed by using a simple auto-detection function: when a signal exceeded a trigger level, the system started to store the signal for 1 s. An instrument-based noise of 0.008 V was determined, and signals higher than 0.01 V (the trigger level) were stored. The stored packets of AE were afterwards analysed using Matlab software, and compared with the simultaneous measurements of EN and elongation.

Elongation of the tensile specimen was measured by means of an inductive probe fixed to the weights that were hung directly on the tensile specimen. Resolution of the elongation measuring system was 1 μm, but only changes larger than 2 to 6 μm (taking into account the presence of noise during individual measurements) were stored. The size of the stored changes was defined for each case individually taking into account the present noise. Two individual experiments are presented in this paper. The minimum size of the stored changes was 2 μm in the first experiment, and 6 μm in the second experiment.

The surfaces of the working and reference electrodes that were exposed to the corrosive medium, as well as the fracture surfaces of fracture, were examined after the experiment was finished. Visual and scanning electron microscope inspection techniques were used.

The specimens were made from austenitic stainless steel type AISI 304. The material was treated before the specimens were produced in the following manner: 1) heated to 1050°C, kept at this temperature for 1 hour - water quenched, 2) heated to 650°C in a nitrogen atmosphere, kept at this temperature for 24 hours, cooled down in air. Such heat treatment causes the growth of austenitic grains, which in our case had a size of approximately 250 μm. Chromium carbides $Cr_{23}C_6$ were precipitated at the grain boundaries. It is known [44] that the described microstructure is very sensitive to SCC processes.

The experiments were performed in two different corrosive solutions, and at two different load levels: 1) in a diluted 0.5 M aqueous solution of sodium thiosulphate ($Na_2S_2O_3$), at a load -corresponding to

approximately 85 % of the yield point of the material, 2) in a diluted 1.4 % aqueous solution of sodium thiocyanate (NaSCN), at a load corresponding to approximately 90 % of the tensile strength of the material. In the first case stress-corrosion cracks propagated mainly across the crystal grains – TGSCC, whereas in the second case cracks were propagated along the crystal boundaries - IGSCC.

3 RESULTS AND DISCUSSION

In the interpretation of the results, sudden changes in all three measured signals (fluctuations, discontinuities) were mainly inspected. It was expected that the characteristics of IGSCC and TGSCC could be described on the basis of analyses of simultaneous events.

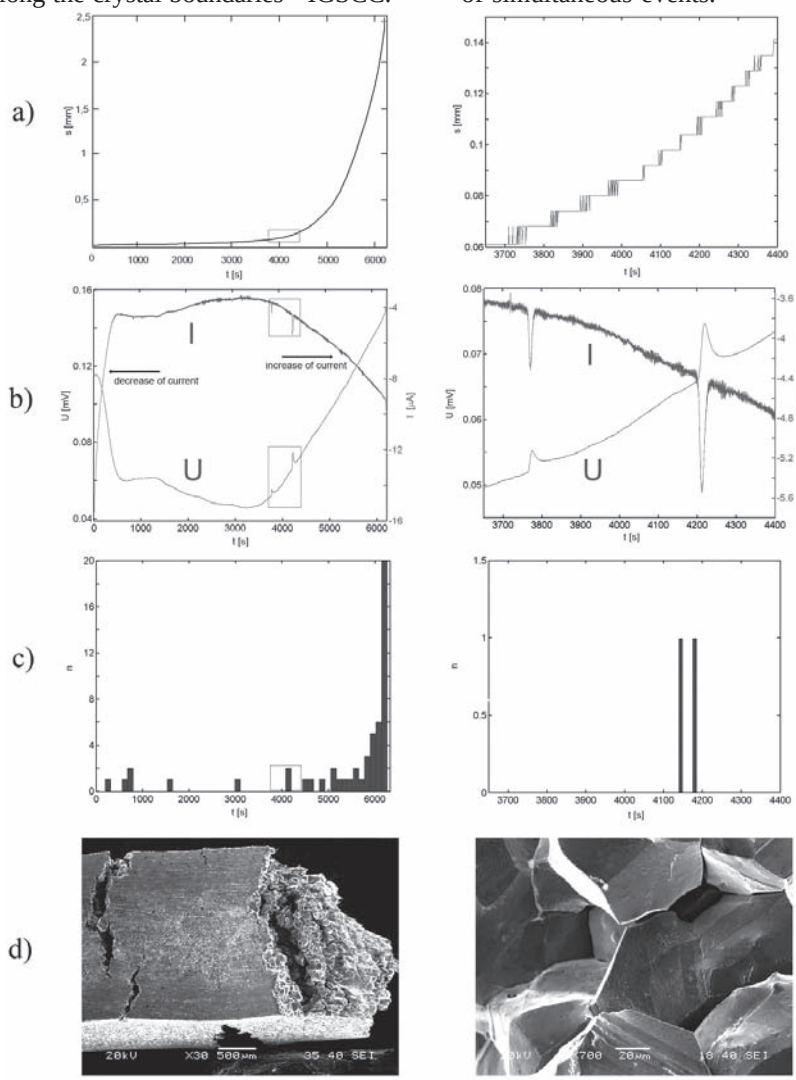

Fig. 3. *Results of measurements during intergranular stress-corrosion cracking of the heat treated stainless steel AISI 304: a – left) entire elongation (l), a – right) enlarged detail from the left-hand diagram (the detail is marked with a frame in the left-hand diagram), b – left) EN: potential and current for the entire measurement, b – right) enlarged detail from left-hand diagram (the detail is marked with a frame in the left-hand diagram) with two events, c – left) AE histogram: number of AE events (n) for the entire measurement, c – right) enlarged detail from the left-hand diagram (the detail is marked with a frame in the left-hand diagram) with the finest division of events in the time intervals (shorter time intervals), d – left) SEM image of the specimen surface with a magnification of 30x, and d – right) SEM image of the fracture surface with a magnification of 700x.*

Typical results of all three measuring techniques during the entire duration of the experiment carried out in a diluted aqueous solution of $Na_2S_2O_3$ are presented in the left-hand diagrams in Figure 3. On the right-hand side of Figure 3 there is an enlarged time detail from the last part of the experiment. The first diagram (Fig. 3a – left) shows an elongation measurement, which was monitored together with AE and EN in order to obtain a better understanding of the deformation processes during the experiment. It can be seen that the elongation increased uniformly, without any sudden jumps that could be expected due to sudden crack propagation or opening. In this case the elongation measurement did not provide useful information about individual events. In the first part (the first 500 seconds) of the measured EN signals (Fig. 3b – left), a large decrease in the measured current can be seen, which was the consequence of passive film growth on the surface of electrodes. The passive film protects the surface of the electrodes against the corrosion, resulting in a smaller corrosion current. In the last part of the measurement a large increase in the DC component of the measured current can be seen. This increase could be related to the initiation and growth of cracks. Also in the last part of the experiment (40 minutes before failure) two typical EN transients (Fig. 3b – right), which could be related to individual SCC events, were detected. However, these transients did not correspond in time with increases in AE activity (Fig. 3c – right), or with any observable sudden increase in elongation. The observed EN transients could have been generated by alternating dissolution at the crack tip (according to the slip-dissolution model [45]), but it is more probable that they were generated by the initiation of pits [6] to [10], which were observed on all electrodes after the experiment was finished. The AE signal did not show any sudden increases in AE activity, but the AE activity increased monotonically and approximately exponentially until failure. For these reasons individual events could not be determined from the presented simultaneous measurements.

In order to determine the prevailing mode of cracking and to characterize the intensity of the process, analysis of the specimen's surface (Fig. 3d – left) and fracture (Fig. 3d – right) were performed using a scanning electron microscope. It was found that a good two-thirds of the fracture was brittle and that less than one third was ductile. Fractographic analysis of the brittle part of the fracture showed that it was caused by propagation of the main intergranular crack. On the other parts of the specimen quite a lot of large cracks propagating perpendicular to the load direction were observed. Some of these large cracks can be seen on the left-hand side of Figure 3d.

From the description above it can be concluded that despite the great number of cracks observed in the case of IGSCC, the detection of individual crack formation or crack growth steps was not successful. This indicates that the process is probably fairly smooth or continuous. On the other hand a relationship between the DC component of the electrochemical current, AE activity and elongation was established. For this reason it can be assumed that these techniques enabled monitoring of the cumulative process of IGSCC.

More information about individual SCC events was obtained by analyzing the three types of measurements during the SCC of specimens exposed to a dilute aqueous solution of NaSCN. Typical results across the entire duration of the experiment are presented in the left-hand diagrams in Figure 4. On the right-hand of Figure 4 is an enlarged time detail from the last part of the experiment, before failure. The characteristics of the measured EN, AE signals and elongation are rather different than in previous case. It can be clearly seen that in this case the signals are much less smooth and more variegated. Also, the duration of the experiment was much longer than in the previous case, although the load level was higher (above the yield point) in this experiment. Two significant increases in the elongation can be seen in the elongation measurements (Fig. 4a – left). The increase in elongation at the beginning of the measurement was probably due to plastic deformation or yielding of the specimen, which was loaded beyond its yield point. The final increase in elongation was the result of final fracture. Two bigger jumps (discontinuities) in the elongation increase can also be seen before the final increase of elongation. In the first part (the first two hours) of the measured EN signal (Fig. 4b – left) a large decrease in the measured current can be seen, which is, as in the previous experiment, a consequence of passive film growth on the surfaces of the electrodes. After the initial decrease, the current stabilized, and did not increase as in case of IGSCC.

Two characteristic events, which are more pronounced in the potential measurement than in the current measurement, can be seen in the last part of the experiment, before fracture. Both events occurred together with the above mentioned discontinuities in the elongation (Fig. 4a) and with the increases in AE activity (Fig. 4c). The highest AE activity was expected to be observed at the fracture, as it was in the case of IGSCC. In Figure 4c an increase in AE activity in the last part of measurement can be seen, but the AE activity was not the highest when fracture occurred. The AE activity was also somewhat higher at the beginning of the measurement. This increase was probably the result of specimen's plastic deformation immediately after loading, which also caused

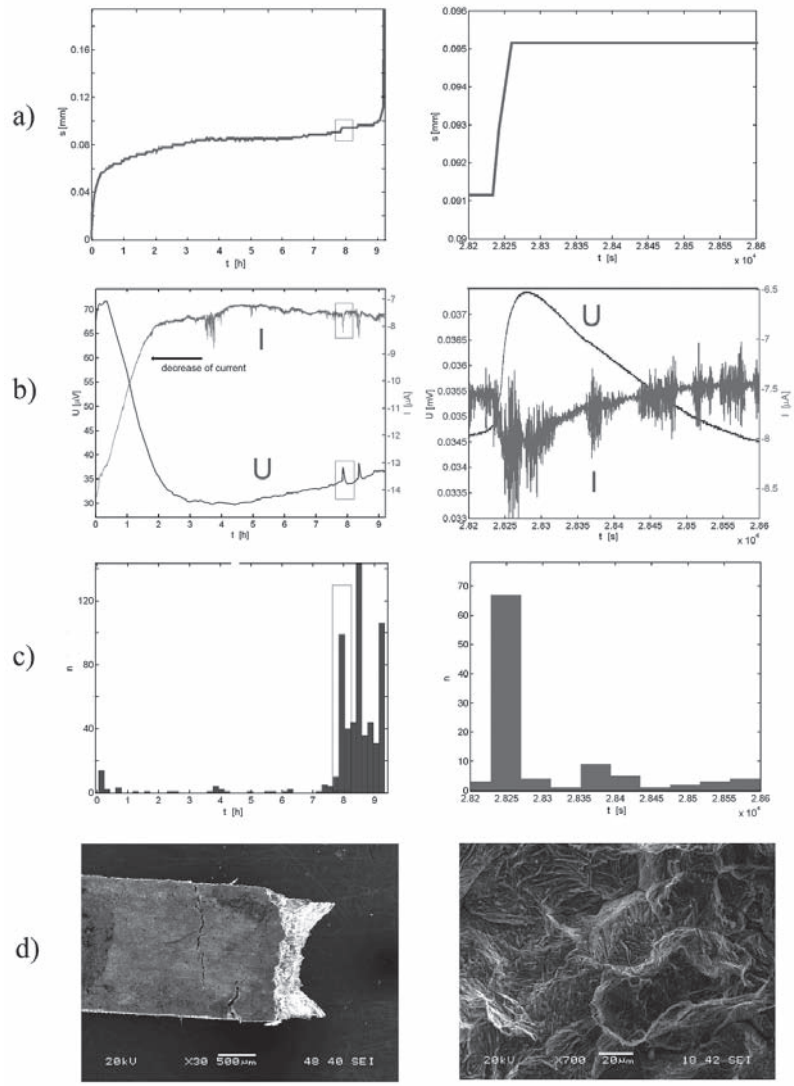

Fig. 4. *Results of measurements during intergranular transgranular stress-corrosion cracking of the heat treated stainless steel AISI 304: a – left) entire elongation (l), a – right) enlarged detail from the left-hand diagram (the detail is marked with a frame in the left-hand diagram), with an elongation jump, b – left) EN: potential and current for the entire measurement, b – right) enlarged detail from left diagram (the detail is marked with a frame in the left-hand diagram) with a characteristic event, c – left) AE histogram: number of AE events (n) for the entire measurement, c – right) enlarged detail from the left-hand diagram (the detail is marked with a frame in the left-hand diagram) with the finest division of events in the time intervals (shorter time intervals), d – left) SEM image of the specimen surface with a magnification of 30x, and d – right) SEM image of the fracture surface with a*

growth of the elongation over the same time interval.

On the right-hand diagrams of Figures 4a, b, c, a typical SCC event detected by all three systems can be seen. On the basis of the measurement results (presented in Fig. 4), and taking into account the resolution of the measurements, it can be concluded that mechanical events occurred first. These mechanical events caused the occurrence of new surface, and were detected as a sudden increase in elongation, combined with a simultaneous increase in AE activity. At the same time a sudden decrease in current, and an increase in potential, followed in both cases by a slower return to the initial levels, was observed. Such a shift of the EN signals in the anodic direction (from the point of view of the working electrode), and its return to the initial levels, is characteristic for the occurrence and passivation of new surface at the crack tip during crack propagation. The analysis showed that not all EN transients were accompanied by increases in AE activity and elongation (Fig. 4). These characteristic events were probably generated by the initiation of pits. The presence of pits on the surfaces of the specimens was confirmed by visual and SEM inspection after each experiment. On the other hand, no AE activity increases and sudden jumps of elongation were found without accompanying EN transients, meaning that, in the case of the selected parameters, no significant noise occurred in the results of the AE and elongation measurements. It needs to be stressed that the measured elongation jumps were very small and close to the limit of the resolution of the measuring system. Thus it would be very difficult to predict the growth or opening of cracks just on the basis of detected elongation jumps, without corresponding increases in AE activity. An important fact is also the reduced resolution due to the elimination of noise, because of which some useful signals were probably not captured. This was most likely in the case of the AE measurements, where it was very difficult to set a proper trigger level above which signals should be stored. This is also probably the most important reason that the number of observed cracks on the specimen was larger than the number of detected events, which were characteristic for the development of cracks.

As in the previous case, analysis of the surface of the specimen (Fig. 4d – left) and of the fracture (Fig. 4d – right) was performed using a scanning electron microscope after the experiment had finished. It was found that a little less than two thirds of the final fracture was completely brittle, caused by the SCC process, whereas a little more than one third was a ductile fracture, caused by specimen overloading due to the reduced cross-section. Besides the main crack that caused failure of the specimen, also two bigger cracks and several small cracks were observed during the analysis (Fig. 4d – left). These cracks propagated perpendicular to the loading direction. From the observations it was assumed that all the cracks, except the three major ones, stayed in the initial phase, and did not propagate further. Fractographic analysis of the fracture surface showed that the larger part of the fracture caused by SCC was transgranular – the crack propagated across the crystal grains. TGSCC on the austenitic stainless steel could be described by the slip-dissolution model. The model consists of two main processes: dissolving at the crack tip, and a mechanical event – slip of the crystal planes [45]. These two processes act alternately, so that the propagation of the crack is probably non-uniform or discontinuous. The results of our measurements indicate this manner of cracking, because from the typical shapes of the signals from all three measuring techniques, a discontinuous process can be assumed.

From the results of the measurements and analysis of the two different experiments a question arises how big is the possibility for the detection of individual event during IGSCC with the simultaneous use of AE and EN. As has been previously mentioned, TGSCC is clearly a discontinuous process, which can be detected by measurements of AE and EN, which has also been shown in the case of our measurements. On the other hand, the results of the measurements indicated that IGSCC is a much more continuous process, although it is believed that it is not completely continuous. This is also in agreement with the results of some other researchers [40] and [41], who are also convinced that IGSCC is not a completely continuous process. However, researchers have stressed that the detection of IGSCC by means of AE is not reliable due to the very small amount of energy that is relaxed during deformation. The relaxed energy could be below the detection limit of the measuring method.

Interpretation of EN results for the IGSCC process is also difficult. As has been mentioned in the introduction cathodic surfaces in long cracks can be located on the crack walls or close to the mouth of crack. In such cases the measured electrochemical current represents only a small proportion of the total corrosion current, so that small events are probably undetectable. Some researchers have tried to avoid this problem by using of so-called compact tension specimens, where most parts of the specimen is protected by means of an anticorrosion coating, and only the active crack is exposed to the electrolyte [29] and [30]. In this case, the coupling current between the CT specimen and the electrode placed directly ahead of the crack mouth is measured. But even in this case cathodic surfaces are not completely eliminated, and the distribution of the current is not completely clear.

Even though our measurements of EN and AE during IGSCC processes did not detect individual characteristic SCC events (Fig. 3), which at the same time proves the statement that IGSCC progresses more continuously than TGSCC, the nature of the IGSCC process can be partly described from the main characteristics of all three measurements. In the last part of this experiment (Fig. 3b) the DC component of the measured electrochemical current increased monotonically, whereas the DC component of the electrochemical current in the TGSCC experiment was more or less constant (Fig. 4b). This observation is in agreement with those of some other authors [28-30], who also found a similar increase in the DC component of the measured current, and an absence of characteristic EN events. The increase of current in the anodic direction was probably the consequence of new anodic surface formation occurring at the crack tip. On the basis of the increasing current, it can be assumed that the rate of new surface formation, and thus the propagation of the crack, increased until the final fracture, or that at the same time the number of cracks, and thus the number of new anodic surfaces at the crack tip, increased. This assumption was additionally confirmed by the approximately simultaneous increase in elongation (Fig. 3a – left), which was a consequence of crack growth or opening, and also partly confirmed by the increase in AE activity in the last part of the experiment, which showed an approximately exponential increase until the failure of specimen. The increased AE activity in the last part of the experiment was probably generated by plastic deformation of the specimen, caused by passing the yielding point due to crack propagation that reduced the cross-section of the specimen. The second possibility for the generation of AE events was mechanical breakage of ligaments at the crack tip. On the basis of our research, it cannot be confirmed that AE signals are a consequences of the first, second or both processes, but based on previous experience it can be assumed that the first mentioned source of AE is more probable. Further research is needed to confirm our observations, to determine the prevailing source of AE during IGSCC, and to eliminate the possibility that the increasing current was caused by the initiation and growth of pits. From the measurements during IGSCC it was additionally observed that the increasing signals (the DC component towards the end of measurement, AE activity and elongation) were fairly smooth. This indicates smaller steps in the IGSCC process, and grater continuity of the process in comparison with the TGSCC process.

4 CONCLUSIONS

The possibility of the combined use of EN and AE for the detection and characterization of different types of SCC was investigated on the basis of experiments performed on austenitic stainless steel. AE and EN were measured simultaneously. Additionally, elongation of the specimens was measured simultaneously. On the basis of the presented results from the AE, EN and elongation measurements, it was established that the successfulness of the used AE and EN methods strongly depends mainly on the type of SCC.

Detection was only partly successful in the case of IGSCC. Some specific EN events were detected, but they did not correspond in time with changes in elongation or changes in AE activity, that these EN events could not be related to individual SCC events. On the other hand, a constant increase in the DC component of the measured current was detected in the second half of the experiment. It is believed that this shift in the current was the result of new anodic surface being formed at the crack tip. This assumption cannot be proved because the EN measurements cannot reliably distinguish between the propagation of intergranular cracks with dissolution, and the

growth of stable pits or crevices. However, the above statement can be supported by the simultaneously observed increase in elongation and the approximately simultaneous increase in AE activity. However, the exact source of the AE during IGSCC cannot be determined from the results of the measurements. Based on previous experience, it is believed that the plastic deformations caused by the reduced cross-section are more probable sources of AE than mechanical breakages of ligaments at the crack tip. The main reason that no individual simultaneous events were detected probably lies in the way of progress of IGSCC the processes. This is because these processes advance relatively continuously, which is also reflected in the greater smoothness of the measured signals.

The detection of TGSCC with the simultaneous use of all three measuring techniques was more successful. During the TGSCC processes several simultaneous AE, EN and elongation events that were assigned to the SCC process were detected. Taking into account the time resolution of the measurements, it was concluded that the mechanical events occurred first. These mechanical breakages at the crack tip were detected by a sudden increase in elongation and a simultaneous increase in AE activity, whereas the following rapid fluctuations in current and potential were the consequence of the occurrence and passivation of a new surface at the crack tip.

It can be concluded that the detection of an individual SCC event by simultaneous measurements of EN and AE depends mainly on the discontinuity of the SCC processes. For this reason the detection of the more discontinuous TGSCC process is more reliable than the detection of the more continuous IGSCC process. Simultaneous use of the three techniques in the case of TGSCC makes it possible to obtain information about sequences of electrochemical and mechanical events, as well as information about the characteristics of these events. On the basis of the results so far obtained, it is expected that, with certain improvements to individual measuring systems, it would be possible to detect individual events of IGSCC, besides the monitoring of the cumulative progress of the IGSCC process. On the basis of the measurements some new data about SCC processes could be obtained, and this information would contribute to a better understanding of SCC mechanisms.

5 REFERENCES

[1] Gangloff, R.P., Ives, M.B. (Eds.). *Environmental-induced cracking of metals*. Houston, Texas: NACE Publication, 1990.

[2] Jones, R.H. *Stress-corrosion cracking – Material performance and evaluation*. ASM International Materials Park, 1992.

[3] Baboian, R., et al. (Eds.). *Corrosion tests and standards: Application and interpretation*. Philadelphia, PA: ASTM Publication, 1995.

[4] Liu, A. F. *Structural life assessment methods*, Ohio: ASM international, 1998.

[5] Kearns, J.R., Scully, J.R., Roberdge, P.R., Reichert, D.L., Dawson, J.L. (Eds.). *Electrochemical noise measurements for corrosion applications*, STP 1277. Philadelphia, PA: ASTM Publication, 1996.

[6] Isaacs, H., Bertocci, U., Kruger, J., Smialowska, S. (Eds.). *Advances in localized corrosion*. Houston, Texas: NACE International, 1990.

[7] Frankel, G.S., Stockert, L., Hunkeler, F., Boehni, H. Metastable pitting of stainless steel. *Corrosion*, 1987, 43, p. 429-436.

[8] Burstein, G.T., Mattin, S.P. Nucleation of corrosion pits on stainless steel. *Philosophical Magazine Letters*, 1992, 66, pp. 127-131.

[9] Legat, A., Dolecek, V. Chaotic analysis of electrochemical noise measured on stainless steel. *J. Electrochem. Soc.*, 1995, 142, p. 1851-1858.

[10] Yang, M.Z., Wilmott, M., Luo, J.L. Analysis of the electrochemical noise for localized corrosion of type A516-70 carbon steel. *Corrosion*, 1998, 54, p. 869-876.

[11] Lunt, T.T., Pride, S.T., Scully, J.R., Hudson, J.L., Mikhailov, A.S. Cooperative stochastic behavior in localized corrosion. *J. Electrochem. Soc*., 1997, 144, p. 1620-1629.

[12] Legat, A., Osredkar, J., Kuhar, V., Leban, M. Detection of various types of corrosion processes by the chaotic analysis of electrochemical noise. *Mater. Sci. Forum*, 1998, 289-2, p. 807-811.

[13] Conde, A., Williams, D.E. Crevice corrosion and pitting detection on 304 stainless steel using electrochemical noise. *Mater. Corros.*, 1999, 50, p. 585-590.

[14] Wharton, J.A., Mellor, B.G., Wood, R.J.K., Smith, C.J.E. Analysis of electrochemical potential noise measurements on type 304 stainless steel in chloride solutions. *J. Electrochem. Soc.*, 2000, 147, p. 3294-3301.

[15] Kolman, D.G., Gaudett, M.A., Scully, J.R. modeling of anodic current transients resulting from oxide Rupture of plastically strained b + a titanium. *J. Electrochem. Soc.*, 1998, 145, p. 1829-1840.

[16] Yang, M.Z., Wilmott, M., Luo, J.L. Crevice corrosion behavior of A516-70 carbon steel in

solutions containing inhibitors and chloride ions. *Thin Solid Films*, 1998, 326, p. 180-188.

[17] Schneider, M., Galle, K., Pohl, H. Inhibitor efficiency inside small crevices investigated by electrochemical noise analysis. *Mater. Corros.*, 2003, 54, p. 966-973.

[18] Newman, R.C., Sieradzki, K., Woodward, J. in: A. Turnbull (Eds.). Current fluctuations during transgranular stress-corrosion cracking. *Proceedings of the Conference on Corrosion Chemistry within Pits, Crevices and Cracks, NPL*, Teddington, Middlesex, 1987, p. 203-212.

[19] Loto, C.A., Cottis, R.A. Electrochemical noise generation during stress corrosion cracking of alpha-brass, *Corrosion*, 1987, 43, p. 499-504.

[20] Loto, C.A., Cottis, R.A. Electrochemical noise generation during stress corrosion cracking of the high-strength aluminum AA 7075-T6 alloy. *Corrosion*, 1989, 45, p. 136-141.

[21] Flanagan, W.F., Wang, M., Zhu, M., Lichter , B.D. A fully plastic microcracking model for transgranular stress-corrosion cracking in planar slip materials, *Metall. Mater. Trans. A*, 1994, 25, p. 1391-1401.

[22] Wells, D.B., Stewart, J., Davidson, R., Scott, P.M., Williams, D.E., SCC of steel in dilute thiosulphate solution. *Corros. Sci.*, 1992, 33, p. 39-71.

[23] Watanabe, Y., Kondo, T. Current and potential fluctuation characteristics in intergranular stress corrosion cracking processes of stainless steels. *Corrosion*, 2000, 56, p. 1250-1255.

[24] Leban, M., Legat, A., Dolecek, V., Kuhar, V., Electrochemical noise as a possible method for detecting stress-corrosion cracking. *Mater. Sci. Forum*, 1998, 289-2, p. 157-161.

[25] Leban, M., Dolecek, V., Legat, A. Comparative analysis of electrochemical noise generated during stress corrosion cracking of AISI 304 stainless steel. *Corrosion*, 2000, 56, p. 921-927.

[26] Leban, M., Legat, A., Dolecek, V. Electrochemical noise during non-stationary corrosion processes. *Mater. Corros*., 2001, 52, p. 418-425.

[27] Leban, M., Bajt, Z., Legat, A. Corrosion processes of steel in concrete characterized by means of electrochemical noise. *Electrochim. Acta*, 2004, 49, p. 2795-2801.

[28] MacDonald, D.D. Fate of the coupling current in stress corrosion cracking – Mechanistic and corrosion control implications. *CORROSION 2004 Conference*, New Orleans, Paper No. 04570.

[29] Gomez-Duran, M., MacDonald, D.D. Stress corrosion cracking of sensitized type 304 stainless steel in thiosulphate solution. II. Dynamics of fracture. *Corrosion Science*, 2006, 48, p. 1608-1622.

[30] Aballe, A., Newman, R.C., Cottis, R.A. Electrochemical noise study of stress corrosion cracking of sensitized 304H in thiosulfate. *CORROSION 2003 Conference*, San Diego, Paper No. 03403.

[31] Grabec, I. Acoustic emission. *Stroj. vestn.- Journal of Mechanical Engineering*, 1975, 3-4, p. 41-48. (In Slovenian).

[32] Nicholas, R.W. *Acoustic emission*, London: Applied Science Publishers Ltd, 1976.

[33] Miller, R.K., Hill, E., Moore, P.O. *Nondestructive testing handbook*, 3rd ed., Vol. 6, Acoustic emission testing. Ohio: American Society for Nondestructive Testing, Inc., 2005.

[34] Grabec I. Relation between development of defects in materials and acoustic emission. *Ultrasonic*, 1980, 18 (1), p. 9-12.

[35] Možina, J. *Acoustic emission induced by energy changes on metal surface*, PhD Thesis. University of Ljubljana, Faculty of Mechanical Engineering, 1980. (In Slovenian).

[36] Bajt, Ž. *Detection of cracking of construction elements with help of acoustic emission technique*, Master's Thesis. University of Ljubljana, Faculty of Civil and Geodetic Engineering, 1980. (In Slovenian).

[37] Grabec, I., Govekar, E., Susič, E., Antolovič, B. Monitoring manufacturing processes by utilizing empirical modeling. *Ultrasonics*, 1998, 36 (1-5), p. 263-271.

[38] Govekar, E., Gradišek, J., Grabec, I. Analysis of acoustic emission signals and monitoring of machining processes. *Ultrasonics*, 2000, 38 (1-8), p. 598-603.

[39] Newman, R.C., Sieradzki, K. Corrosion of acoustic and electrochemical noise in the stress corrosion cracking of a-brass. *Scripta Metall. Mater*., 1983, 17, p. 621-624.

[40] Jones, R.H., Friesel, M.A., Gerberich, W.W. Acoustic Emission from intergranular subcritical crack growth. *Metall. Trans.* A, 1989, 20, p. 637-648.

[41] Jones, R.H., Friesel, M.A., Pathania, R. Evaluation of stress corrosion cracking initiation using acoustic emission. *Corrosion*, 1991, 47, p. 105-115.

[42] Munch, E., Duisabeau, L., Fregonese, M., Fournier, L. Acoustic emission detection of environmentally assisted cracking in zircalloy-4 alloy. *EUROCORR 2004 Conference*, Nice.

[43] Van Nieuwenhove, R., Bosch, R.-W. Acoustic emission detection during stress corrosion cracking at elevated pressure and temperature. *J. Acoustic Emission*, 2000, 18, p. 293-299.

[44] Vehovar, L. *Corrosion of metals and corrosion tests*. Ljubljana: self-publishing house, 1991. (In Slovenian).

[45] Newman, R.C. Developments in the slip-dissolution model of stress corrosion cracking. *Corrosion*, 1994, 50, p. 682-686.

Strojniški vestnik - Journal of Mechanical Engineering 54(2008)1, 37-48
UDC 658.5:669.712
Paper received: 27.12.2006
Paper accepted: 28.9.2007

Production Scheduling Model in Aluminium Foundry

Gordana Matičević[1,*] - Niko Majdandžić[1] - Tadija Lovrić[2]
[1]University of Osijek, Mechanical Engineering Faculty, Croatia
[2]ININ Ltd., Croatia

There are numerous methods and strategies for production management which are successfully implemented in the metal industry and in the automobile and machine tools industry in particular. However, little research has been published regarding scheduling foundry operations. Therefore, the main goal of this paper is to develop a new mathematical model for scheduling foundry operations based on the MRP II (Manufacturing Resource Planning), JIT (Just in Time) and OPT (Optimized Production Technology) concepts. The research strategy includes a review of available literature and integration of the developed mathematical model into a foundry for testing the model with real data. The proposed model is successfully implemented into the ERP (Enterprise Resource Planning) system of Aluminium Ltd. in Mostar. The conclusions offered in this paper are based on the results of the tests carried out in that single foundry so that further work is required to validate the findings at other foundries and other manufacturing areas.

Keywords: aluminium production, scheduling, mathematical models, tardiness minimization

0 INTRODUCTION

In today's competitive industrial environments the main goal of a company is to earn profit. Meeting customer demands completely and in time and offering them high-quality products is a must if the goal is to be reached. Among other factors the existence of a good and effective planning and scheduling system is a major precondition to achieve the necessary competitiveness and fulfil the given task. But the planning and scheduling issues are very complex because of the ever changing needs of customers and the existing constrains in different manufacturing fields, including the metal industry. Therefore, researches have been conducted aimed at finding the solution to the problem.

The research carried out by Van Voorhis and Peters [1] about production system practices of steel foundries in the USA has pointed out that there is no widely accepted software system that has essentially solved the problem of generating pouring schedules for steel foundries. According to the research, only a few foundries used software to assist in scheduling, while most of them schedule operations manually [1] to [3]. Therefore, there is a need to address this problem by developing a new mathematical model and software for pouring scheduling. The paper proposes a mathematical model to find a feasible pouring schedule based on the MRP II (Manufacturing Resources Planning), JIT (Just in Time) and OPT (Optimized Production Technology) concepts. The proposed model was implemented into the ERP (Enterprise Resource Planning) system of Aluminium Ltd. in Mostar and successfully applied for the furnace and pouring scheduling. Section 1 of the paper gives a review of literature, section 2 describes the problem and the mathematical model of pouring scheduling. Section 3 deals with the results of the model implementation into the ERP system by the system screenshots. Section 4 gives the conclusions and ends the paper.

1 LITERATURE REVIEW

1.1 General Production Scheduling Problem

Special attention has been given to scheduling problems ever since the fifties of the last century. Following the appearance of Gantt chart a number of papers has been published that discuss the models and methods for solving scheduling problems. In the literature on production planning and scheduling various models and methods are used: mathematical programming, e.g. [4] to [8], and artificial intelligence, e.g. [9] to [11], [49] and [50]. The models mentioned in literature can be classified as deterministic and stochastic, and as static and dynamic.

*Corr. Author's Address: University of Osijek, Mechanical Engineering Faculty in Slavonski Brod, Trg I. Brlić-Mažuranić 2, HR-35000 Slavonski Brod, Croatia, gordana.maticevic@sfsb.hr

The published papers treating the production scheduling problem deal with different types of production. In their paper [12] the authors treat a single-machine batch scheduling problem, and the objective of established model is to minimize the maximum lateness. In the paper [13] the authors compare various methods for the flow-shop scheduling problem with late work objective function. The problem of scheduling a multiprocessor task model with parallel work on several processors that is often used in modern manufacturing systems is discussed in [14]. The paper applies scheduling in time windows for the objective function of maximum lateness and schedule length. An overview of development and approaches to solving the flow-shop problem is given in the paper [15]. A concise review of the techniques developed up to that time for solving the job shop scheduling problem is presented in the paper [16]. The authors of the paper [17] deal with the job shop scheduling problem for flexible manufacturing system. To solve the job-shop scheduling problem a new time and memory efficient representation of the disjunctive graph is given in the paper [18]. In the papers [19] and [20] the authors discuss the optimization of multiple conflictuous criteria for flowshop scheduling problem. The authors of the paper [21] treat the resource-constrained project scheduling problem. The review of the fundamental approaches for project scheduling under uncertainty is given in the paper [22]. The authors of the paper [23] elaborate the activities scheduling problem aiming at minimizing the project duration with the possibility to perform the activities in several variants. The project scheduling problem classification is also given. The authors of the papers [24] and [25] the scheduling problem with the setup time included, in contrast to most models that disregard the machine setup time or consider it as part of the processing time. The authors of the paper [26] deal with the family scheduling model which includes the setup times when there are family setup times aimed at minimizing total earliness and total tardiness. In their paper [27] the authors treat the problem of scheduling orders with various priority rules.

1.2 Foundry Operations Scheduling

Most papers about scheduling problems in the metal industry deal with various planning and scheduling models for steel production. In the paper [28] a mixed integer linear programming model is given. The objective function is to minimize the total completion time. In the paper [29] a mathematical model for steel billets production scheduling is presented. Linear programming method is used and the objective function is to make a maximum profit on selling the billets. The mathematical model for steelmaking-continuous casting production scheduling based on the just-in-time (JIT) concept is given in the paper [30]. The linear programming method is applied and the objective function is to minimize the cost function. According to [30] no systematic research has been realized so far on the general structure, model and algorithm which can be applied to steelmaking plants. In the paper [31] authors reviewed the planning and scheduling systems developed for steel production. However, little research has been published regarding scheduling foundry operations. An example of Gantt chart (from 1903) for foundry operations scheduling is shown in the paper [32]. A recent survey on this topic may be found in the papers [1], [2] and [33] to [37]. Mathematical model for pouring scheduling, formulated by integer programming, is given in the paper [1]. The authors of the paper [33] suggest mixed integer linear programming formulation for the scheduling problem. The objective function is to minimize total tardiness. In the paper [34] the authors apply a mixed integer linear programming method to model the production planning and scheduling in small foundries. The authors [35] use ant colony optimization metaheuristic to solve the aluminium casting scheduling problem by computerized scheduling application. The paper [36] presents a software solution for aluminium production complex process management. The authors of the paper [37] describe a lot-sizing model for foundry. Objective function is to minimize the total production costs. The paper [2] describes the application of multiobjective evolution algorithms in multicriteria optimization of operational production plans in foundry.

1.3 ERP System

The papers [38] and [39] compare several ERP systems (recognized global solutions and local solutions) used in Croatia. There is an ample supply of the software for financial operations,

management of human resources and payroll accounts while the supply of the software for commodity and material transactions is less adequate. However, the supply of production software and that for production management in particular is completely inadequate. The mentioned research has shown that compared to imported commercial packages the Croatian solutions are better, cheaper and easier to implement. The most important parts of the ERP system are planning and scheduling [40]. However the researchers think that the applied methods of planning built in the computer systems are too simple. Not even the linear programming methods are in most cases included into the standard program packages for planning and scheduling [41]. The ERP system manufacturers are beginning to include the operation research optimisation methods (e.g. mixed-integer programming) to upgrade the quality of operations planning and scheduling [42]. Most software manufacturers avoid getting involved in solving this problem. Further research is necessary in order to find an efficient and user friendly computer-aided tool for scheduling. The ERP system practical application advantages and disadvantages are often discussed in professional journals, but the research on ERP and applied planning and scheduling methods are under-represented in literature, except for the researches on reasons for implementation or the ERP system implementation itself, e.g. [43] to [46].

According to the AMR Research[1] the world five largest ERP system manufacturers: SAP, Oracle, Sage Group, Microsoft, SSA Global, control nearly 80% of the ERP system market. Most of the ERP systems available are modular. Typical modules are accounting, human resources, production and logistics. Each module contains specific business processes, access to common data base and ability to operate as independent application. Thus the system structure can be quickly changed and upgraded. The software of the above mentioned software manufacturers is used in some foundries. However, the expensive, large and computer equipment demanding ERP systems are not available to small and medium companies especially when they have particularities the ERP system has to be adjusted to [40]. It is also highly complicating to modify the commercial software so as to adjust it to the requirements of the foundry operational processes.

2 PROBLEM DEFINITION

This paper deals with scheduling issues in foundries. The production of aluminium casting products (blocks, ingots, wire) is a combined continuous discrete production with processes: electrolysis in electrolytic cells, pouring into transfer crucibles, transfer and pouring of alloy to the furnace, molten metal control and purification by adding the required ingredients according to the customer's alloy specification, pouring into moulds, control, product cutting and delivering. Figure 1 gives a scheme of production lines in the foundry Aluminium Ltd. in Mostar. The production process encompasses five production lines with ten furnaces and a finishing workshop for production of aluminium cast items:

- line CC3 for producing billets with furnaces P10 and P9,
- line CC2 for producing T-ingots with furnaces P8 and P7,
- line CC1 for producing blocks with furnaces P6 and P5,
- line BROCHOT for producing alloyed ingots with furnaces P3 and P2,
- line - wire rolling mill CLESIM with furnace P1.

Tasks set to the production of aluminium casting products scheduling system are:

- to calculate the available furnace capacity for the total of 24 hours,
- to group products according to alloy specification,
- to group products according to dimensions of moulds,
- to open production order with the products grouped as mentioned above,
- to create daily plan for production based on work shifts,
- to schedule daily production for the lines and available capacities of furnaces.

Furnaces cause bottlenecks. Based on the OPT concept, bottlenecks are identified as critical manufacturing resources and scheduled first. Also, furnaces and moulds must be coordinated. The mathematical model and algorithm for pouring scheduling is developed based on algorithm [47] with adjustment to the specific problem of scheduling foundry operations. The objective is to find feasible production schedule. Let $S_o = \{i_a | i \in a\}$ be a set of items which can be produced by the

[1] http://www.simplysap.com/sap-news/sap-articles/erp-software-will-grow-to-$29-billion-in-2006.htm (20.1.2007)

same alloy and $\mu_o = \{m_i | i \subset S\}$ a set of moulds for items with similar dimensions. Thus the items are grouped to production order o.

The following notation is used:

Indices:

$a = 1,...., A$	alloys
$c = 1,...., C$	charges
$f = 1,...., F$	furnaces
$i = 1,...., I$	items
$j = 1,...., J$	operations
$l = 1,...., L$	production lines
$m = 1,...., M$	moulds
$o = 1,...., O$	production orders
$t = 1,...., T$	periods

Parameters:

b_i	weight of item i [kg]
$dd_{i,o}$	delivery date for item i and order o
K_i	tardiness of item i [day]
$k_{l,f}$	utilization factor of furnace f on production line l
$K^R_{l,f,t}$	available capacity of furnace f in a day t [hours]
$K^{cap}_{l,f}$	capacity of furnace on production line per hour [kg/hour]
$n_{a,t}$	number of charges for alloy a
N^R_m	available quantity of moulds type m [pieces]
n^h_s	number of hours in shift s
$\delta_{s,t}$	number of shifts in a day
o^h	number of overtime hours
$\Pr(i)$	priority of item i
$q_{i,c}$	quantity of items i from one charge [pieces]
$q_{i,o}$	quantity of items i per production order o [pieces]
$q_{i,t}$	quantity of produced items i in period t [pieces]
$q^n_{i,t}$	ordered quantity of item i [pieces]
$q^z_{i,t}$	inventory of item i in period t [pieces]
Q_{raw}	total quantity of melted aluminium [kg]
Q_l	quantity of melted aluminium for line l [kg]
$Q_{l,f,c}$	quantity of melted aluminium for charge in furnace f on line l [kg]
$t_{i,j}$	processing time of operation j of item i [hours]
$t_{l,f,c}$	processing time of charge c in furnace f on production line l [hours]
$t^{pour}_{l,f,c,i}$	duration of pouring of item i from furnace f on production line l [hours]
tm_m	time of assuring necessary quantity of mould type m
$tp^{pour}_{l,f,c,i}$	start time of pouring operation of item i
$tp_{l,f,c}$	start time of processing charge c in furnace f on production line l
$tz_{i,o}$	finish time of item i on production order o
$tz^{pour}_{l,f,c,g}$	finish time of pouring
$\delta_{s,t}$	number of shifts s in a day t
ε	transportation time between pouring and succeeding operations
$\tau_{l,f,c,c+1}$	time between charges

Decision variables:

$x_{i,m}$	binary variable, $x_{i,m} = 1$ if item i is produced in mould type m, otherwise $x_{i,m} = 0$
$y_{a,c}$	binary variable, $y_{a,c} = 1$ if alloy a is produced in charge c, otherwise $y_{a,c} = 0$
$y_{i,c}$	binary variable, $y_{i,c} = 1$ if item i is produced from charge c, otherwise $y_{i,c} = 0$
$\zeta_{g,c}$	binary variable, $\zeta_{g,c} = 1$ if item g is produced from same charge c as item i

Mathematical model is formulated as follows:

Minimize

$$H = \sum_i K_i \tag{1}$$

subject to:

$$K_i = \begin{cases} 0 & if \quad dd_{i,o} \geq tz_{i,o} \\ tz_{i,o} - dd_{i,o} & otherwise \end{cases} \tag{2}$$

$$q_{i,o} \geq \max\left(0, q^n_{i,t} - q^z_{i,t}\right) \tag{3}$$

$$\sum_t q_{i,t} \geq q^n_{i,t} \qquad \forall i \tag{4}$$

$$\sum_c q_{i,c} = q_{i,o} \qquad \forall o \tag{5}$$

$$q_{i,c} \leq \min\left\{q_{i,o}, \frac{Q_{l,f,c}}{b_i} - q_{g,o} \cdot b_g \cdot \zeta_{g,c}\right\} \tag{6}$$

$$\sum_a n_{a,t} \cdot Q_{l,f,c} \leq K^R_{l,f,t} \cdot K^{cap}_{l,f} \tag{7}$$

$$b_i \cdot N^R_m \leq Q_{l,f,c} \tag{8}$$

$$K^R_{l,f,t} = \left[\sum_s \delta_{s,t} \cdot n^h_s + o^h\right] \cdot k_{l,f} \tag{9}$$

$$\sum_l Q_l \leq Q_{raw} \tag{10}$$

$$\sum_i x_{i,m} \cdot q_{i,o} \leq N^R_{m,t} \tag{11}$$

$$tp^{pour}_{l,f,c,i} \geq \max\left(y_{a,c} \cdot \left(tp_{l,f,c} + t_{l,f,c}\right), \sum_i x_{i,m} \cdot tm_m, \psi_{i,g} \cdot tz^{pour}_{l,f,c,g}\right) \quad g \neq i,\ \Pr(g) \geq \Pr(i) \tag{12}$$

$$t_{i,j=1} \geq tp^{pour}_{l,f,c,i} + t^{pour}_{l,f,c,i} + \varepsilon \tag{13}$$

$$\sum_j t_{i,j} + t_{l,f,c,i} \leq dd_{i,o} - tp_{l,f,c,i} \tag{14}$$

$$tp_{l,f,c+1} \geq tp_{l,f,c} + t_{l,f,c} + 1 + \tau_{l,f,c,c+1} \tag{15}$$

$$\sum_a y_{a,c} = 1 \quad \forall c \tag{16}$$

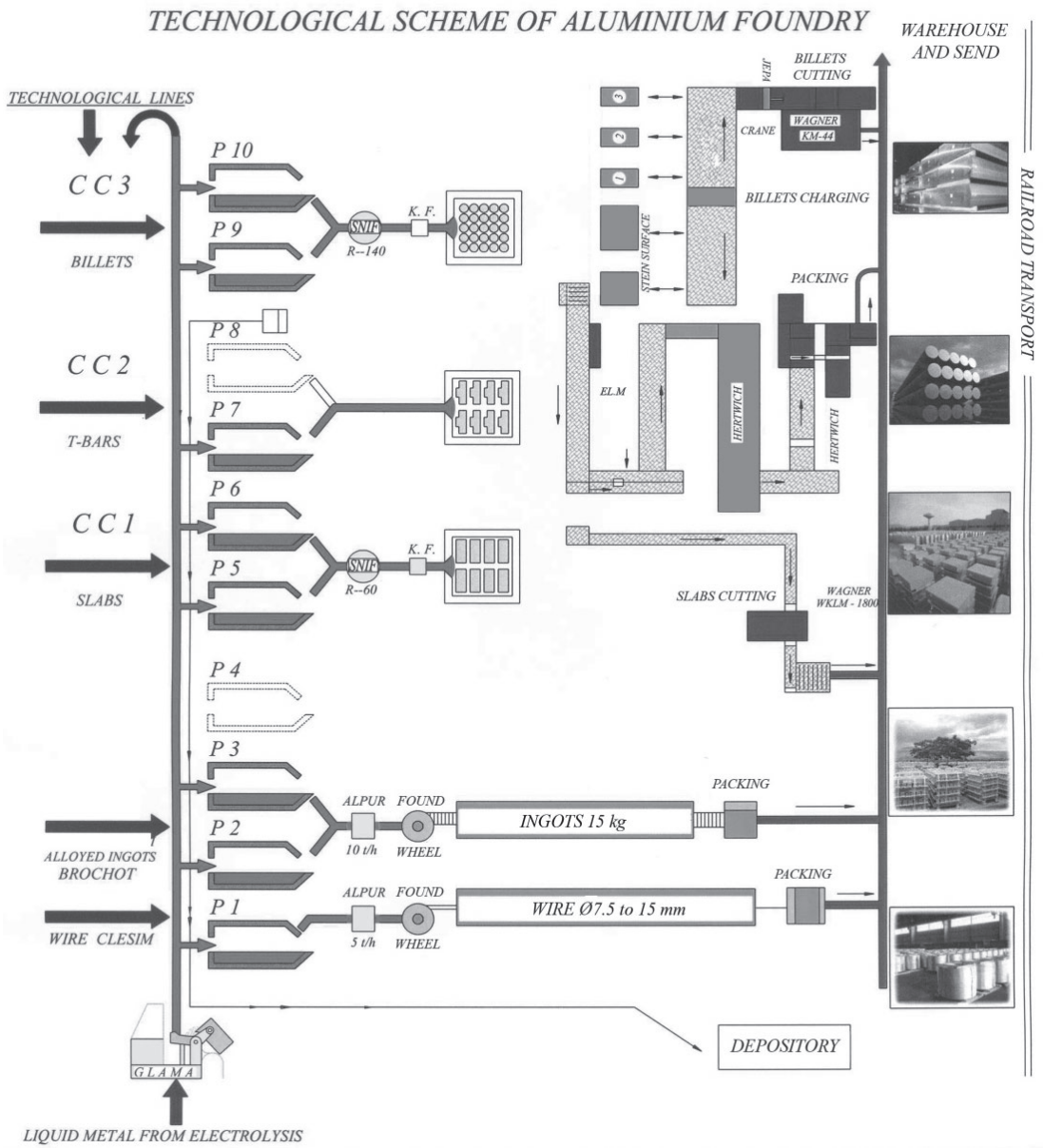

Fig.1 *Technological scheme of aluminium foundry*[2]

$$\sum_{a} y_{i,a} = 1 \quad \forall i \tag{17}$$

The objective function is to minimize tardiness of production order (1). Tardiness can be expressed by the term (2). Constraint (3) determines the order quantity for item *i* of production order *o*. Constraint (4) ensures that the quantity of produced items in the planning horizon is equal to the ordered quantity. Constraint (5) ensures that the total quantity of items *i* from all charges is equal to the production order quantity. Constraint (6) determines the quantity of item *i* for producing from charge *c* according to the available quantity of alloy in the charge. Constraint (7) determines that the total quantity of different alloy for period *t* is equal to or less than the available furnace capacity. Constraint (8) ensures enough mould capacity. The mathematical term (9) determines the available capacity of furnace *f* on production line *l* for day *t*. Constraint (10) guarantees that the consumption of the total required quantity of melted aluminium for all production lines does not exceed the

[2] http://www.aluminij.ba/About_us-Technological%20scheme%20of%20the%20foundry.htm (18.8.2006)

available melted aluminium. Constraint (11) ensures that the consumption of moulds does not exceed the available quantity of moulds. Constraint (12) determines the starting time of pouring items *i* from charge *c* in furnace *f* on production line *l*. The operation of pouring item *i* is assigned to the furnace according to the defined priority of items. Also, according to the MRP II concept all needed resources (e.g. moulds) must be provided for the start of operation. Constraint (13) ensures the starting time of subsequent operations on item *i* (after pouring into moulds). Constraint (14) enforces that the sum of the charge processing time in the furnace and subsequent operations times is less than or equal to the difference between due date and starting time of the charge *c* processing in the furnace *f*. That enforces production according to the JIT concept. Constraint (15) ensures that the succeeding charge is started only when the preceding charge is finished and poured. The time between charges is taken into account. Constraint (16) ensures that there is only a single alloy in each charge. Constraint (17) ensures that each product is made from just one alloy.

3 IMPLEMENTATION OF MATHEMATICAL MODEL

The model, Croatian solution of the ERP system [40], has been used in the Aluminium Ltd. foundry in Mostar since March 2006. Some screenshots of the developed planning and scheduling system are given and discussed below.

The ERP system contains information about the capacities that will be monitored during the foundry operations process. Bottlenecks as critical capacities are defined. Furthermore, the definition of technological operations is given. Each operation is defined in view of its duration and capacity. Figure 2 shows the technological operations for production of aluminium casting products. After creating orders the next task is to determine the production order (production line and quantity from one charge are automatically offered) and the basic plan. By the selection of the number of charges the basic plan for that day is determined. Figure 3 shows the procedure for determining the basic production plan. Figure 4 shows the basic plan that defines the deadlines and also shows the realisation of contracted times (planned finishing time with regard to the deadline).

Detailed scheduling with the dates, shifts and hours of the pouring operations start times for every production order is determined after the basic plan has been generated. After the selection of the date and production line, the system offers all production orders planned for that day. Afterwards, the selection of production order is performed and the process of scheduling starts. Figure 5 shows the start-up for the generation of the detailed plan.

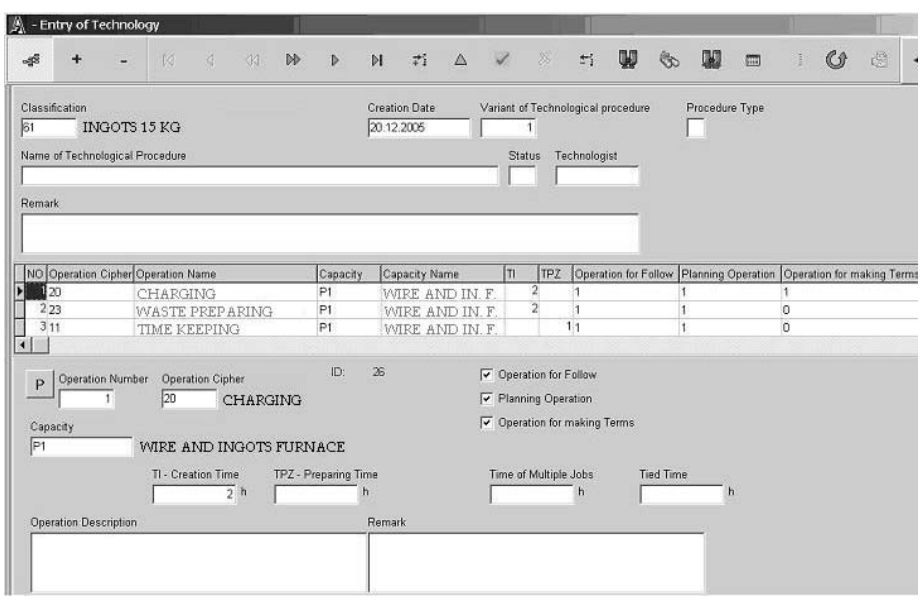

Fig. 2. *Technological operations for production of aluminium casting products*

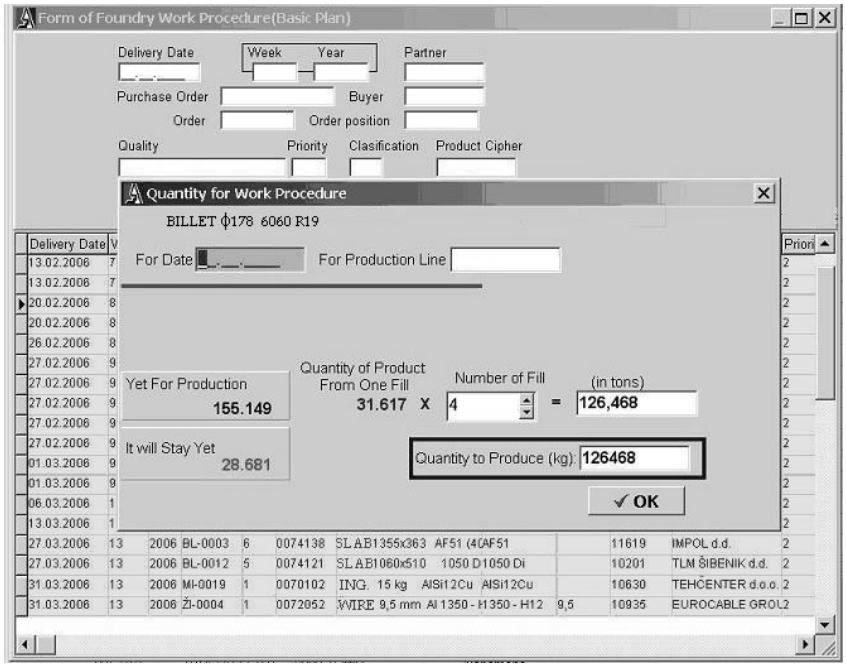

Fig. 3. *Procedure for the generation of basic plan*

ALUMINIJ d.d. Mostar

Basic Plan of Production
FROM 28.09.2006 TILL 03.10.2006

Num:1
Date 27.09.2006

Production Line	The Num. of Fill		Buyer	Order	Purchas Order	Quality	Dimension	Product	Quantity for Production(kg	Produced (kg)	Yet for Production	Date/Week of Delivery	
28.09.2006	7	7											
CC3	7	7											
	1	1	VIBA SrL	TR-0046	390	6060 VIBA	7000; fi 178	0073143	130.	125.145	4.855	25.09.2006	39
	4	4	FEAL d.o.o. za	TR-0086	10/200	6060 FEAL	7000; fi 178	0073048	800.000	122.827	677.173	30.10.2006	44
	2	2	ESTRAL SpA	TR-0083	418	6060 EST	7000; fi 178	0073090	100.000	62.314	37.686	29.09.2006	39
29.09.2006	6	6											
CC3	6	6											
	2	2	ESTRAL SpA	TR-0083	418	6060 EST	7000; fi 178	0073090	100.000	119.036	-19.036	29.09.2006	39
	4	4	ALCOA KOEFEM	TR-0082	417	6060.36	7000; fi 178	0073114	200.000	122.355	77.645	04.10.2006	40
30.09.2006	4	4											
CC3	4	4											
	2	2	ALCOA KOEFEM	TR-0082	417	6060.36	7000; fi 178	0073114	200.000	185.624	14.376	04.10.2006	40
	2	2	ALCOA KOEFEM	TR-0082	417	6060.36	7000; fi 178	0073114	200.000	62.805	137.195	03.10.2006	40
01.10.2006	7	7											
CC3	7	7											
	5	5	ALCOA KOEFEM	TR-0082	417	6060.36	7000; fi 178	0073114	200.000	216.794	-16.794	03.10.2006	40
	1	1	FIN.AL SPA	TR-0084	419	6060 FINAL	7000; fi 178	0073077	100.000	29.766	70.234	09.10.2006	41
	1	1	ANODALL	TR-0090	424	6060 ANOD	7000; fi 178	0073095	300.000		300.000	16.10.2006	42
02.10.2006	6	6											
CC3	6	6											
	3	3	FIN.AL SPA	TR-0084	419	6060 FINAL	7000; fi 178	0073077	100.000	123.268	-23.268	09.10.2006	41
	3	3	FEAL d.o.o. za	TR-0086	10/200	6060 FEAL	7000; fi 178	0073048	800.000	272.634	527.366	30.10.2006	44
03.10.2006	7	7											
CC3	7	7											
	7	7	FEAL d.o.o. za	TR-0086	10/200	6060 FEAL	7000; fi 178	0073048	800.000	493.145	306.855	30.10.2006	44

Fig. 4. *Screenshot of the basic plan of production*

Figure 6 shows the screenshot of the detailed plan. A particular task of the system is the rescheduling that solves:

- priority changes for the previously generated plan of pouring,
- changes caused by certain problems in the preparation of pouring.

A new production plan is generated whenever a change in production and orders occurs.

According to the previously published research on foundry operations scheduling the authors have concluded that in most cases the foundries schedule operations manually and that only a few of them use software to assist in

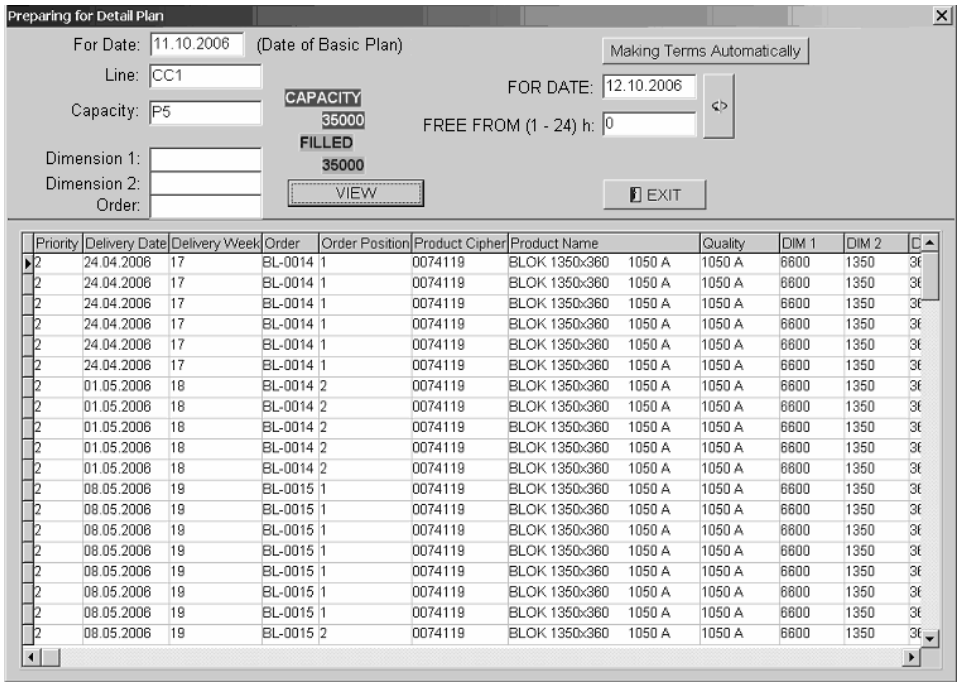

Fig. 5. *Scheduling procedure*

ALUMINIJ d.d. Mostar

Plan of Production

FROM 05.03.2006 TILL 05.03.2006

Num.1
Date 27.09.2006

IN	Buyer	FILL	PRODUCT			Planed Quantity	Capacity		Date	Begin	End
10201	TLM ŠIBENIK d.d.	607789	0074118	SLAB 1560x510	1050 Di	28.341 kg					
							P6	SLABS FURNACE CC1	05.03.2006	6	7
							P6	SLABS FURNACE CC1	05.03.2006	7	10
							P6	SLABS FURNACE CC1	05.03.2006	10	11
							CC1	TL slabs Wagstaff	05.03.2006	11	14
10201	TLM ŠIBENIK d.d.	607790	0074118	SLAB 1560x510	1050 Di	28.341 kg					
							P5	SLABS FURNACE CC1	05.03.2006	9	10
							P5	SLABS FURNACE CC1	05.03.2006	10	13
							P5	SLABS FURNACE CC1	05.03.2006	13	14
							CC1	TL slabs Wagstaff	05.03.2006	14	17
10201	TLM ŠIBENIK d.d.	607791	0074118	SLAB 1560x510	1050 Di	28.341 kg					
							P6	SLABS FURNACE CC1	05.03.2006	14	15
							P6	SLABS FURNACE CC1	05.03.2006	15	18
							P6	SLABS FURNACE CC1	05.03.2006	18	19
							CC1	TL slabs Wagstaff	05.03.2006	19	22
10201	TLM ŠIBENIK d.d.	607792	0074121	SLAB 1060x510	1050 Di	28.090 kg					
							P7	SLABS FURNACE CC2	05.03.2006	6	7
							P7	SLABS FURNACE CC2	05.03.2006	7	10
							P7	SLABS FURNACE	05.03.2006	10	11

Fig. 6. *Production schedule*

scheduling. Thus the development of the operations scheduling model for the manufacture of aluminium casting products renders the present research original and of considerable industrial significance. So the OPT method can be used not only in the production of car parts but also for pouring processes. The mathematical scheduling model has been successfully applied to the foundry,

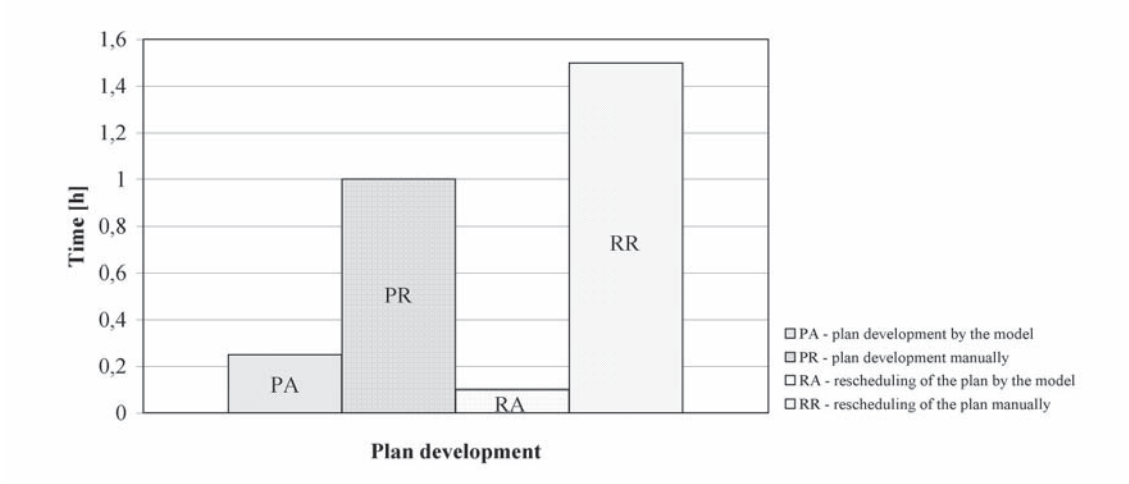

Fig. 7. *Comparison of the time needed for plan development manually and by the model*

and it has significantly improved the set-up process and the scheduling of furnace operations. It is also a precondition for better monitoring of obtained results.

The analysis of the classical and new approach to scheduling is made by comparing the times required for the plan development (shown in Fig. 7). To develop the plan by the model takes 15 min while to do it manually takes 60 min. Rescheduling of the plan by the model takes 6 min while doing it manually takes 90 min.

The other data (monitoring of the quantity produced per day, reduction of production flow, reduction of waiting time in foundry and of consumption of energy required for keeping the foundry temperature constant) will be available only after a year–long monitoring.

4 CONCLUSION

The main goal of this paper was to develop a new mathematical model for scheduling foundry operations based on the MRP II (Manufacturing Resource Planning), JIT (Just in Time) and OPT (Optimized Production Technology) concepts. A considerable effort was made to link academic research with industry requirements in order to achieve this goal. The researches carried out at the Mechanical Engineering Faculty in Slavonski Brod confirmed that the JIT and OPT approach can be applied to solve the foundry operations scheduling problems. The researches also showed that the JIT and OPT concepts, originally developed for discrete production, can be applied for the combination of the process - discrete production, such as the production of aluminium casting products. In this paper a mathematical model is proposed to find a feasible pouring schedule. The use of this mathematical model for scheduling the operations of a foundry reduces the time needed for generating pouring schedules and enables the control of tardiness and adherence to the contracted due dates. The advantage of the proposed model and algorithm in comparison with other algorithms is in its multi-stage approach to planning and scheduling.

The model put forward in this paper is the Croatian solution of the ERP system. It is implemented into the ERP system of the firm Informatics Engineering ININ Ltd. in Slavonski Brod. The mathematical model, an integral part of the ERP system, is successfully applied and tested in the foundry Aluminium Ltd. in Mostar. This practical aspect makes the paper original and of importance to both academic researchers and actual practitioners in the metal industry. With minimum modifications, other foundries and other industries (e.g. food and paper industries) can also integrate this model into their systems.

Acknowledgements

The authors would like to thank the reviewers whose relevant comments and suggestions helped to improve this paper. This research (project 152-2235) was financially supported by the Ministry of Science, Education and Sports of the Republic of Croatia.

5 REFERENCES

[1] Van Voorhis, T., Peters, F., Johnson, D. Developing software for generating pouring schedules for steel foundries. *Computers & Industrial Engineering*, 3-4, 2001, p. 219-234.

[2] Duda, J., Osyczka, A. Multiple criteria lot-sizing in a foundry using evolutionary algorithms in proceedings evolutionary multi-criterion optimization. Third International Conference, EMO 2005, Guanajuato, Mexico, 2005. Coello Coello, C.A., Aguirre, A.H., Zitzler, E. (Ed.). Berlin/Heidelberg: Springer-Verlag, *Lectures Notes in Computer Science*, 2005, vol. 3410, p. 651-663.

[3] Peters, F., Van Voorhis, T. *Re-engineering casting production systems*, Final Report 03/02/1998 – 03/01/2001, Work Performed Under Contract No. DE-FC07-98ID13614, 2001. Available online 26.10.2006, www.osti.gov/bridge/servlets/purl/792021-FdatY9/native/792021.pdf.

[4] Błażewicz, J., Pesch, E., Sterna, M. Job shop scheduling by disjunctive graph analysis. *Fifth International Symposium on Methods and Models in Automation and Robotics MMAR'98*, Miedzyzdroje, Poland, 25-29. August 1998, p. 1029-1033.

[5] Brucker, P., Knust, S. A linear programming and constraint propagation-based lower bound for the RCPSP, *European Journal of Operational Research*, 2 (2000), p. 355-362.

[6] Demeulemeester, E., De Reyck, B., Foubert, B., Herroelen, W., Vanhoucke, M. New computational results on the discrete time/cost trade-off problem in project networks. *Journal of Operational Research Society*, 49 (1998), p. 1153-1163.

[7] Luh, P.B., Hoitomt, D.J. Scheduling of manufacturing systems using the Lagrangian relaxation technique. *IEEE Transactions Automatic Control*, 6 (1993), p. 1066-1080.

[8] Harjunkoski, I., Grossmann, I.E. Decomposition techniques for multistage scheduling problems using mixed-integer and constraint programming methods. *Computers & Chemical Engineering*, 11 (2002), p. 1533-1552.

[9] Schneeweiss, C. Distributed decision making––a unified approach. *European Journal of Operational Research*, 2 (2003), p. 237-252.

[10] Kuhlmann, T., Lamping, R., Massow, C. Agent-based production management. *Journal of Materials Processing Technology*, 1-3 (1998), p. 252-256.

[11] Agarwal, A., Pirkul, H., Varghese, S.J., Augmented neural networks for task scheduling. *European Journal of Operational Research*, 3 (2003), p. 481–502.

[12] Ghosh, J.B., Gupta, N.D. Batch scheduling to minimize maximum lateness. *Operations Research Letters*, 2 (1997), p. 77-80.

[13] Błażewicz, J., Pesch, E., Sterna, M., Werner, F. A comparison of solution procedures for two-machine flow shop scheduling with late work criterion. *Computers & Industrial Engineering*, 4 (2005), p. 611-624.

[14] Błażewicz, J., Dell'Olmo, P., Drozdowski, M., Maczka, P. Scheduling multiprocessor tasks on parallel processors with limited availability. *European Journal of Operational Research*, 2 (2003), p. 377-389.

[15] Gupta, J.N.D., Stafford Jr., E.F. Flowshop scheduling research after five decades. *European Journal of Operational Research*, 3 (2006), p. 699-711.

[16] Jain, A.S., Meeran, S. Deterministic job-shop scheduling: Past, present and future. *European Journal of Operational Research*, 2 (1999), p. 390-434.

[17] Golenko-Ginzburg, D., Gonik, A. Job-shop resource scheduling via simulating random operations. *Mathematics and Computers in Simulation*, 5 (1997), p. 427-440.

[18] Błażewicz, J., Pesch, E., Sterna, M. The disjunctive graph machine representation of the job shop scheduling problem. *European Journal of Operational Research*, 2 (2000), p. 317-331.

[19] T'kindt, V., Billaut, J-C., Proust, C. Solving a bicriteria scheduling problem on unrelated parallel machines occurring in the glass bottle industry. *European Journal of Operational Research*, 1 (2001), p. 42-49.

[20] T'kindt, V., Gupta, J.N.D., Billaut, J-C. Two-machine flowshop scheduling with a secondary criterion. *Computers & Operations Research*, 30 (2003), p. 505–526.

[21] Brucker, P., Drexl, A., Mohring, R., Neumann, K., Pesch, E. Resource-constrained project scheduling: Notation, classification, models, and methods. *European Journal of*

Operational Research, 1 (1999), p. 3–41.
[22] Herroelen, W., Leus, R. Project scheduling under uncertainty: Survey and research potentials. *European Journal of Operational Research*, 2 (2005), p. 289-306.
[23] De Reyck, B., Herroelen, W. The multi-mode resource-constrained project scheduling problem with generalized precedence relations. *European Journal of Operational Research*, 2 (1999), p. 538-556.
[24] Lee, Y.H., Pinedo, M. Scheduling jobs on parallel machines with sequence-dependent setup times. *European Journal of Operational Research*, 3 (1997), p. 64-474.
[25] Alahverdi, A., Gupta, J.N.D., Aldowaisan, T. A review of scheduling research involving setup considerations. *Omega*, 2 (1999), p. 219-239.
[26] Schaller, J.E., Gupta, J.N.D. Single machine scheduling with family setups to minimize total earliness and tardiness. *European Journal of Operational Research*, (2006), doi:10.1016/j.ejor.2006.06.061.
[27] Leung, J.Y.-T., Li, H., Pinedo, M. Scheduling orders for multiple product types to minimize total weighted completion time. *Discrete Applied Mathematics*, 8 (2007), p. 945-970.
[28] Bellabdaoui, A., Teghem, J. A mixed-integer linear programming model for the continuous casting planning. *International Journal of Production Economics*, 2 (2006), p. 260-270.
[29] Zanoni, S., Zavanella, L. Model and analysis of integrated production–inventory system: The case of steel production. *International Journal of Production Economics*, 93-94 (2005), p. 197-205.
[30] Tang, L., Rong, A., Yang, Z. A mathematical programming model for scheduling steelmaking-continuous casting production. *European Journal of Operational Research*, 2 (2000), p. 423-435.
[31] Tang, L., Liu, J., Rong, A., Yang, Z. A review of planning and scheduling systems and methods for integrated steel production. *European Journal of Operational Research*, 1 (2001), p. 1-20.
[32] Wilson, J.M. Gantt charts: A centenary appreciation. *European Journal of Operational Research,* 2 (2003), p. 430-437.
[33] Nonas, S.L., Olsen, K.A. Optimal and heuristic solutions for a scheduling problem arising in a foundry. *Computers & Operations Research,* 9 (2005), p. 2351-2382.
[34] de Araujo, S.A., Arenales, M.N., Clark, A.R., Lot sizing and furnace scheduling in small foundries. *Computers & Operations Research*, Available online 25.07.2006, http://www.sciencedirect.com.
[35] Gravel, M., Price, W.L., Gagné, C. Scheduling continuous casting of aluminum using a multiple objective ant colony optimization metaheuristic. *European Journal of Operational Research*, 1 (2002), p. 218-229.
[36] Majdandžić, N., Budić, I., Novoselović, D. Integrated informational system for an aluminum smelter company - ISAL. *Metalurgija*, 3 (2003), p. 197-201.
[37] dos Santos-Meza, E., dos Santos, M.O., Arenales, M.N. A lot-sizing problem in an automated foundry. *European Journal of Operational Research*, 3 (2002), p. 490-500.
[38] Fertalj, K., Mornar, V., Kovač, D., Hađina, N., Pale, P., Žitnik, B. *Comparative analysis of information system software in Croatia*. Project of IT implementation, Faculty of Electrical Engineering and Computing, University of Zagreb, 2002. Available online, http://www.unibis.hr/ERP-HR.pdf, 12.7.2004.
[39] Fertalj, K., Kalpić, D. ERP software evaluation and comparative analysis. *Journal of Computing and Information Technology – CIT*, 3 (2004), p. 195-209.
[40] Majdandžić, N. *Building Information systems for production enterprises*. Mechanical Engineering Faculty in Slavonski Brod, 2004.
[41] Jacobs, F.R., Bendoly, E. Enterprise resource planning: Developments and directions for operations management research. *European Journal of Operational Research*, 2 (2003), p. 233–240.
[42] Clark, A.R. Optimization approximations for capacity constrained material requirements planning. *International Journal of Production Economics*, 2 (2003), p. 115–131.
[43] Umble, E.J., Haft, R.R., Umble, M.M. Enterprise resource planning: Implementation procedures and critical success factors. *European Journal of Operational Research*, 2 (2003), p. 241–257.
[44] Mabert, V.A., Soni, A., Venkataramanan, M.A. The impact of organization size on enterprise resource planning (ERP) implementations in

the US manufacturing sector. *Omega*, 3 (2003), p. 235-246.

[45] Hong, K.K., Kim, Y.G. The critical success factors for ERP implementation: an organizational fit perspective. *Information & Management*, 1 (2002), p. 25-40.

[46] Yen, H.J.R., Sheu, C. Aligning ERP implementation with competitive priorities of manufacturing firms: An exploratory study. *International Journal of Production Economics*, 3 (2004), p. 207-220.

[47] Matičević, G. *Hierarchical planning and scheduling model for one-piece and small batch production*, PhD dissertation. University of Osijek, Mechanical Engineering Faculty in Slavonski Brod, 2005. 166 p.

[49] Tsourveloudis N., Ioannidis S., Valavanis K. Fuzzy surplus based distributed control of manufacturing systems. *Advances in production engineering & management*, Volume 1: Number 1 (2006), p 5-12.

[50] Nestler A., Dang T.N. The application of a multi-gent system for process management and NC data transfer aided by a DNC system. *Advances in production engineering & management,* Volume 3: Number 1 (2008), p 3-16.

Strojniški vestnik - Journal of Mechanical Engineering 54(2008)1, 49-55
UDC 658.5.012.7
Paper received: 26.4.2006
Paper accepted: 19.12.2007

Optimum Selection of Information Terminals for Production Monitoring in Manufacturing Industries

Jani Kleindienst[1] - Đani Juričić[2,*]
[1]Kolektor Sinabit Ltd., Slovenia
[2]"Jožef Stefan" Institute, Slovenia

The purpose of automated acquisition of production data in manufacturing industries is aimed to provide accurate data about the performance of the scheduled tasks and the production process. Hence, easier and more effective production control can be achieved. The information acquired includes the duration of each operation, the number of manufactured items of products, the amount of scrap as well as the duration of downtimes and their root-causes. A way to acquire relevant data makes use of special-purpose information terminals. The problem that arises here is how to select the optimum number of the terminals in order to minimize the overall losses. The approach presented below relies on optimization of a stochastic criterion function, which combines the terminal costs and costs related to the waiting times during busy sessions. The solution suggested is based on using the distribution of events, recorded during the past production session. A case study dealing with optimum selection of terminals in a real production process is presented in detail.

Keywords: production systems, optimization, production monitoring, production control

0 INTRODUCTION

More and more manufacturing companies are introducing multi-information terminals (MIT) in order to allow peer monitoring of the production process. These systems complement business information systems, such as ERP's (Enterprise Resource Planning). There are many ways in which relevant production data can be collected [1] and [2]:

- entirely manually by filling up special forms,
- automatically from the machines,
- on demand and on-line through special purpose terminals.

Data of considerable relevance for the production process encompass the following items: execution times needed to complete an operation from the work order, number of manufactured parts, the amount of scrap parts and duration as well as root-causes for downtimes.

In order to assure best quality data, events are recorded at the time and the site of their origin. According to [3], the quality of information is measured by accessibility, accuracy, timeliness, integrity, density, suitability, understandability, and objectivity.

Specially tailored information terminals represent a convenient means to record the production events (Fig. 1). Different technologies for data entry can be employed, however the most frequent one is the bar code [5]. Bar code is also widely used with different working sheets and personal identification cards.

Fig. 1. *A terminal used to record production events (manufactured by Kolektor Sinabit Ltd.)*

Prior to implementing the terminals in the production process, the following issues have to be considered:

- distribution of events, typical for the underlying production process,
- duration of events,
- distances between working places and terminals,

*Corr. Author's Address: "Jožef Stefan" Institute, Department of Systems and Control, Jamova 39, SI-1000 Ljubljana, Slovenia, dani.juricic@ijs.si

- terminals cost, including costs for installation and maintenance.

Terminal costs can be reduced by cutting the number of terminals. However, new costs are introduced because of idle times workers have to spend while waiting for a free terminal. Hence, our problem is to find the optimum number of terminals, which minimizes the *overall* costs.

The paper is organized as follows. In the first section the problem of optimum selection of terminals is stated in the form of a stochastic optimization problem. Basically, the idea is to employ a record of production events from the production history. The second section describes a simple procedure for solving the optimization problem by means of simulation. The third section reports on results, obtained in a real production plant.

1 PROBLEM STATEMENT

Organization of the manufacturing process

Let us first shortly outline the organization of a production process in a typical manufacturing industry.

The basic item is *work order*, the result of which are manufactured products. Work order is usually divided into many discrete operations defined by the technological procedure. Each worker is responsible for his/her own *workplace* and for handling *operations* assigned to it. A workplace consists of one or more machines, which are capable of executing the specified operations.

In order to get clear insight into the production efficiency, the following events have to be recorded [4]:

- start of each operation,
- end of work,
- start of a downtime,
- end of a downtime.

The origin of waiting times

At each registration, e.g. at the start of work, the operator has to enter data about who will perform the operation (personal number), the allocation of operation (machine number) and the code of operation along with the underlying work order. When a downtime has to be registered, the worker has to enter additional data regarding the root cause for it. Downtime code can be found on a printed bar-code list. The registration procedure is depicted in Figure 2.

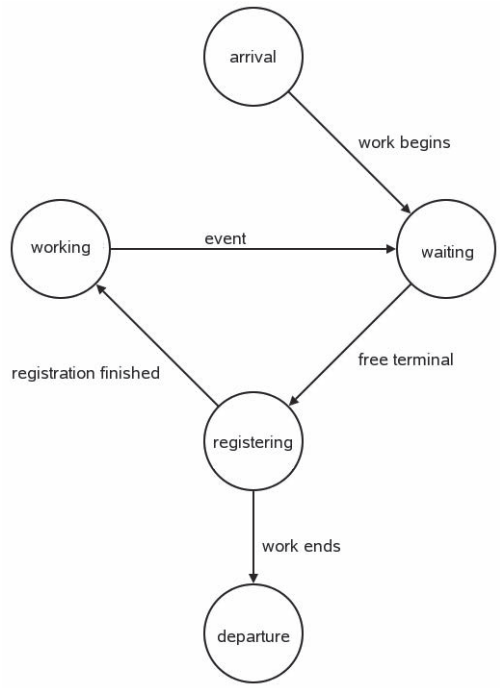

Fig. 2. *Particular stages in the event registration procedure and emergence of the waiting times*

In order to *register* an event, one has to access the terminal and enter the relevant data. Provided the terminal is busy, one has to wait in a queue. In this paper it is assumed that any of the available terminals can be freely selected. Time needed to access the terminal is neglected.

In principle, waiting times could be entirely eliminated by installing sufficiently many terminals. However, such a solution is not an optimum one since by raising the number of terminals their costs increase monotonicaly. Therefore, we have to choose a criterion function that will include both types of costs.

Criterion function

Let N be the number of terminals and $J_{cost}(N)$ their cost normalized per day. This cost is calculated according to the amortization period of 4 years. The annual cost implied by a terminal is thus a sum of amortization costs and maintenance costs. The former and the latter are as high as one quarter and one tenth of the purchasing price respectively.

Let $J_w(N)$ represent daily costs due to the waiting times. This can be simply expressed as

$$J_w = c_w \tau(N) \quad (1),$$

where c_w represents labour cost per employee and $\tau(N)$ stays for daily accumulated waiting time.

Comment 1

The time required to enter the data in the terminal is about 30 secs and this is not considered as loss caused by waiting.

Comment 2

The accumulated daily waiting time $\tau(N)$ is random variable with a probability density function $p(\tau(N))$ defined on the open interval $[0,\infty)$. Its analytical expression is not known.

Because of the dispersion in waiting times, we are looking for such a τ_α, that the probability $P(\tau \leq \tau_\alpha)$ equals $1-\alpha$. Here $0 \leq \alpha \leq 1$ is the degree of significance. For example, when $\alpha=0.05$ there is 95% probability that the waiting time at the given number of terminals N will be $\tau(N) \leq \tau_{0.05}(N)$ [6].

The following stochastic optimization problem should be solved in order to find the optimum number of terminals:

$$N^* = \arg\min_{N \geq 1} \left(J_{cost}(N) + c_w \tau_\alpha(N) \right) \quad (2).$$

Comment 3

Because of the strictly monotonically increasing function $J_{cost}(N)$ on the right side of (2) and strictly monotonically decreasing function $\tau_\alpha(N)$, the criterion function (2) is unimodal. In that case, there exists N^*, such that the criterion function reaches its minimum.

2 SOLVING THE OPTIMIZATION PROBLEM

To solve the problem (2), the knowledge of event distribution is required. The frequency of events differs during the working day, depending on the type of production. In order to estimate the daily profile of the density of events, some recorded realization of events is needed. These data are referred to as the *learning data set*.

Preparation of the learning data set

The acquisition of learning data is done by means of the *currently available* acquisition system. This can be purely manual in some cases. In other cases process history or diverse information sources can be utilized. Each recorded event carries information about the start and the end of an activity. Accuracy of the learning data is of considerable importance here so that problems might occur in cases where data resolution is poor. For example, manually entered data are rounded to a half an hour or an hour instead of a second or minute. A typical consequence of rounding can be seen in higher density of events around full hours, which results in higher values of the estimated waiting times.

Calculation of waiting times on the learning set

Each event is associated a time stamp, i.e. the date and time of its occurrence. The algorithm for calculation of waiting times is executed within 5 steps:

1. find the terminal, which will first become available;
2. estimate the time a terminal will become available (if terminal is already free, registration can start immediately);
3. waiting time is calculated as the difference between the time of availability of the terminal and the occurrence of the event;
4. waiting time is extended with time required for data entry;
5. calculated waiting time in step 3 is added to the daily accummulated waiting time.

The algorithm results in a sequence of waiting times:

$$T = \{\tau_1, \ldots, \tau_M\} \quad (3),$$

calculated for each day separately. The complexity of the algorithm is $O(m*N_{max})$, where m is the number of events in the learning set and N_{max} is the highest assumed number of terminals.

Figure 3 illustrates a simple case in which waiting times for one and two terminals are calculated respectively. In both cases there are three events, which occur at times 2, 7 and 13. Every event is 7 time units long. The first event, which occurs at time 2, is immediately processed in both cases. The same happens with events 2 and 3 in the case of two terminals. In the case of one terminal, the first event is still being processed when the second appears at time 7. In the same manner the second event is still being processed when the third one occurs at time 13. Therefore, handling of the last two events has to be delayed

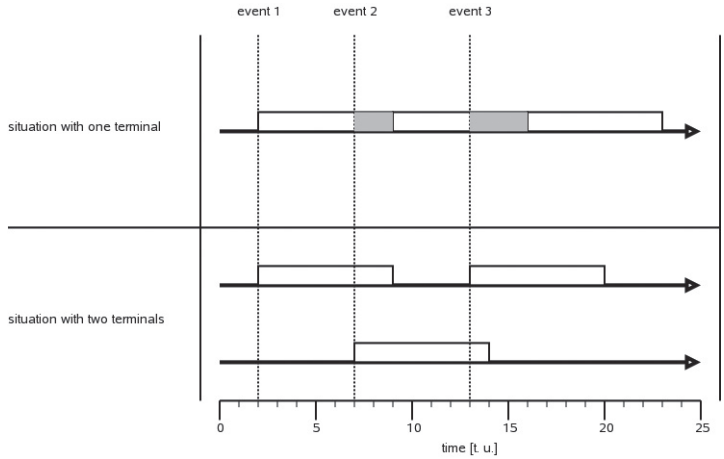

Fig. 3. *Illustrated calculation of waiting times*

from time 7 to time 9 for the second and from time 13 to time 16 for the third event. The diagram shows waiting times in gray color. To sum up, in the situation with two terminals there is no waiting time while in the situation with one terminal, the waiting time equals 5 units.

Determination of the critical waiting times

In order to approximate the probability density function of the random variable τ_d one can calculate the histogram derived from the set T (see Eq. (3)). The distribution function varies with respect to the number of terminals and its shape is hard to define analytically.

Optimization method

Let's first notice that the argument of the criterion function (2) is integer. In this case we deal with the one-dimensional problem, which is relatively simple. Given the fact that the expected optimum number of terminals is not high, we apply a simple optimum seeking procedure, which reads as follows:

N_{opt} = 0, J_{opt} = 1e10
for N = 1 to N_{max} do begin
calculate the histogram of waiting times for N terminals
calculate the critical waiting time τ_α
calculate the criterion function J(N)
if J(N) < J_{opt} do begin
N_{opt} = N
J_{opt} = J(N)
end
end

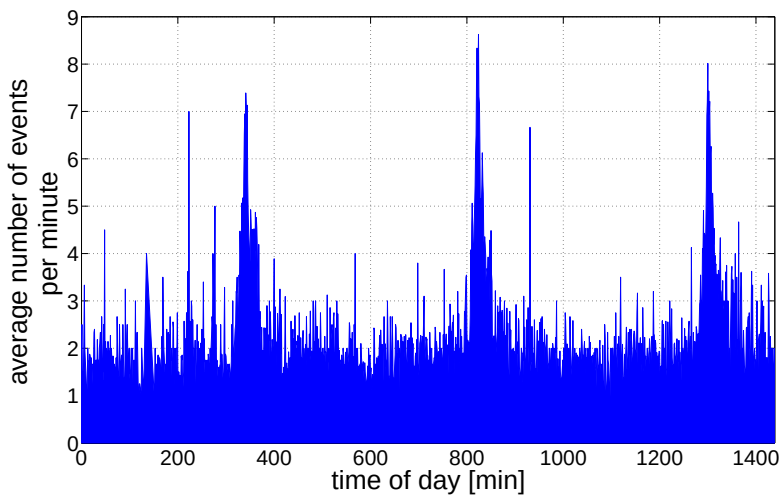

Fig. 4. *The average number of events per minute during the day. Peaks at 6 am, 2 pm an 10 pm coincide with the shift changes.*

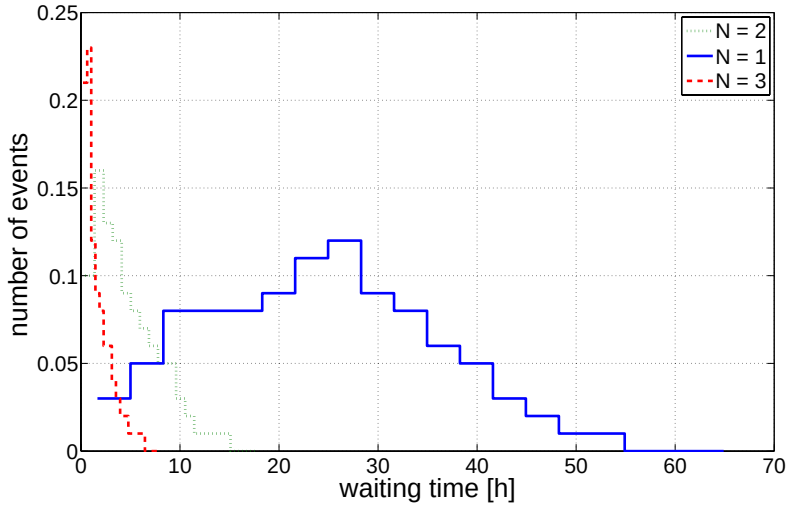

Fig. 5. *Histograms of waiting times for various numbers of terminals. When increasing the number of terminals, critical expected time approaches zero.*

3 CASE STUDY

The approach above has been applied in a case study related to the manufacturing industry. The underlying production line employs 60 workers in the morning and afternoon shift. Figure 4 presents the frequency of events recorded on the daily basis.

The learning set includes 1205 working days. We have collected 331448 events during this time period. Cost parameters c_w=4.6 and c_0=1500[1] were applied in the optimization procedure.

During the optimum search, a new histogram is calculated for each newly selected number of terminals. Figure 5 shows histograms for N=1, 2, 3. The critical expected time $\tau_\alpha(N)$ approaches zero with the raising number of terminals.

Figure 6 shows the values of the criterion function (2) in dependence of the number of terminals.

Figure 7 shows the way the optimum N* varies with respect to the parameter α. When increasing α, the optimum number of terminals decreases. This could be explained by the fact that increased α leads to the overoptimistic (too short) waiting times. The recommended value is α=0.05.

4 DISCUSSION

The results deserve some comments:

1. The proposed solution depends very much on the quality of the learning data set. Special attention has to be paid to that issue. Namely, incorrect time stamps, associated with the recorded events, do not reflect the actual state of the production process.
2. Surprisingly, the solution presented in this case study turns to be very similar to the heuristic solution applied so far in practice. The rule of thumb being used suggests one terminal for 10 to 15 workers, depending on the size of the plant.
3. Our solution provides clear insight into the expected costs due to the waiting times conditioned with the number of terminals. Moreover, Figure 6 is helpful in figuring out the cost of additional redundancy. More precisely, though the optimum is reached for N*=5, additional costs to install one or even 2 more terminals are almost negligible. However, the overall system s much more robust in case that one or more terminals fail to operate properly.
4. In this stage we did not take into consideration the site distribution of the terminals. Instead, we were only searching for the optimum number of them assuming that the terminals are distributed uniformly along the production plant and the paths between work places and the terminals do not differ much.

5 CONCLUSION

In this paper the problem of optimum terminal arrangement in the production plant is

[1] The units are intentionally omitted.

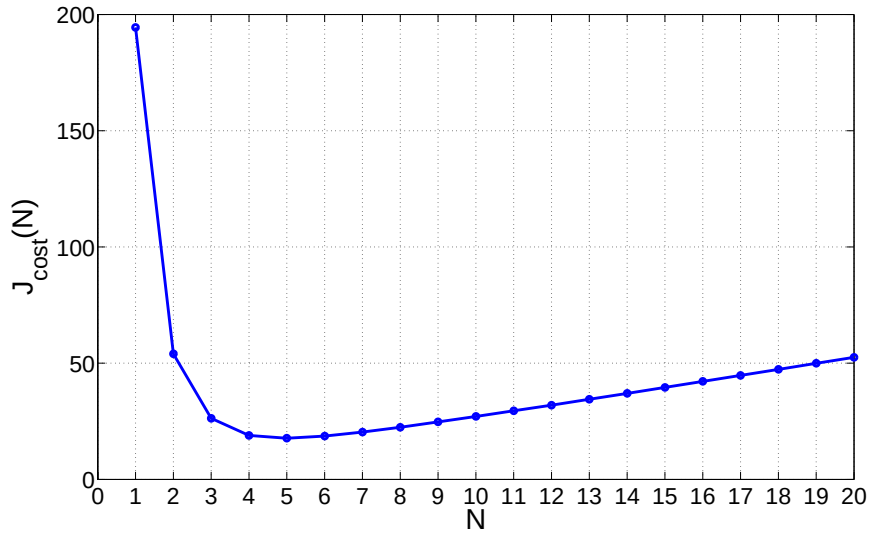

Fig. 6. *Criterion function J_{cost}, for a given critical value α=0.05, shown as a function of the number of terminals N. The lowest value of 17,73 is reached at N = 5.*

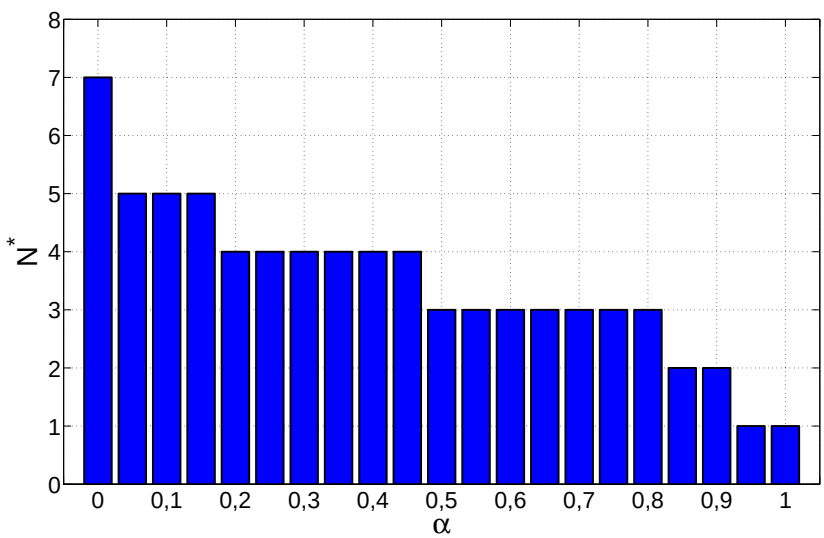

Fig. 7. *Dependence of the optimum number of terminals from the parameter $\alpha \in [0,1]$*

addressed. The problem has been formulated as optimisation of a stochastic criterion function. Main goal of this study was to develop the algorithm for determination of the optimum number of terminals in the manufacturing industries. The proposed criterion function takes into account two types of costs: those due to the waiting times and those caused by the installation of the terminals. One possible upgrade of the presented solution would also consider the geographical dimension of the problem. Namely, it is not possible to install a terminal at any site in the production plant. Availability of power and communication outlets should also be considered. Possible upgrade should concern the application of the information terminals, though they are more expensive than the traditional ones.

6 REFERENCES

[1] Boyer, S. *SCADA: Supervisory Control and Data Acquisition*. ISA, Research Triangle Park, 1999.

[2] Kleindienst J. *The development and implementation of an information system for production monitoring*, MSc. Thesis. Faculty of Economics, University of Ljubljana, 2004. (In Slovenian)

[3] Gradišar, M., Resinovič, G. *Information sciences in business environment*. Faculty of Economics, University of Ljubljana, 2001. (In Slovenian)

[4] Kokošar, S. The information system support to the manufacturing process. *Monitor*, p. 34. (In Slovenian).

[5] Wallace, T., Kremzar, M. *ERP: Making it happen*. New York: John Wiley & Sons, 2001.

[6] Wasserman, L. *All of Statistics: A Concise Course in Statistical Inference*. New York: Springer, 2004.

Strojniški vestnik - Journal of Mechanical Engineering 54(2008)1, 56-61
UDC 621.9.04
Paper received: 26.6.2006
Paper accepted: 28.9.2007

Control of the Cutting Forces in Turning by Entry Angle and Cutting Inserts Geometry

Toma Udiljak* - Stephan Škorić - Damir Ciglar
University of Zagreb, Faculty of Mechanical Engineering and Naval Architecture, Croatia

Machinability is assessed by a set of criteria or machinability functions, the knowledge of which is needed in optimising the machining process. New cutting tool materials and new concepts of the machine tools provide new possibilities and cause quantitative changes in machinability functions. This research has studied the cutting forces function, as one of the crucial machinability functions. The research was done at longitudinal turning of steel 16MnCr5. Coated carbide inserts for roughing and finishing with different inclination angles were used, and tool clamping system has enabled the changes of entry angle. Obtained results confirm that entry angle and geometry of cutting insert significantly influence cutting forces especially thrust cutting force.

Keywords: turning, cutting forces, cutting tool inserts, inserts geometry

0 INTRODUCTION

Main aims of modern machining processes are productivity, economy, accuracy and quality of machined surface, which are achieved by continuous analysis of machinability indicators. Machinability is a very complex term, and it is most often described as the basic technological characteristic of the material and evaluated by a set of criteria or functions of machinability. In metal cutting, the basic set of machinability functions include [1] and [2]:

- function of tool life,
- function of cutting forces,
- function surface roughness,
- function of the chip forms.

Apart from the basic functions, also a number of additional functions are applied such as temperature, material removal rate, built-up-cutting edge, power, etc.

The study of the machinability results also in obtaining the guidelines for the development of the cutting tools. It has contributed to very intensive development of the cutting tools, particularly in the area of high-speed machining, hard machining and dry machining. Improvement of existing and development of new cutting tool materials, same as the new concepts of machine tools, provide new possibilities and change quantitatively the machinability indicators. Therefore, the study of machinability represents a continuous process [3] to [6].

Force modelling in metal cutting is important for a multitude of purposes, including design of machine tools, thermal analysis, tool life estimation, chatter prediction, tool condition monitoring etc. Numerous approaches, in orthogonal and oblique cutting, have been proposed to model metal cutting forces with various degrees of success [7].

1 STUDY OF INFLUENCE OF TECHNOLOGICAL PARAMETERS ON THE CUTTING FORCES

1.1 Goal, methodology and condition of study

The goal of the research is to define the cutting forces as the functions of influencing parameters. Among a great number of influencing parameters, for this research the major entry angle (κ_r) (Fig. 1), machining depth (a_p), feedrate (f), and geometry of cutting insert are selected as independent factors.

The experiment was made in the Laboratory for machine tools of Faculty of Mechanical Engineering and Naval Architecture, University Zagreb, at universal turning machine. Longitudinal turning process has been used, cutting speed 120 m/min, without coolants. A steel for cementation (16MnCr5) was selected. Three different coated carbide inserts have been used:

1) positive cutting insert ($\lambda = 0^o$) for finishing marked as DCMT11T304-FF1 TP2000,

*Corr. Author's Address: University of Zagreb, Faculty of Mechanical Engineering and Naval Architecture, Ivana Lučića 5, HR-10000 Zagreb, Croatia, toma.udiljak@fsb.hr

2) negative cutting insert (λ = -6°):
   a) cutting insert for finishing marked as DNMG150604-FF1 TP2000,
   b) cutting insert for roughing marked as DNMG150604-M5 TP2000.

Tool clamping system has enabled the changes of entry angle (Fig. 1). The measurement of cutting forces was made by three-component measuring device "Kistler 9257B".

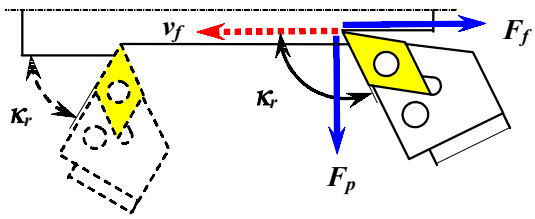

Fig. 1. *Scheme of longitudinal turning with exchangeable (adaptable) entry angle* κ_r

1.2 Research results obtained with positive cutting insert for finishing (λ = 0°)

Statistical analysis of experimental data (SW Statistica) resulted with mathematical models presented by:

$$F_c = 1207.5 - 26.5\ \kappa_r + 0.14\ \kappa_r^2 + 1.6\ \kappa_r\ a_p + 2196.5\ a_p\ f \quad (1)$$

$$F_f = -223.2 + 201.7\ a_p + 1.57\ \kappa_r\ a_p + 1025.6\ a_p\ f \quad (2)$$

$$F_p = -403.3 + 0.049\ \kappa_r^2 + 708\ a_p + 3206.5\ f - 7.45\ \kappa_r\ a_p - 28.26\ \kappa_r\ f \quad (3).$$

Graphical interpretations of the obtained mathematical models are presented in Figures 2 to 4.

Figure 2 shows that the main cutting force slightly increases with the increase of the entry angle. More adequate explanation is obtained by single-factorial analysis, whose results are shown on Figure 5.

Figure 3 shows that feed cutting force also slightly increases by increasing the entry angle even when it's value exceeds 90°. Such result differs from Kienzle's formula and can be caused by the same reasons as the increase of the main cutting force.

Figure 4 shows that passive cutting force is considerably reduced by increasing the entry angle. Furthermore, for certain combination of cutting data, passive cutting force can take negative values.

Single-factorial analysis (Fig. 5) shows that significant increase of main cutting force happens when entry angle exceeds 90°. It is the situation in which contact length between the cutting edge and the workpiece is increased and the end cutting edge angle, κ_r', is reduced. As a result there is a significant amount of friction from three sides, as shown on Figure 1. That fact can be cause of formidable increase in roughness of the machined surface, as shown in Figure 6.

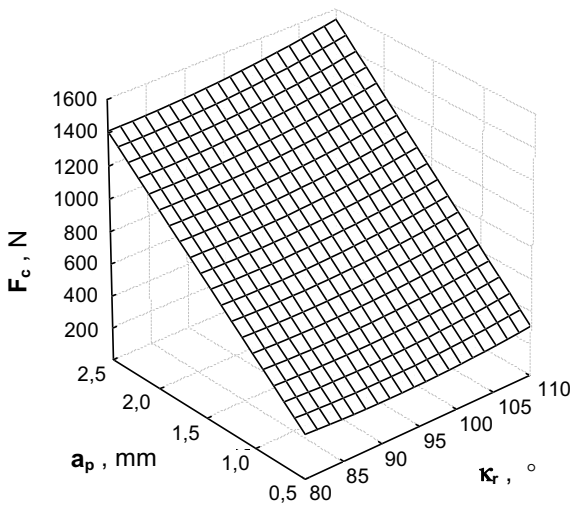

Fig. 2. *Main cutting force as a function of cutting depth and entry angle (cutting insert for finishing,* λ = 0°, *f = 0.2 mm)*

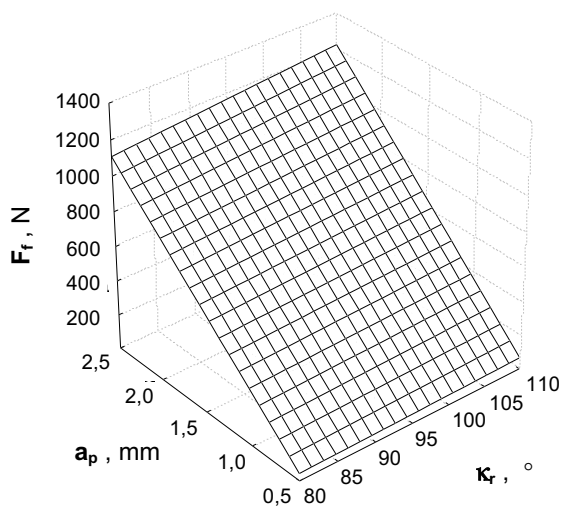

Fig. 3. *Feed cutting force as a function of entry angle and cutting depth (cutting insert for finishing,* λ = 0°, *f = 0.2 mm)*

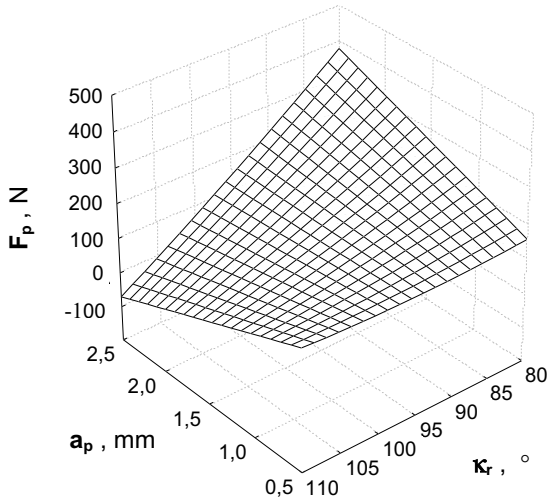

Fig. 4. *Passive cutting force as a function of entry angle and cutting depth (cutting insert for finishing, $\lambda = 0^o$, $f = 0.2$ mm)*

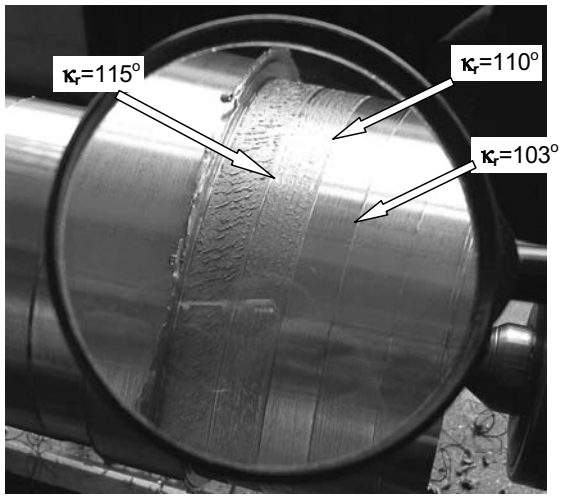

Fig. 6. *Roughness of the machined surface as a function of entry angle (v_c =120 mmin $^{-1}$, a_p =2.5 mm, f = 0.16 mm)*

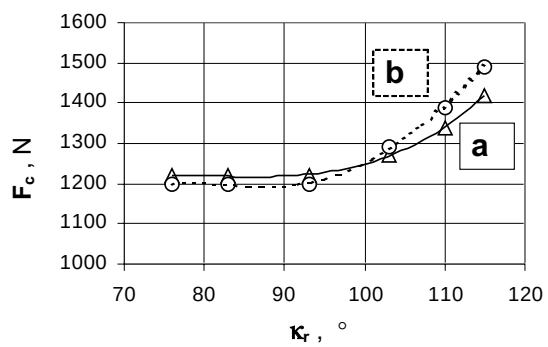

Fig. 5. *Main cutting force as a function of entry angle (a_p =2.5 mm, f = 0.16 mm)*
a – positive cutting insert for finishing,
b – negative cutting insert for finishing

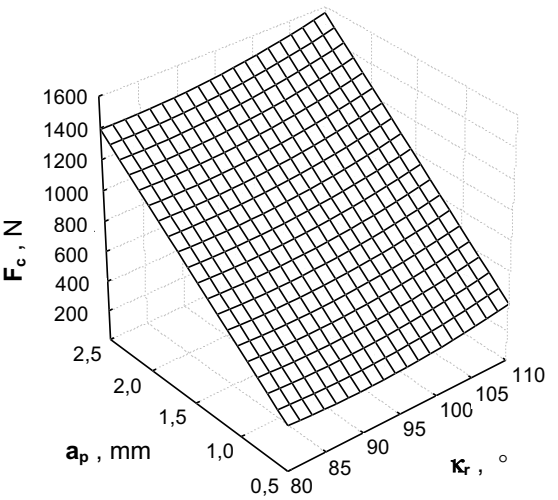

Fig. 7. *Main cutting force as a function of cutting depth and entry angle (cutting insert for finishing, $\lambda = -6^o$, $f = 0.2$ mm)*

1.3 Research results obtained with negative cutting insert ($\lambda = -6^o$)

1.3.1 Cutting insert for finishing

Statistical analysis of experimental data (SW Statistica) resulted with mathematical models presented by:

Figure 7 shows that by increasing the entry angle, the main cutting force is increased. Also, obtained results don't show significant difference compared to positive cutting insert, except in the area of greater values of entry angle. In that area

$$F_c = 1742.8 - 38.36\ \kappa_r + 0.21\ \kappa_r^2 + 1.52\ \kappa_r a_p + 2113.5\ a_p f \quad (4)$$

$$F_f = -158.12 + 188.43\ a_p + 1.54\ \kappa_r a_p + 982.36\ a_p f \quad (5)$$

$$F_p = -462.84 + 0.053\ \kappa_r^2 + 607.24\ a_p + 4234.6\ f - 6.3\ \kappa_r a_p - 37.9\ \kappa_r f \quad (6).$$

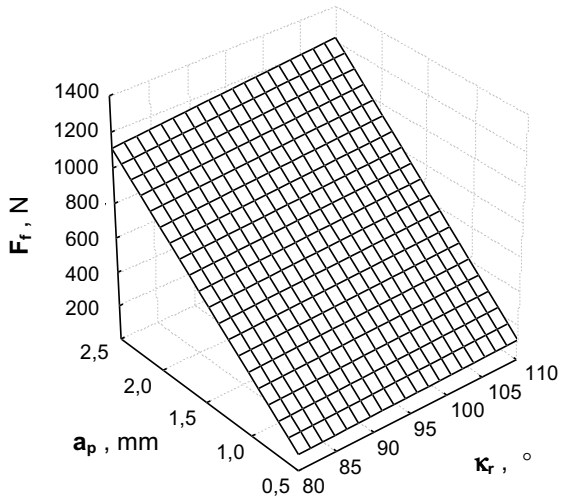

Fig. 8. *Feed cutting force as a function of cutting depth and entry angle (cutting insert for finishing, λ = -6°, f = 0.2 mm)*

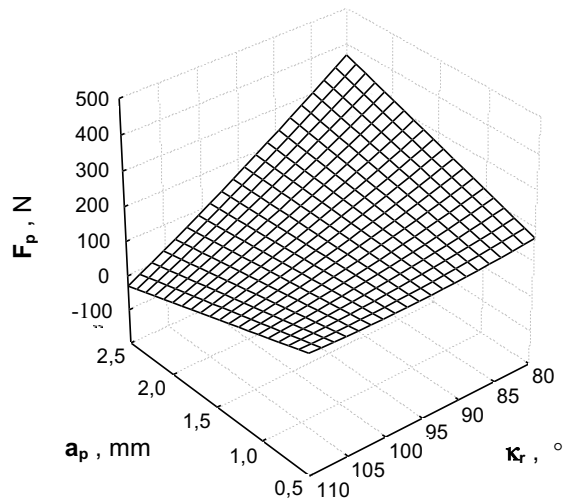

Fig. 9. *Passive cutting force as a function of entry angle and cutting depth (cutting insert for finishing, λ = -6°, f = 0.2 mm)*

(Fig. 5) was measured more significant increase of main cutting force, caused by the fact that tools with negative cutting insert (λ_s= -6°) have formidably reduced end clearance angle.

Figure 8 shows that by increasing the entry angle, the feed cutting force is increased even when its value exceeds 90°. Also, obtained results don't show significant difference compared to positive cutting insert.

Figure 9 shows that by increasing the entry angle, the passive cutting force is formidably reduced. Furthermore, passive cutting force can take negative values for certain cutting data combinations. However, negative values are harder to achieve than using positive cutting insert. This is mainly consequence of the fact that tools with negative cutting insert have formidably reduced end clearance angle.

1.3.2 Cutting insert for roughing

Statistical analysis of experimental data (SW Statistica) resulted with mathematical models presented by:

Graphical interpretations of the obtained mathematical models are presented in Figures 10, 12 and 13. Graphical presentation of single-factorial analysis of main cutting forces for negative cutting inserts (for roughing and finishing) as a function of entry angle is given in Figure 11.

Analysis of Figures 10 and 11 shows that shape of main cutting force, obtained with cutting insert for roughing, differ in some elements from shape of main cutting force, obtained with cutting insert for finishing. In the area with lesser values of entry angle and higher values of cutting depth, measured values of main cutting force obtained with cutting insert for roughing are smaller. However, in the area with higher values of entry angle measured values are formidably increased.

Analysis of Figure 12 shows that shape of feed cutting force, in the area of all values of entry angle, is similar as for main cutting force.

Analysis of Equation 9 and its graphical presentation, Figure 13, shows that the increase entry angle, at higher values of cutting depth formidably reduces the passive cutting force. However, passive cutting force can't take negative values.

$$F_c = 2948.76 - 62.28\kappa_r + 0.34\kappa_r^2 - 196.3a_p + 2.52\kappa_r a_p + 2052.1a_p f \quad (7)$$

$$F_f = 1551.7 - 34.05\kappa_r + 0.2\kappa_r^2 + 1.15\kappa_r a_p + 883.43a_p f \quad (8)$$

$$F_p = 1599.3 - 35.75\kappa_r + 0.21\kappa_r^2 + 311.38a_p + 1586.9 f - 3.65\kappa_r a_p - 13.95\kappa_r f + 293.7a_p f \quad (9).$$

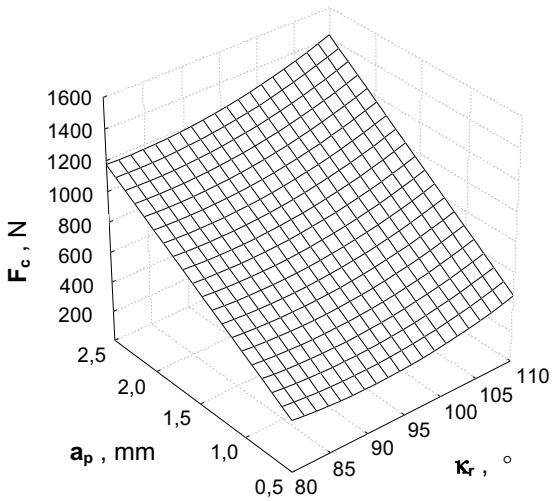

Fig. 10. *Main cutting force as a function of entry angle and cutting depth (cutting insert for roughing, λ = -6°, f = 0.2 mm)*

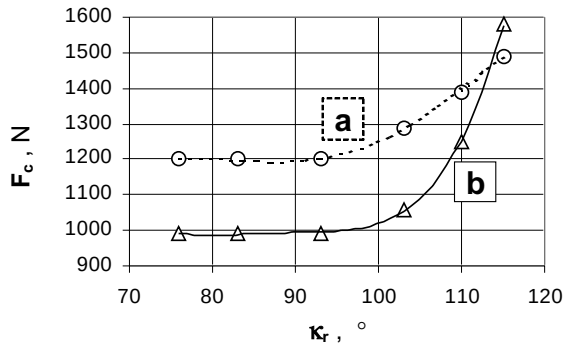

Fig. 11. *Main cutting force as a function of entry angle (a_p =2.5 mm, f = 0.16 mm) a – cutting insert for finishing, b – cutting insert for roughing*

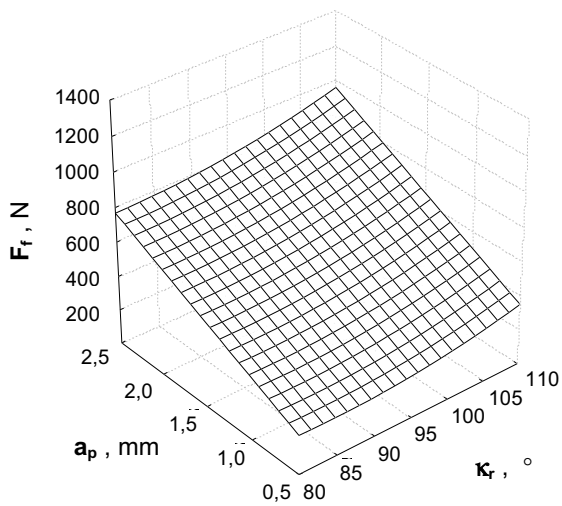

Fig. 12. *Feed cutting force as a function of entry angle and cutting depth (cutting insert for roughing, λ = -6°, f = 0.2 mm)*

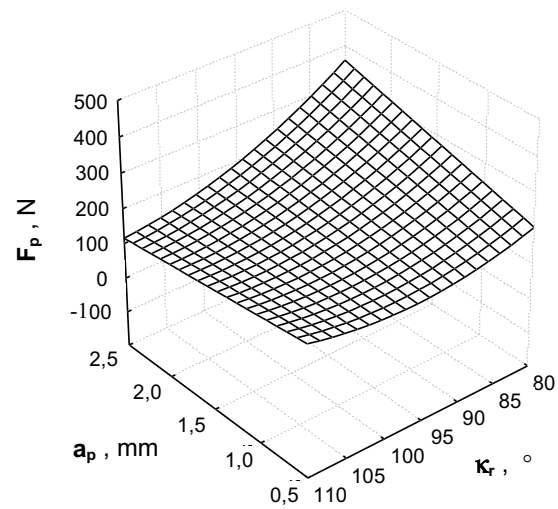

Fig. 13. *Passive cutting force as a function of entry angle and cutting depth (cutting insert for roughing, λ = -6°, f = 0.2 mm)*

2 CONCLUSION

Obtained results confirm the possibility to control the thrust cutting force with entry angle, what is particularly important when turning lean workpieces (high ratio length/diameter), and thin wall workpieces. Analysis of mathematical models and their graphical presentations, shows that the increase of the entry angle, at higher values of cutting depth, formidably reduces the passive cutting force. However, passive cutting force, by cutting insert for roughing, can't take negative values.

However, it should be noted that there is no research of cutting tool temperature, chattering or surface roughness. In situation when cutting tool has significant amount of friction from three sides, and generated heat is almost captured, the complete picture of influence of entry angle is still missing. The generated heat in conjunction with reduced cutting tool cross section (caused with increased entry angle) could significantly reduce tool life, what would, in great extent, neutralize the positive effect of reduced thrust cutting force. Potential field of application would be adaptive control of

B axis with carefully selected limits. That would open possibility to optimize the machining conditions by adjusting entry angle in contour turning operations.

3 REFERENCES

[1] König, W. *Fertigungsverfahren*, Band 1. Düsseldorf: *VDI Verlag,* 1990.

[2] Škorić, S. *Study of suitability of machining by orthogonal turn-milling*, Dissertation. Zagreb: FSB, 2002. (In Croatian).

[3] Oxley, P.L.B. Modelling machining processes with a view to their optimization and to the adaptive control of metal cutting machine tools. *Robotics & Computer-Integrated Manufacturing*, 1988, Vol. (4)(1/2), p. 103-119.

[4] Čuš, F., Balič, J. Selection of cutting conditions and tool flow in flexible manufacturing system. *J. mater. process. technol.*, 2001, Vol. 118, p. 485-489.

[5] Kopač, J. Cutting tool wear during high-speed cutting. *Strojniški vestnik - Journal of Mechanical Engineering*, 2004, Vol. 50, No. 4, p. 195-205.

[6] Udiljak,T., Mulc, T. Monitoring of cutting tool wear by using control system signal. *6th International Scientific Conference on Production Engineering*, Lumbarda, 2000. p. I-077 I-094. ISBN 953-97181-2-0.

[7] Altintas, Y. *Manufacturing automation*, Cambridge: Cambridge University Press, 2000.

Strojniški vestnik - Journal of Mechanical Engineering 54(2008)1, 62-67
UDC 621.3.077.2
Paper received: 18.12.2006
Paper accepted: 19.12.2007

Exponential Tracking Control of an Electro-Pneumatic Servo Motor

Dragan V. Lazić
University of Belgrade, Faculty of Mechanical Engineering, Serbia

According to the fundamental importance of the tracking theory on technical systems, the main goal of this paper is a further development of the theory and the application of the tracking, especially to the practical tracking concept.

The new definition of the practical exponential tracking is shown. The practical tracking is defined by the output vector, which is different from the former definitions, given by the output error vector. The defined exponential tracking is elementwise. The new criterion of the practical exponential tracking is shown. Based of the new criteria, the control algorithm of practical exponential tracking is determined by using the self-adaptive principle. The structural characteristic of such a control system is the existence of two feedback sources: the global negative of the output value and the local positive of the control value. Such a structure ensures the synthesis of the control without the internal dynamics knowledge and without measurements of disturbance values.

The plant under consideration is an electro-pneumatic servo motor. This system is often applied as the final control element of a controller in automatic control systems. The correction device for the mentioned plant will be a digital computer. The mentioned control forces the observed plant output to track the desired output value with prespecified accuracy. In this paper the simulation results produced by practical tracking control algorithm on an electro-pneumatic servosystem will be presented.

The results show a high quality of the practical exponential tracking automatic control. The type of the control ensures the change of the output error value according to a prespecified exponential law.

Keywords: electro-pneumatic servo systems, servo motors, non-linear systems, self adaption

0 INTRODUCTION

The practical tracking concept is very important from the technical viewpoint. The consideration of the dynamics behavior of technical plants during a limited time interval, with a prespecified quality of that behavior, imposes a practical request and necessities, which can be placed to any technical plant. For many plants the most adequate tracking concept is the practical tracking concept. The concept most completely satisfies practical technical requirements on the dynamics behavior as well as the quality of the dynamics behavior. The practical tracking concept includes physically possible and realizable initial deviations of the output value, maximum deviations of the output value permitted in relation to the desired output value (according to the desired accuracy), a set of expected and unexpected disturbances during such a time interval, which is of a technical interest. The elementwise exponential tracking has been defined. Each element of vector y should exponentially approach the appropriate element of vector y_d. Elementwise exponential tracking was introduced by Grujic and Mounfield [1] to [6]. In those papers the Lyapunov approach to the exponential tracking study is used. The approach assumes the existence of the bound (envelope of the output error vector) which limits the exponential evolution of the output error vector, but that bound is not predefined. In this framework the bounds are predefined and determined with the function set $I_A(\cdot)$ and scalar β.

The nonuniform practical exponential tracking is introduced by Lazic [7], where definitions, criteria and algorithms for such tracking are presented for a certain class of technical objects.

*Corr. Author's Address: University of Belgrade, Faculty of Mechanical Engineering, Automatic Control Department, Kraljice Marije 16, 11120 Belgrade, Serbia, dragan.lazic@gmail.com

1 PROBLEM STATEMENT AND SIGNIFICANCE

The object considered can be described by a mathematical model expressed by the state and the output equations:

$$\dot{\mathbf{x}}(t)=\mathbf{f}\left[\mathbf{x}(t),\mathbf{d}(t)\right]+B\mathbf{u}(t)$$
$$\mathbf{y}(t)=\mathbf{g}\left[\mathbf{x}(t)\right] \quad (1).$$

The admitted bounds of the vector y of the object real dynamic behavior are determined by the vector of desired dynamic behavior $\mathbf{y}_d$ and sets E_I and E_A, as follows:

$$I_I(\mathbf{y}_{d0};E_I)=\left\{\mathbf{y}_0:\mathbf{y}_0=\mathbf{y}_{d0}-\mathbf{e}_0,\mathbf{e}_0\in E_I\right\} \quad (2),$$

$$I_A(t;\mathbf{y}_d(\cdot);E_A)=\left\{\mathbf{y}:\mathbf{y}=\mathbf{y}_d(t)-\mathbf{e},\mathbf{e}\in E_A\right\} \quad (3).$$

2 DEFINITION

The system Eq. (1) controlled by $\mathbf{u}(\cdot)\in S_u$ exhibits the practical exponential tracking with respect to $\left\{\tau,\Lambda,\beta,I_I(\cdot),I_A(\cdot),S_d,S_z\right\}$, (Fig. 1), if $\left[\mathbf{y}_0,\mathbf{y}_d(\cdot),\mathbf{d}(\cdot)\right]\in I_I(\mathbf{y}_{d0})\times S_d\times S_z$ implies:

$$\mathbf{y}\left[t,\mathbf{y}_0,\mathbf{u}(\cdot),\mathbf{y}_d(\cdot),\mathbf{d}(\cdot)\right]\in I_A(t),\forall t\in R_\tau \quad (4),$$

and for $\forall i\in\{1,2,\ldots,n\}$ and $\forall t\in R_\tau$ holds

$$y_i\left[t,y_{i0},\mathbf{u}(\cdot),\mathbf{y}_d(\cdot),\mathbf{d}(\cdot)\right]\geq y_{di}(t)-\alpha_i\left(y_{di0}-y_{i0}\right)e^{-\beta t},\ y_{i0}\leq y_{di0} \quad (5),$$

and

$$y_i\left[t,y_{i0},\mathbf{u}(\cdot),\mathbf{y}_d(\cdot),\mathbf{d}(\cdot)\right]\leq y_{di}(t)-\alpha_i\left(y_{di0}-y_{i0}\right)e^{-\beta t},\ y_{i0}\geq y_{di0} \quad (6).$$

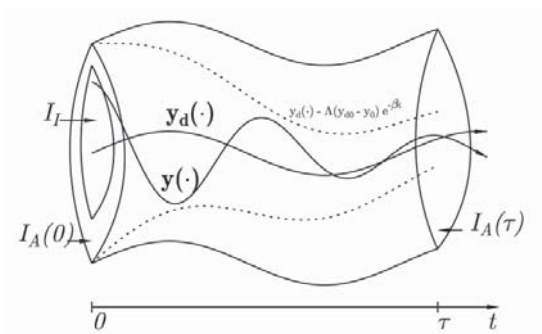

Fig. 1. *Practical exponential tracking*

3 CRITERIA

In order for the system Eq. (1) controlled by $\mathbf{u}(\cdot)$ to exhibit practical exponential tracking with respect to $\left\{\tau,\mathrm{I},\beta,I_I(\cdot),I_A(\cdot),S_d,S_z\right\}$ it is sufficient that control $\mathbf{u}(\cdot)$ guaranties:

$$\mathbf{e}\left[t,\mathbf{e}_0,\mathbf{u}(\cdot),\mathbf{y}_d(\cdot),\mathbf{d}(\cdot)\right]=-\gamma\mathbf{e},\forall\left[t,\mathbf{e}_0,\mathbf{y}_d(\cdot),\mathbf{d}(\cdot)\right]\in R_\tau\times E_I\times S_d\times S_z \quad (7),$$

where $\gamma\in[\beta,+\infty[$.

Arbitrary $\mathbf{y}_d(\cdot)\in S_d$, $\mathbf{d}(\cdot)\in S_z$, $e_{i0}\in E_{Ii}$ and $i\in\{1,2,\ldots,n\}$ is considered. From Eq. (7) it follows that:

$$e\left(t;\mathbf{e}_0;\mathbf{u}(\cdot),\mathbf{y}_d(\cdot),\mathbf{d}(\cdot)\right)=\mathbf{e}_0e^{-\gamma t},\ \forall t\in R_\tau,$$

or in scalar form:

$$e_i\left[t;e_{i0};\mathbf{u}(\cdot),\mathbf{y}_d(\cdot),\mathbf{d}(\cdot)\right]=e_{i0}e^{-\gamma t},\ \forall t\in R_\tau \quad (8).$$

This equation expresses exponential decrease of the function $e_i(\cdot)$, from starting value e_{i0} towards zero. Since $e_{i0}\in E_{Ii}\subseteq E_{Ai}$ the value of the error in any time is less than e_{iMA}, and greater than e_{imA}. It means that the object exhibits practical tracking with respect to $\left\{\tau,I_I(\cdot),I_A(\cdot),S_d,S_z\right\}$, Lazić [7]:

$$\mathbf{y}\left[t;\mathbf{y}_0;\mathbf{u}(\cdot),\mathbf{y}_d(\cdot),\mathbf{d}(\cdot)\right]\in I_A(t)$$
$$\forall\left[t,\mathbf{y}_0,\mathbf{y}_d(\cdot),\mathbf{d}(\cdot)\right]\in R_\tau\times I_I(\mathbf{y}_{d0})\times S_d\times S_z \quad (9).$$

Based on Eq. (8) and the condition of theorem $\gamma\in[\beta,+\infty[$, it follows that

$$e_i\left[t;e_{i0};\mathbf{u}(\cdot),\mathbf{y}_d(\cdot),\mathbf{d}(\cdot)\right]\leq e_{i0}e^{-\beta t},\ \forall t\in R_\tau,\ e_{i0}>0 \quad (10),$$

$$e_i\left[t;e_{i0};\mathbf{u}(\cdot),\mathbf{y}_d(\cdot),\mathbf{d}(\cdot)\right]\geq e_{i0}e^{-\beta t},\ \forall t\in R_\tau,\ e_{i0}<0 \quad (11),$$

and

$$e_i\left[t;0;\mathbf{u}(\cdot),\mathbf{y}_d(\cdot),\mathbf{d}(\cdot)\right]=0,\ \forall t\in R_\tau,\ e_{i0}=0 \quad (12).$$

Now, using Eq. (10), Eq. (11), Eq. (12), $e_i(t)=y_{di}(t)-y_i(t)$, $\forall t\in R_\tau$, the function set definitions $I_I(\cdot)$ and $I_A(\cdot)$, Eq. (2) and Eq. (3), and $\alpha_i=1$, $\Lambda=\mathrm{I}$, one gets:

$$y_i\left[t;y_{i0};\mathbf{u}(\cdot),\mathbf{y}_d,\mathbf{d}(\cdot)\right]\geq y_{di}(t)-\alpha_i\left(y_{di0}-y_{i0}\right)e^{-\beta t},\ y_{i0}\leq y_{di0},\ \forall t\in R_\tau \quad (13),$$

$$y_i\left[t;y_{i0};\mathbf{u}(\cdot),\mathbf{y}_d,\mathbf{d}(\cdot)\right]\leq y_{di}(t)-\alpha_i\left(y_{di0}-y_{i0}\right)e^{-\beta t},\ y_{i0}\geq y_{di0},\ \forall t\in R_\tau \quad (14),$$

which considering the arbitrary chosen $\left[e_{i0},i,\mathbf{y}_d,\mathbf{d}(\cdot)\right]\in E_{Ii}\times\{1,2,\ldots,n\}\times S_d\times S_z$, together with Eq. (9) satisfies the definition and proofs the theorem.

4 ALGORITHM

The algorithm is based on the natural tracking control concept introduced by Grujic. The main characteristic of this concept, which follows from the self-adaptive principle, Grujic [8] to [10], is the existence of the local positive feedback in the control **u** (with possible derivative and/or integrals of **u**). The local positive feedback compensates for the influences of the disturbances and the internal dynamics of the controlled object, since, during the control construction the information about them is not used.

The main negative feedback loop in the output y (with possible derivatives and/or integrals of y) provides the desired quality of the error evolution.

The values of all vector elements $\mathbf{y}(t)$ and $\dot{\mathbf{y}}(t)$ from Eq. (1) are measurable in any time instant $t \in R_\tau$.

Let Assumption 1 hold, let $S_u = \{\mathbf{u}(\cdot)\}$ and control $\mathbf{u}(\cdot)$:

$$\mathbf{u}(t) = \mathbf{u}(t^-) + \mathrm{D}^T\left(\mathrm{DD}^T\right)^{-1}\left[\dot{\mathbf{e}}(t) + \gamma\mathbf{e}(t)\right] \quad \forall\left[t, \mathbf{e}_0, \mathbf{y}_d, \mathbf{d}(\cdot)\right] \in R_\tau \times E_I \times S_d \times S_z \tag{15},$$

where D is an arbitrary matrix satisfied $\det\left(\mathrm{DD}^T\right) \neq 0$, and $\gamma \in [\beta, +\infty[$.

System Eq. (1) controlled by $\mathbf{u}(\cdot)$, Eq. (15), exhibits The practical exponential tracking with respect to $\{\tau, \mathrm{I}, \beta, I_I(\cdot), I_A(\cdot), S_d, S_z\}$.

If there is no delay in the feedback loop than $\mathbf{u}(t) = \mathbf{u}(t^-)$, Grujic [8] to [10], and following the vector equation Eq. (15) one gets:

$$\mathrm{D}^T\left(\mathrm{DD}^T\right)^{-1}\left[\dot{\mathbf{e}}(t) + \gamma\mathbf{e}(t)\right] = \mathbf{0} \quad \forall\left[t, \mathbf{e}_0, \mathbf{y}_d(\cdot), \mathbf{d}(\cdot)\right] \in R_\tau \times E_I \times S_d \times S_z \tag{16}.$$

By multiplying that equation with matrix D from the left side, the following equation is obtained:

$$\dot{\mathbf{e}}(t) = -\gamma\mathbf{e}(t), \ \forall\left[t, \mathbf{e}_0, \mathbf{y}_d(\cdot), \mathbf{d}(\cdot)\right] \in R_\tau \times E_I \times S_d \times S_z \tag{17},$$

which, based on $\gamma \in [\beta, +\infty[$ and the former theorem proves this theorem.

This algorithm presents a further justification of the approach of the natural tracking control by Grujic and Mounfield. The natural trackability condition is not considered here. A further implementation of this algorithm in the present paper is a simplify attempt and matrix D will be chosen as an arbitrary matrix.

5 APPLICATION

In this case an electro-pneumatic servo motor as a plant, presented in Figure 2, is considered. It consists of:

1. a single acting membrane pneumatic motor,
2. potentiometer (displacement transducer),
3. electro-pneumatic transducer (EPT).

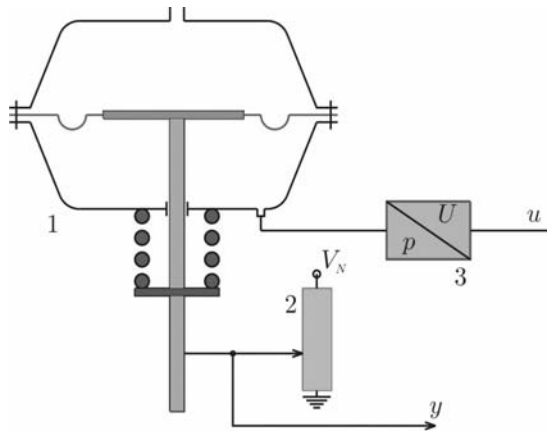

Fig. 2. *Electro-pneumatic servo motor*

The mathematical model of the mentioned plant is shown Lazic [11]. Here the first order EPT is accepted and verified by experimental results. The electrical part of EPT is very fast and the air volume of pneumatic line and motor chamber are relatively small. For this plant that simplification is very closed to the exact mathematical model of EPT with a pneumatic motor when their air volume determines variable τ_p by a very complex formula.

$$\tau_p \frac{dp(t)}{dt} + p(t) = K_p u(t)$$
$$B_v \frac{dy(t)}{dt} + K_o y(t) + c_t \operatorname{sgn}\left[\dot{y}(t)\right] = A_m p(t) \tag{18},$$

where:

y - motor spindle displacement,
u - voltage control signal,
p - EPT output pressure.

A block diagram of the considered plant is shown in Figure 3.

The technical characteristics of the plant are:

$\tau_p = 0.45$ s - EPT time constant,
$K_p = 0.229 \cdot 10^5$ Pa/V - EPT gain,
B_v = 63050 Ns/m - damping factor,
c_t = 93.5 N - Coulomb friction coefficient,
R_L = 175 Ω - EPT coil resistance,
K_o = 150857.14 N/m - motor spring stiffness,

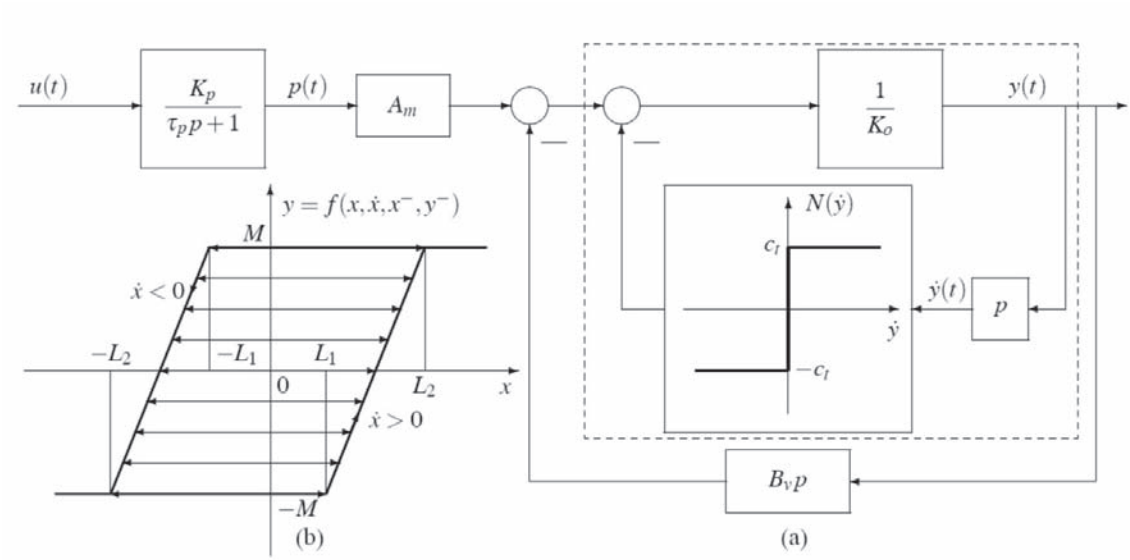

Fig.3. *(a) The plant block diagram, (b) the equivalent nonlinearity of the plant part shown in the dashed box of (a)*

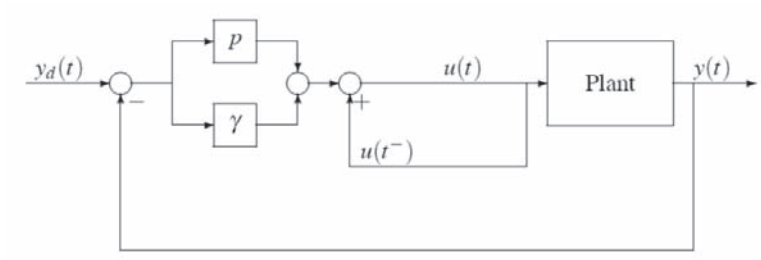

Fig. 4. *Control system block diagram*

A_m = 330·10^{-3} m^2 - membrane area,
y_{max} = 17.5 mm - maximum motor spindle displacement.

A symbolic block diagram of the control system is presented in Figure 4.

The digital computer simulation of the practical exponential tracking control algorithm, based on the self-adaptive principle, in the form:

$$u(t) = u(t^-) + \mathrm{D}\left[\dot{e}(t) + \gamma e(t)\right] \qquad (19),$$

for a prespecified $\beta = 1$, chosen $\gamma = 1.5$ $(\gamma \in [\beta, +\infty[)$, and $\mathrm{D} = 0.1$ is done. The illustration of the results achieved by the practical exponential tracking algorithm simulation can be seen in Figures 5 to 8.

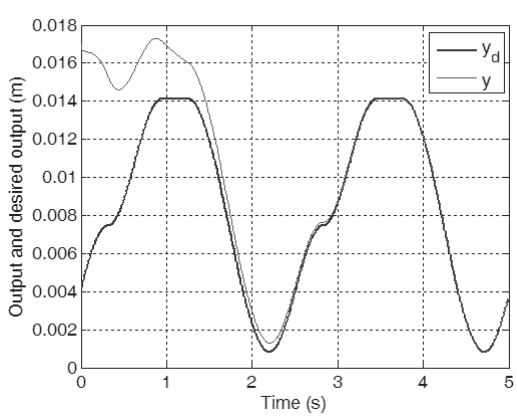

Fig. 5. *Output and desired output*

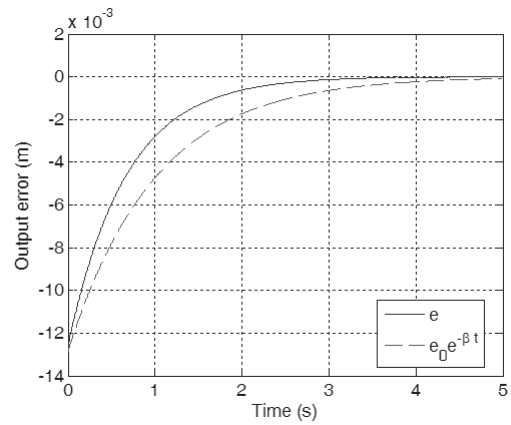

Fig. 6. *Output error behavior*

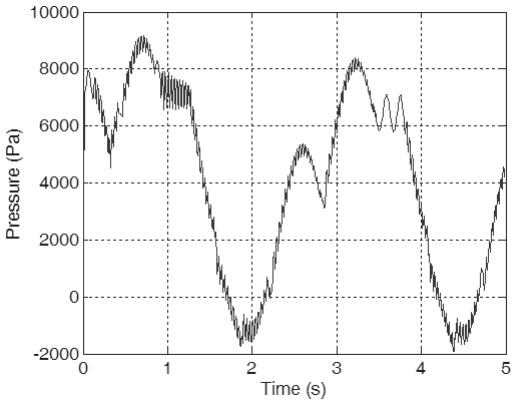

Fig. 7. *Electro-pneumatic transducer: output pressure signal*

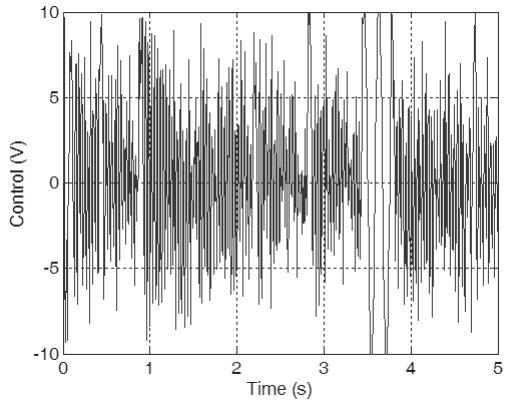

Fig. 8. *Control signal*

From Figure 5 it can be seen that the real output *y* is very smooth, and the difference between *y* and y_d is in permitted boundaries, which can be seen in Figure 6, the exponential error change $e(\cdot)$ is in permitted boundaries $e_0 e^{-\beta(\cdot)}$.

The command pressure (electro-pneumatic transducer pressure) signal behavior is illustrated in Figure 7. The control value **u** (Fig. 8) is rather rough but lies in the standard signal range -10V to +10V, without saturations. High frequency components in the control signal are a consequence of physical sources - existence of the hysteresis nonlinearity in the plant.

6 CONCLUSIONS

The results show a high quality of the practical exponential tracking automatic control. This type of control ensures a change of output error value according to a prespecified exponential law. For the control design, the internal dynamics of the controlled object need not be known and the measurement of the real output values only is required. The practical tracking control algorithm is based on the self-adjustment principle. The main characteristic of this principle is the existence of the local positive feedback in the control u. The algorithm has been proved based on an assumption that there is no delay in the local positive feedback loop. Over a digital computer simulation, the smaller time step provides the better approximation of the proposed algorithm. Since very small sampling period can be realized by using the up-to-date digital computers, no possible limitations are expected during the implementation on a real system.

7 NOMENCLATURE

$B \in R^{q \times r}$ matrix
$D \in R^{n \times q}$ arbitrary matrix
$\mathbf{d}(\cdot): R \to R^p$ the disturbance vector function
$\mathbf{d}(t)$ the disturbance vector at time *t*
$\mathbf{d} \in R^p$ the disturbance vector
$E_A \subset R^n$ the set of all admitted errors $\mathbf{e}(t)$ on R_τ; closed connected neighborhood of $\mathbf{0}_e$
$E_I \subset R^n$ the set of all admitted initial errors $\mathbf{e}(0) = \mathbf{e}_0$; closed connected neighborhood of $\mathbf{0}_e$
$E_{(\cdot)i} = \left\{ e_i : e_i \in R, e_{im(\cdot)} \le e_i \le e_{iM(\cdot)} \right\}$, $(\cdot)=A,I$
$\mathbf{e}\left[\cdot; \mathbf{e}_0; \mathbf{u}(\cdot), \mathbf{y}_d(\cdot), \mathbf{z}(\cdot)\right]: R \to R^n$ the output error response, which at time t represents the output error vector $\mathbf{e}(t)$ at the same time $\mathbf{e}\left[t; \mathbf{e}_0; \mathbf{u}(\cdot), \mathbf{y}_d(\cdot), \mathbf{z}(\cdot)\right] = \mathbf{e}(t)$
$\mathbf{e} \in R^n$ the output error vector, $\mathbf{e} = \mathbf{y}_d - \mathbf{y}$
$\mathbf{e}_{m(\cdot)} = \min\left\{ \mathbf{e} : \mathbf{e} \in E_{(\cdot)} \right\}$, $(\cdot)=A,I$, elementwise minimization
$\mathbf{e}_{m(\cdot)} = \left(e_{1m(\cdot)} \; e_{2m(\cdot)} \; \ldots \; e_{nm(\cdot)} \right)^T$, $(\cdot)=A,I$
$\mathbf{e}_{M(\cdot)} = \max\left(\mathbf{e} : \mathbf{e} \in E_{(\cdot)} \right)$, $(\cdot)=A,I$, elementwise maximization
$\mathbf{e}_{M(\cdot)} = \left(e_{1M(\cdot)} \; e_{2M(\cdot)} \; \ldots \; e_{nM(\cdot)} \right)^T$, $(\cdot)=A,I$
$\mathbf{f}(\cdot): R^q \times R^p \to R^q$ the continuous vector function, $\mathbf{f}(\mathbf{x}, \mathbf{z}) \in C\left(R^q \times R^p\right)$, which describes plant internal dynamics
$\mathbf{g}(\cdot): R^q \to R^n$ the output function
$I_A(\cdot): R \times R^n \times 2^{R^n} \to 2^{R^n}$, the set function of all admitted vector functions $y(\cdot)$ on R_τ with respect to $\mathbf{y}_d(\cdot)$ and E_A
$I_A(t) = I_A\left[t; \mathbf{y}_d(\cdot); E_A\right]$, the set value of the set function $I_A(\cdot)$ at time t, with respect to $\mathbf{y}_d(\cdot)$ and E_A
$I_I(\cdot): R^n \times 2^{R^n} \to 2^{R^n}$, the set function of all admitted vector functions $\mathbf{y}_0$ with respect to $\mathbf{y}_{d0}$ and E_I

$I_I(\mathbf{y}_{d0}; E_I)$ the set value of the set function $I_I(\cdot)$ at time t, with respect to $\mathbf{y}_{d0}$ and E_I; if $\mathbf{y}_{d0}$ is chosen $\Rightarrow I_I(\mathbf{y}_{d0}; E_I) = I_I$

$R^+ =]0, +\infty[= \{t : t \in R, 0 < t < +\infty\}$

$R_0 = [t_0, \infty[$

$R_\tau = [0, \tau[$

$S_d \subset R^n$ the set of all admitted $y_d(\cdot)$ on R_τ; $\mathbf{y}_d(\cdot) \in S_d \Rightarrow \mathbf{y}_d(t) \in C(R_\tau, R^n)$

$S_z \subset R^p$ the set of all admitted $\mathbf{d}(\cdot)$ on R_τ

t time

$\mathbf{u}(\cdot): R \times ... \rightarrow R^r$ the vector function which describes evolution of the control vector

$\mathbf{u}(t)$ the value of the function $\mathbf{u}(\cdot)$ at time t

$\mathbf{u} \in R^r$ the control vector

$\mathbf{x} \in R^q$ the state vector

$\mathbf{y}[\cdot; \mathbf{y}_0; \mathbf{u}(\cdot), \mathbf{y}_d(\cdot), \mathbf{d}(\cdot)]$ the real output response, which at time t equals the real output vector at same time,

$\mathbf{y}[t; \mathbf{y}_0; \mathbf{u}(\cdot), \mathbf{y}_d(\cdot), \mathbf{d}(\cdot)] = \mathbf{y}(t)$

$\mathbf{y} \in R^n$ the real output vector

$\mathbf{y}_d(\cdot): R \rightarrow R^n$ the desired output vector function

$\mathbf{y}_d(t)$ the desired output vector at time t

$\mathbf{y}_d \in R^n$ the desired output vector

$\beta \in R^+$

$\gamma \in [\beta, +\infty[$

$\Lambda \in R^{n \times n}$, $\Lambda = \mathrm{diag}\{e_{1MA}\ e_{2MA}\ ...\ e_{nMA}\}$

$\tau \in]0, +\infty]$ the final moment

$\mathbf{0} = (0\ 0\ ...\ 0)^T \in R^q$

8 REFERENCES

[1] Mounfield,W.P., Grujić, L.T. High-gain PI natural control for exponential tracking of linear single-output systems with state-space description. *RAIRO-APII*, 1992, Vol. 26, p. 125-146.

[2] Grujić, L.T., Mounfield, W.P. Natural tracking PID process control for exponential tracking. *American Institute of Chemical Engineers Journal*, 1992, Vol. 38, No. 4, pp. 552-562.

[3] Mounfield, W.P., Grujić, L.T. *Natural tracking control for exponential tracking: Lateral high-gain PI control of an aircraft system with state-space description*. Neural, Parallel & Scientific Computations, 1993, Vol. 1, No. 3, p. 357-370.

[4] Mounfield, W.P., Grujić, L.T. High-gain PI natural tracking control for exponential tracking of linear MIMO systems with state-space description. *International Journal of Systems Science*, 1994, Vol. 25, No. 11, p. 1793-1817.

[5] Grujić, L.T., Mounfield, W.P. Natural PD exponential tracking control: State-space approach to linear systems. *Proceedings of The Cairo Third IASTED International Conference Computer Applications in Industry*, Cairo, Egypt, December 26-29, 1994, p. 432-435.

[6] Mounfield, W.P., Grujić, L.T. Natural PD exponential tracking control, Part II: Computational resolutions", *Proceedings of The Cairo Third IASTED International Conference Computer Applications in Industry*, Cairo, Egypt, December 26-29, 1994, p. 436-439.

[7] Lazić, D.V. *Analysis and synthesis of automatic practical tracking control*, Ph.D. thesis. Belgrade, Serbia: Faculty of Mechanical Engineering, 1995 (In Serbian).

[8] Grujić, L.T. Tracking with prespecified performance index limits: Control synthesis for non-linear objects. *Proceedings of II International Seminar and Symposium: Automaton and Robot, SAUM and ZZEE*, Belgrade, October 27-29, 1987, p. S-20 to S-52.

[9] Grujić, L.T. Tracking versus stability: Theory. *Proceedings of 12th World Congress on Scientific Computation, IMACS*, Paris, July 18-22, 1988, Vol. 1, p. 319-327.

[10] Grujić, L.T. Tracking control obeying prespecified performance index. *Proceedings of 12th World Congress on Scientific Computation, IMACS*, Paris, July 18-22, 1988, Vol. 1, p. 332-336.

[11] Lazić, D.V. *Dynamical analysis of Continuous structurally variable control systems*, M.S. thesis. Belgrade, Serbia: Faculty of Mechanical Engineering (In Serbian).

Strojniški vestnik - Journal of Mechanical Engineering 54(2008)1, 68-76
UDC 658.562.4:669.71
Paper received: 19.12.2007
Paper accepted: 14.1.2008

Laser Supported Optical Control of High Pressure Aluminium Cast Products

Valter Gruden[1] - Drago Bračun[2] - Janez Možina[2,*]
[1]Hidria-Rotomatika Ltd, Slovenia
[2]University of Ljubljana, Faculty of Mechanical Engineering, Slovenia

We present a new method for surface quality control of aluminium high pressure cast products. By this method it is aimed to improve efficiently the existing practice of castings being only visually checked for surface defects such as laminations, non-fills and cold shots. The method is based on laser triangulation principle. The measured cloud of points is analysed using software designed specifically for automatic detection of surface defects. The paper describes a measurement system, measuring procedure focussed on the detection of surface defects and the comparison of the results with a visual inspection.

Keywords: aluminium pressure casting, surface quality control, laser 3D-measurement, optical control

0 INTRODUCTION

Today, the automotive industry requires complete traceability of each part used. This means that data on the exact date of production, production conditions and quality have to be provided for each part made [1] and [2]. The quality of a die-casting is determined by checking the precast final dimensions, casting quality, in particular with regard to porosity and surface defects, and the chemical composition of materials. The existing mechanical methods used for the purpose are the following: mechanical standard measurements, go-no-go gauges and 3D coordinate measuring machines (precast final dimensions), X-ray (porosity) and emission spectrometers (chemical composition of materials) [3] and [4]. In high pressure casting of aluminium, surface defects are relatively common. Normally, these occur on thin casting walls as laminations, non-fills and cold shots [5]. Surface defects may result from incorrect settings of the high pressure die-casting process, and the wear and cracks on die-casting tools. The traditional method of inspecting the quality of a die-casting is that a machine operator visually checks the quality of the product. The method depends on the skill of the operator and is as such highly subjective.

The paper proposes a new method for inspecting the surface quality of die castings, which is based on an optical measurement system and appropriate software to allow fast accurate measurement analyses. The new method shall be demonstrated on a cast product built for automobiles as an electronic component support (Fig. 1).

The support casting is made from aluminium alloy $AlSi_{12}$, and the casting dimensions are 190 x 150 x 10 mm with a minimum mean wall thickness of 1.5 mm. The inner surface of the casting has to be smooth to allow adhesion of an

Fig. 1. *Electronic component support made by aluminium high pressure die-casting*

*Corr. Author's Address: University of Ljubljana, Faculty of Mechanical Engineering, Aškerčeva 6, SI-1000 Ljubljana, Slovenia, janez.mozina@fs.uni-lj.si

electronic circuit board. Surface defects (e.g. small humps, slivers) protruding from the surface of the casting may cause short-circuit in the attached electronic circuit board and lead to the assembled set being rejected. According to the specifications, the maximum curvature of a casting shall not exceed 0.4 mm and the size of a surface defect shall not exceed 0.08 mm. Currently, three dimension prototypes are used in assessing casting quality: height, width and flatness. Assessment of surface defects, however, is entirely dependent on the visual capabilities of the assessor. On account of being highly subjective, this method is being replaced with a laser based measurement system which both ensures precise measurements of the casting surface quality and improves quality traceability.

High pressure die-casting is a modern casting technique for mass production of complex components characterised by thin walls and good mechanical characteristics. The mentioned die-casting is made on a horizontal pressure die-casting machine with a closing force of 4000 kN with a cold chamber [5]. In pressure die-casting, temperature plays a very important role. It affects the time of solidifying, the quality of molten metal structure and the lifetime of pressure die-casting tools. Thermal cracks, which may occur on the surface of the main tool inserts, reduce the lifetime of the tools. These cracks are caused by high temperature differences (up to 500 °C) between the aggressive aluminium alloy and the cavity surface, alloy velocity at the gate area and the shape of the gate area.

The most common surface-visible die-casting defects include cold shots (Fig. 2-a), non-fills (Fig. 2-b) and laminations (Fig. 2-c, d). Cold shots are normally caused by high surface tension between the alloy-and the inserts as well as from long filling time. In such a case, the alloy cools down and starts to solidify before the entire cavity has been fulfilled. Often the same reason also accounts for the occurrence of non-fills. Laminations are most commonly observed in die castings after sand blasting. This surface defect occurs when the top layer peels from the rest of the casting. It is caused by high velocity of the alloy or by a preheated surface of the cavity.

The most common defects in the die-casting of electronic component supports occur on the thinnest walls of the casting as cold shots or non-fills (cold die-casting tools). Laminations as another type of surface defect may occur as a result of preheated tools and is seen as humps or blisters appearing on the surface.

1 LASER SUPPORTED OPTICAL MEASUREMENT SYSTEM

The measuring system (Fig. 3) consists of an optical measuring instrument using the laser triangulation principle [6] and [7] and a movable table that changes the position of the measured product relative to the instrument. The casting contains precast blind holes which lean against three support balls when mounted onto the movable table, thereby ensuring repeatable mounting of the casting onto the table. The system set-up is made up of a laser projector which illuminates the casting with a thin laser plane, and a CDD camera (Basler 101f). At the point where the laser plane hits the casting, a thin bright line can be seen (intersection curve). The image is captured by the camera positioned at an angle with respect to the direction of illumination (laser triangulation). The process points to the 3D profile of the intersection curve. The image is then translated into a personal computer file, and the intersection curve is extracted and its maximum and minimum values are identified [8] and [9]. The result of one measurement is a profile representing a cross-

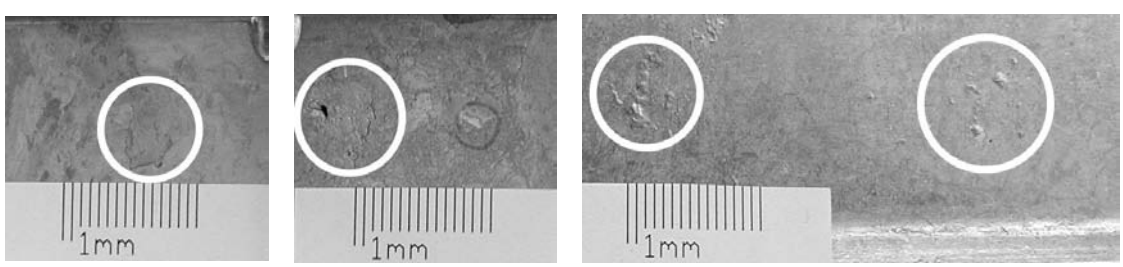

Fig. 2. *A cold shot (a), non-fills (b), laminations (c, d)*

section of the light plane and the illuminated surface $(X,Y)_i$, where X and Y are the coordinates of a particular point, X along the intersection curve and Y perpendicular to the surface; index i runs from 1 to n, where n is the number of points within a profile (e.g. 1300). By changing the position of the table or the measured casting in several steps, new profiles are acquired and joined into a 3D surface image referred to as the cloud of points $(X,Y,Z)_{i,j}$. The Z-coordinate is the position of a particular profile in the direction of table positioning and index j runs from 1 to m (number of profiles). On account of the measurement technique applied, the cloud of points has a matrix structure {n, m}, which simplifies further operations for modelling and presentation of the measured surface. The measurement system (Fig. 4) incorporates built-in optics which magnifies the image 4.5 times more in the direction perpendicular to the casting surface than in the direction along the intersection curve. The optics is assembled from a spherical lens and two cylindrical lenses making up the cylindrical Keplerian telescope [10]. The optical system was set up to the measuring range of 200 x 35 mm (width x height) and a mean resolution of 0.15 mm along the intersection curve and 0.025 mm perpendicular to the measured surface. Measurement uncertainty in a particular measured point is 0.02 mm (σ). The existing system can capture 15 profiles per second, the speed being determined by the image size (1.3 MB) and bandwidth of the 1394 output (alias fire-wire). The measurement system has been set up to capture 750 profiles in 50 seconds. Further increasing of the speed of the system is only possible through development of a new camera supported by modern programmable logic, according to which the image will be processed by the camera and only the profile will be translated along the fire-wire.

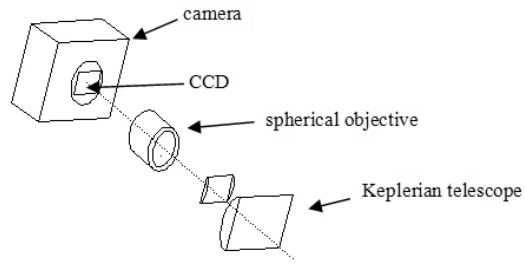

Fig. 4. *Keplerian cylindrical telescope increases measurement resolution in the direction perpendicular to the die-casting surface.*

2 DATA PROCESSING

In developing software for automated detection of surface defects, special emphasis was placed on the speed of action, since a measurement (an average measurement consists of 2 x 10^6 points) is to be made and processed within the casting cycle (approx. 60 seconds). The flowchart for detection of surface defects is presented in Figure 5.

Detection of die-casting defects is only performed in several different non-overlapping regions of interest (ROI). The number, shape and position of the studied regions of interest are

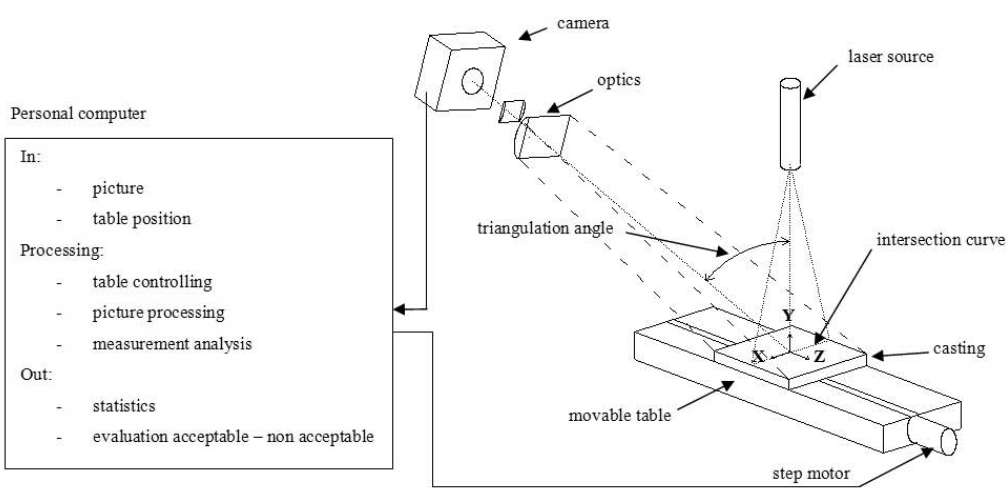

Fig. 3. *A schematic of the new method for inspecting the die-casting surface quality*

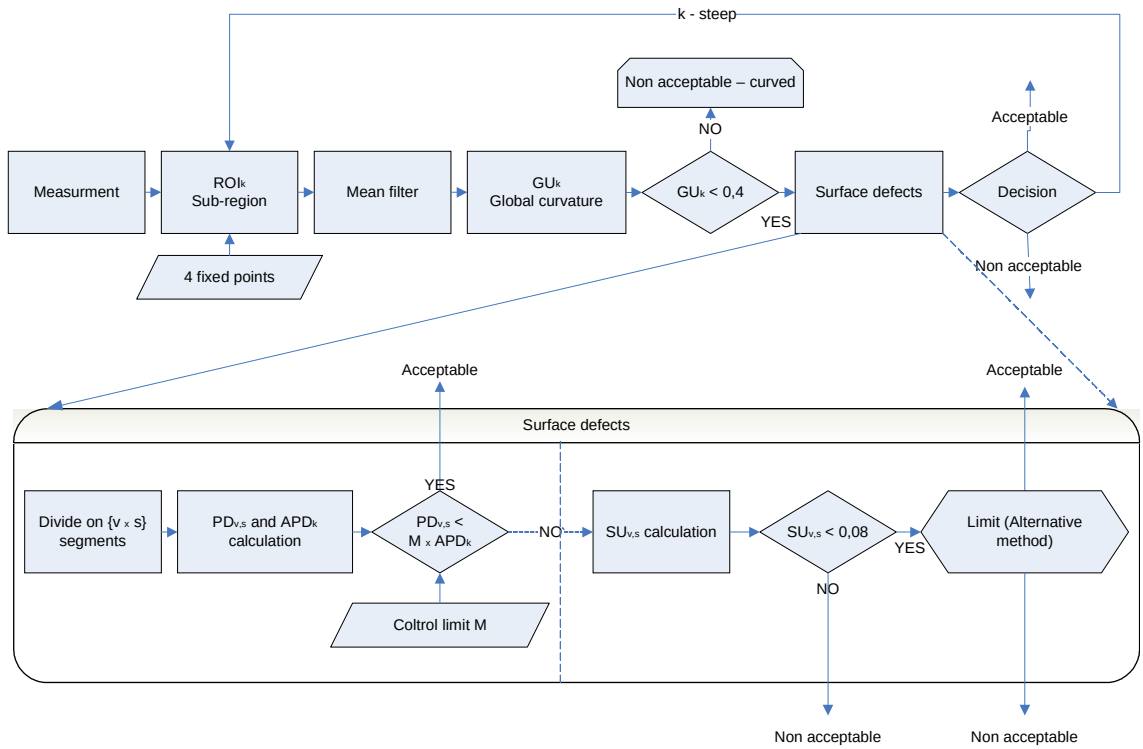

Fig. 5. *The flowchart for detection of surface defects*

selected with regard to the functionality or purpose of various casting surfaces. To this aim, the cloud of points is first divided into several sub-regions $ROI_k = \{(X, Y, Z)_{i,j}; i,j \in k\}$, where $k = 0, 1,..., K$ (K is the number of all ROI). Figure 6 shows OI_1, for which the process of detecting casting defects will be demonstrated in the continuation of the paper. Each ROI is defined with a boundary consisting of four fixed points, positioned into a rectangular pattern. Fixed points are used to ensure

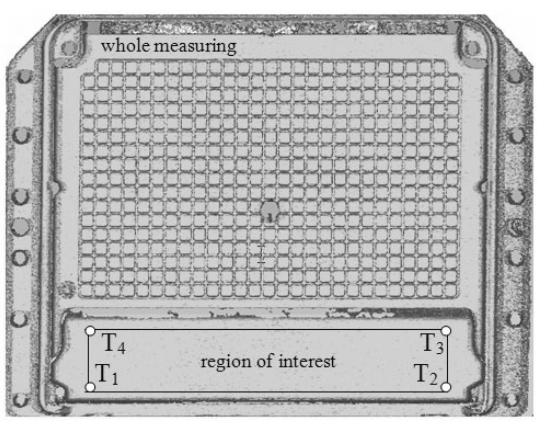

Fig. 6. *A particular region of interest (ROI_k) is defined with four fixed points.*

that the casting measured maintains the same position at all times, which significantly speeds up data processing as it enables us to avoid the invariant analysis.

In the first processing step, the region of interest is filtered.

A mean filter [11] is used to clean up isolated points protruding from the die-casting surface, which have probably been caused by second reflection of the transmitted laser beam on the die-casting. The first important parameter used in assessing the die-casting surface quality is global curvature (GU) of a particular ROI_k. In calculating this parameter, the plane (R_k) is first adjusted to the ROI_k, using the method of least squares [11]. In the next processing step, perpendicular distances D_k are calculated from the points of ROI_k to the plane R_k (Fig. 7). Global curvature GU_k is then determined as a distance between the maximum and the minimum of the D_k. According to the specifications, GU_k of a particular ROI_k may not exceed 0.4 mm.

In the second processing step, detection of surface defects is performed. To this purpose, ROI_k is sub-divided into small segments (Fig. 8), the surface area of which corresponds in size to a

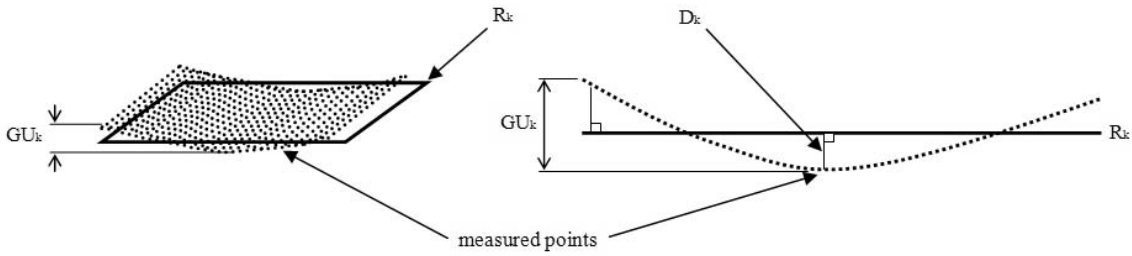

Fig. 7. *Definition of global curvature (GU)*

typical casting defect (e.g. 5 x 5 mm). The underlying idea of segmentation is to perform narrow-band filtering on ROI_k surface to detect geometrical shapes the size of the segment. Figure 8 shows a sample segmentation of ROI_k.

In detecting surface defects, certain parameters are first calculated for each segment and then a statistical analysis of the values obtained is carried out for the entire ROI_k. Calculation of parameters by segment is similar to the calculation of global curvature GU. On every segment $S_{k,v,s} = \{(X, Y, Z)_{i,j};\ i,j \in (k \wedge v \wedge s)\}$, ($v$ = 1, 2, .. V (number of rows) and s = 1, 2, .. S (number of columns)) a plane $R_{v,s}$ is fitted in a least-square sense, and the perpendicular distances $D_{v,s}$ of the $S_{k,v,s}$ points to the plane $R_{v,s}$ are calculated.

The first parameter to be calculated for each segment is local curvature of the matrix segment ($SU_{v,s}$) which is defined similarly as the global curvature GU_k, as a distance between the maximum and the minimum of $D_{v,s}$. Local curvature of the matrix segment $SU_{v,s}$ defines the size of a surface defect.

The second parameter describes the average deviation $PD_{v,s}$ of perpendicular distances $D_{v,s}$

$$PD_{v,s} = \frac{\sum D_{v,s}^{\ 2}}{npts_{v,s}} \qquad (1),$$

where $npts_{v,s}$ is the number of points within a particular matrix segment $S_{k,v,s}$. Both parameters are then statistically analysed along the entire ROI_k.

The research has shown that defect identification through the average deviation $PD_{v,s}$ is considerably more reliable than the detection based on the local curvature of a matrix segment $SU_{v,s}$. In the light of this fact, the mean value of $PD_{v,s}$ is first calculated for all the matrix segments within a ROI_k, generating the average value APD_k, whose multiple M is set as the upper control limit for detection of surface defects. In conclusion, a surface defect is likely to be located in a segment where $PD_{v,s} > M * APD_k$. The multiple M of the upper control limit is determined experimentally; in our case M = 2. The defect found is confirmed by the parameter $SU_{v,s}$ indicating an absolute defect size. When $SU_{v,s}$ exceeds 0.08 mm (specification of surface defect size), the matrix segment {v, s} contains a surface defect, and the casting is marked as »Not acceptable«. Otherwise, the defect is on the verge of acceptance; the casting is marked as "Limit" and needs to be inspected using an alternative method (also visual inspection).

3 EXPERIMENTS

The new method is demonstrated through the shape measurement and surface quality control of a group of 32 castings, which had been visually inspected following production. The method's performance is demonstrated on two castings, focusing in both only on the first region of interest (ROI_1). The first casting E_2 successfully passed visual inspection in the production. Using the new method, the calculated global curvature is GU_1 = 0.15 mm (Fig. 9).

The process of averaging $PD_{v,s}$ generates the value APD_1 = 0.0032 mm; perception threshold for surface defects is 0.0064 mm (M = 2). The graph of perpendicular distances PD (Fig. 10) shows that

Fig. 8. *ROI_1 divided to a matrix of 28 x 4 segments whose average size is 5 x 5 mm*

Fig. 9. *Visualization of D_1 on casting E_2. (light: +0.7 mm above R_k, dark: -0.7 mm below R_k)*

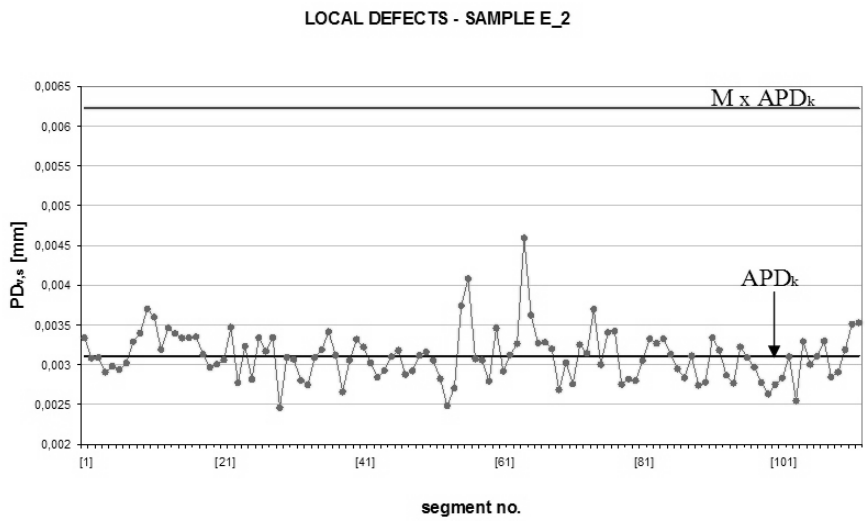

Fig. 10. *Control chart of $PD_{v,s}$ (segment number = (v-1)*S+s)*

all $PD_{v,s}$ are lower than 0.0064 mm indicating there are no surface defects. In cases where such results are obtained, no further analysis of the local curvature SU is performed.

The second casting E_4 is marked as conditionally acceptable in the production visual control. The region of interest ROI_1 shows signs of laminations (cf. Fig. 2 c and d). Using the new method, global curvature is calculated at GU_1 = 0.08 mm (Fig. 11), and found to be within the control limits (< 0. 4 mm). The mean of $PD_{v,s}$ values is APD_1 = 0.0038 mm; perception threshold for surface defects is 0.0074 mm (M = 2). The graph of the parameter PD (Fig. 12) indicates that PD exceeds the perception threshold in segments 46, 53 and 74, indicating occurrence of potential surface defects in these segments. In such cases, the local curvature parameter SU (Fig. 13) is analysed further. It can be observed that in the

Fig. 11. *Visualization of D_k on casting E_4. (light: +0.04 mm above R_k, dark: -0.04 mm below R_k)*

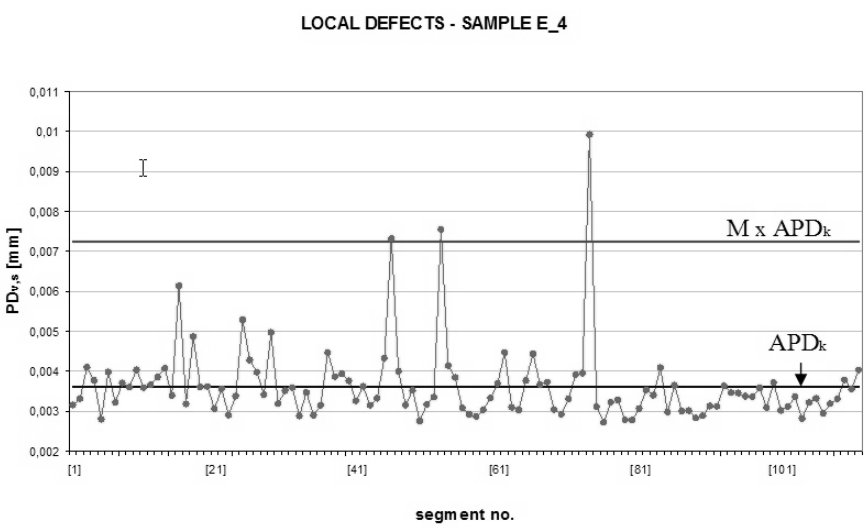

Fig. 12. *Control chart of $PD_{v,s}$*

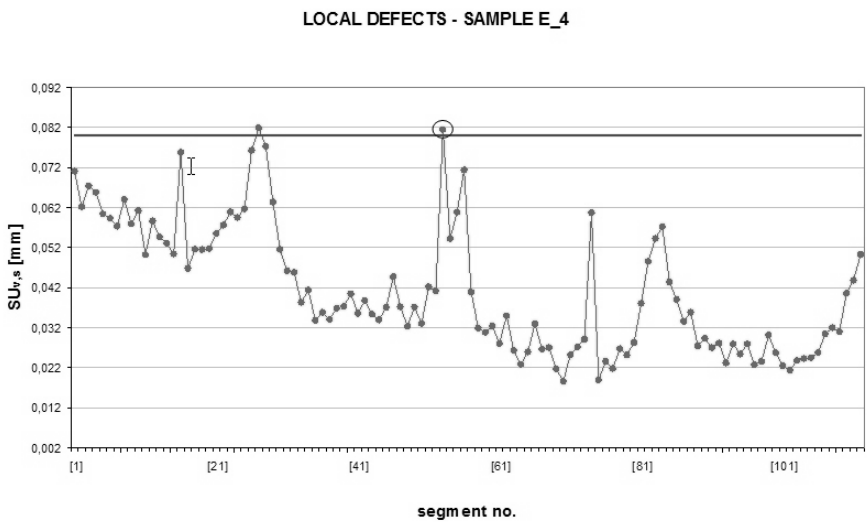

Fig. 13. *Control chart of $SU_{v,s}$*

segment 53 SU exceeds the control limit of 0.08 mm and is therefore marked as containing a surface defect. In segments 45 and 74 SU is below 0.08 mm and these segments are marked as defect limit. As the matrix segment 53 contains a surface defect, the casting is marked "not acceptable" (defective).

The same procedure is used for analysing the remaining die-castings. The results are given in Table 1. The second column presents visual inspection results. Castings containing no defects are marked "Acceptable"; conditionally acceptable castings are marked "Limit" and defective castings are marked "Not acceptable". The results of the new method are given in the third, fourth and fifth columns. The third column indicates segments with surface defects, the fourth column states global curvature and the fifth column states the decision regarding the surface quality of the casting.

A comparison into the columns Visual Inspection and Decision shows that the new method is stricter in inspecting the castings. All the castings which have been marked as defective in the production, have been recognized as such by the new method; additionally, the method yielded several castings with small defects and marked them as "limit" defects. The reason for stricter control lies in currently low control limits (M = 2 and SU = 0.08 mm). If these are increased, the strictness of quality control decreases. Stricter control causes production costs to rise as it increases reject rates and requires additional checking of conditionally acceptable die castings. The results call for an additional fine setting of control limits in the phase of introducing the new method for casting quality control into the production process.

Fig. 14. *Segments with surface defects (46, 53, 74)*

4 CONCLUSIONS

The paper presents the development of a new method for control of die-casting surface quality, which is based on a 3D measurement of the die-casting shape with a laser supported optical measurement system and on analysing the 3D measured shape. In using the new method, the measured shape is sub-divided into several non-overlapping regions of interest, whose size and position are selected with respect to the casting functionality. For each of these regions, global curvature and the position and size of surface defects are calculated. Casting surface quality is assessed by checking whether the calculated values fall within the set control limits. Through this approach, casting surface quality is assigned numerical values and is time-independent, unlike the currently used visual inspection where a worker decides on the

Table 1. *Comparison of the classic (visual) and a new method for quality control*

		New method		
Casting	Visual inspection	Segment with defects	Global curvature [mm]	Decision
E_1	Acceptable	15	0.14	Limit
E_2	Acceptable		0.15	Acceptable
E_3	Acceptable		0.11	Acceptable
E_4	Limit	46,53,74	0.08	Non acceptable
E_5	Non acceptable	19,48,49	0.15	Non acceptable
U_1	Non acceptable	74	0.16	Non acceptable
U_2	Acceptable		0.11	Acceptable
U_3	Acceptable	27	0.17	Limit
U_4	Non acceptable	46,54,67,74 etc.	0.22	Non acceptable
U_5	Non acceptable	2,8,9,10,12 etc.	0.33	Non acceptable
U_6	Acceptable	75	0.14	Limit
U_7	Acceptable		0.15	Acceptable
U_8	Non acceptable	58	0.20	Non acceptable
U_9	Non acceptable	10, 28, 53, 54 etc.	0.33	Non acceptable
U_12	Acceptable		0.11	Acceptable
U_13	Acceptable	8	0.10	Limit
U_14	Acceptable		0.10	Acceptable
A_1	Acceptable		0.11	Acceptable
A_2	Acceptable		0.11	Acceptable
A_3	Acceptable		0.11	Acceptable
A_4	Acceptable		0.12	Acceptable
A_5	Limit	76	0.11	Limit
A_6	Acceptable		0.10	Acceptable
A_7	Acceptable		0.12	Acceptable
A_8	Acceptable		0.09	Acceptable
A_9	Acceptable		0.10	Acceptable
A_10	Acceptable		0.10	Acceptable
A_11	Acceptable		0.12	Acceptable
A_12	Acceptable		0.08	Acceptable
A_13	Acceptable		0.11	Acceptable
A_14	Acceptable	81, 82	0.10	Non acceptable
A_15	Acceptable	37, 65	0.14	Non acceptable

acceptability of a cast product relative to his/her subjective experience.

Tests have proven that the measurement system achieves sufficiently high measurement precision and accuracy (0.025 ± 0.02 mm perpendicular to the casting surface) and that the current speed of measurement (15 profiles per second) is too low to accommodate introduction of the new measurement method into the production process and will therefore need to be increased. Furthermore, a comparison into the results of the quality of test castings has pointed to the need for an additional fine setting of control limits in the phase of introducing the new method for casting quality control into the production process in order to achieve the balance between technological requirements and increasing of costs on the one hand and stricter casting quality control on the other.

5 REFERENCES

[1] Chandra M.J. *Statistical quality controll.* CRC press, 2001.

[2] Keller P. *Quality engineering handbook*, 2nd ed. Marcel Dekker, Inc., 2003.

[3] Leopold J. et al. New developments in fast 3D-surface control. *Measurement*, 2003, 33 p. 179-87.

[4] Shull J. P. *Nondestructive evaluation: theory, techniques and applications*. Marcel Dekker, Inc., 2002.
[5] Andresen B. *Die casting engineering: A hydraulic, thermal and mechanical process*. Marcel Dekker, Inc., 2004.
[6] Donges A., Noll R. *Lasermeßtechnik, Grundlagen und Anwendungen.* Heidelberg: Hüthig, 1993, 214 p.
[7] Girod B., Greiner G., Niemann H. *Principles of 3D image analysis and synthesis*. Kluwer Academic Publishers, 2002.
[8] Bračun D., Jezeršek M., Diaci J. Triangulation model taking into account light sheet curvature. *Meas. Sci. Technol.*, 2006, 17, p. 2191-96
[9] Bouguet J. Y. *Camera calibration toolbox for Matlab*, URL http://www.vision.caltech.edu/bouguetj/calib_doc/index.html (09.10.2007)
[10] O'Shea D. *Elements of modern optical design*. John Wiley &Sons, 1985, 81 p.
[11] *Numerical Recipes: The Art of Scientific Computing*, 3rd ed. Cambridge University Press, 2007.

Instructions for Authors

From 2008 the Journal of Mechanical Engineering is to be published in English only, but with separate Slovene abstracts. The authors are entirely responsible for the correctness of the language. If a reviewer indicates that the language in the paper is poor, the editor will require the author to correct the text with the help of a native English speaker before the paper is reviewed again.

Papers can be submitted electronically to the journal's e-mail address (info@sv-jme.eu) or by post.

Papers submitted for publication should comprise the following:

- Title, Abstract, Keywords,
- Main body of text,
- Tables and Figures (graphs, drawings or photographs) with captions,
- List of References,
- Information about the authors, the corresponding author and a full set of addresses.

For papers from abroad (in the case that none of the authors is a Slovene) the editor will obtain a Slovenian translation of the Abstract.

Papers should be short, about 8 to 12 pages of A4 format, or at most, 7000 words. Longer papers will be accepted if there is a special reason, which should be stated by the author in the accompanying letter. Short papers should be limited to less than 3000 words.

THE FORMAT OF THE PAPER

The paper should be written in the following format:

- A Title, which adequately describes the content of the paper.
- An Abstract, which should not exceed 250 words. The Abstract should state the principal objectives and the scope of the investigation, the methodology employed, summarize the results and state the principal conclusions.
- An Introduction, which should provide a review of recent literature and sufficient background information to allow the results of the paper to be understood and evaluated.
- A Theory and the experimental methods used.
- An Experimental section, which should provide details of the experimental set-up and the methods used for obtaining the results.
- A Results section, which should clearly and concisely present the data using figures and tables where appropriate.
- A Discussion section, which should describe the relationships and generalisations shown by the results and discuss the significance of the results, making comparisons with previously published work.
- Because of the nature of some studies it may be appropriate to combine the Results and Discussion sections into a single section to improve the clarity and make it easier for the reader.
- Conclusions, which should present one or more conclusions that have been drawn from the results and subsequent discussion and do not duplicate the Abstract.
- References, which must be numbered consecutively in the text using square brackets [1] and collected together in a reference list at the end of the paper.

THE LAYOUT OF THE TEXT

Texts should be written in Microsoft Word format. The paper must be submitted in an electronic version, by e-mail or by post on a CD.

Do not use a LaTeX text editor, since this is not compatible with the publishing procedure of the Journal of Mechanical Engineering.

Equations should be on a separate line in the main body of the text and marked on the right-hand side of the page with numbers in round brackets.

Units and abbreviations

Only standard SI symbols and abbreviations should be used in the text, tables and figures. Symbols for physical quantities in the text should be written in italics (e.g., *v, T, n,* etc.). Symbols for units that consist of letters should be in plain text (e.g. m/s, K, min, mm, etc.).

All abbreviations should be spelt out in full on first appearance, e.g., variable time geometry (VTG).

The meaning of symbols and units belonging to symbols should be explained in each

case or quoted in special table at the end of the paper before the References.

Figures

Figures must be cited in consecutive numerical order in the text and referred to in both the text and the caption as Fig. 1, Fig. 2, etc. Pictures should be saved in a resolution good enough for printing, and in any common format, e.g., BMP, GIF or JPG. However, graphs and line drawings should be prepared as vector images, e.g., CDR, AI.

All Figures should be prepared in black and white, without borders and on a white background. All the figures should be sent separately in their original formats.

When labeling axes, physical quantities, e.g., *t, v, m,* etc., should be used whenever possible. Multi-curve graphs should have the individual curves marked with a symbol. The meaning of the symbol should be explained in the figure caption.

In the case that the author wishes, for whatever reason, to publish Figures in colour, the author must pay the resulting costs.

Tables

Tables must be cited in consecutive numerical order in the text and referred to in both the text and the caption as Table 1, Table 2, etc. In addition to the physical quantity, e.g., *t* (in italics), units (normal text), should be added in square brackets. Each column should have the title line. Tables should not duplicate information that is already noted anywhere in the paper.

Acknowledgement

An acknowledgement for cooperation or help can be included before the References. The author should state the name of the research (co)financer.

The list of references

All references should be collected at the end of the paper in the following styles for journals, proceedings and books, respectively:

[1] Wagner, A., Bajsić, I., Fajdiga, M. Measurement of the surface-temperature field in a fog lamp using resistance-based temperature detectors. *Strojniški vestnik – Journal of Mechanical Engineering*, February 2004, vol. 50, no. 2, p. 72-79.

[2] Boguslawski L. Influence of pressure fluctuations distribution on local heat transfer on flat surface impinged by turbulent free jet. *Proceedings of International Thermal Science Seminar II*, Bled, June 13.-16., 2004.

[3] Muhs, D., et al. *Roloff/Matek mechanical parts*, 16th ed. Wiesbaden: Vieweg Verlag, 2003. 791 p. (In German). ISBN 3-528-07028-5

ACCEPTANCE OF PAPERS AND COPYRIGHT

The Editorial Board reserves the right to decide whether a paper is acceptable for publication, obtain professional reviews for submitted papers, and if necessary, require changes to the content, length or language.

The corresponding author must, in the name of all authors, also enclose a written statement that the paper is original unpublished work, and not under consideration for publication elsewhere.

On publication, copyright of the paper shall pass to the Journal of Mechanical Engineering. The JME must be stated as a source in all later publications.

Submitted materials will not be returned to the author. Unpublished materials are not preserved and will not be sent anywhere without the author's consent.

The paper, prepared for publication, will be sent to the author in PDF format. The author should check for any necessary corrections, which should be the minimum required. With this the author confirms that the paper is ready for publication.

PUBLICATION FEE

For all papers the authors will be asked to pay a publication fee prior to the paper appearing in the journal. However, this fee only needs to be paid after the paper is accepted for publication by the Editorial Board. The fee is €180.00 (for all papers with a maximum of 6 pages), €220.00 (for all papers with a maximum of 10 pages) and €20.00 for each additional page. The publication fee includes 25 off-prints of each paper, which will be sent to the corresponding author.

Vsebina

Strojniški vestnik - Journal of Mechanical Engineering
letnik 54, (2008), številka 1
Ljubljana, januar 2008
ISSN 0039-2480

Izhaja mesečno

Uvodnik

Spoštovani bralci,

ob koncu leta 2007 se je spremenil Izdajateljski svet skladno s pravili delovanja Strojniškega vestnika - Journal of Mechanical Engineering. V nov izdajateljski svet sta obe fakulteti za strojništvo želeli vključiti kolege, ki so ali pomembno ustvarjajo pisano besedo na področju strojništva. Povabljenci so se vabilu odzvali s posebnim veseljem. Ob priliki osebnih intervjujev so predstavili svoje poglede na razvoj revije, ki v slovenskem prostoru predstavlja matico znanja na področju znanstvenih člankov. Na že začeti poti mednarodnega uveljavljanja revije izpred desetletja želimo še bolj odpreti prostor za izmenjavo znanja. Skupen evropski prostor nam to sedaj omogoča. Izdajateljski svet se je srečal večkrat, da bi lahko utrl pot novemu uredniškemu odboru, še posebej pa glavnemu uredniku in njegovemu namestniku. Spremembe v vsebinskem in oblikovnem konceptu so sedaj pred Vami. Ocenite jih in napišite Vaše mnenje.

Spremembe v vsebinskem delu so predvsem v tem, da se članki ne razvrščajo med strokovne ali znanstvene. V reviji bomo objavljali samo še znanstvene članke, ki bodo v recenzijskem postopku zagotavljali čim višjo raven. Za tak pogumen korak se moram v imenu novega IS zahvaliti predvsem staremu uredniku prof. Alujeviču in njegovemu namestniku doc. Karižu. Kakovost in vplivnost revije sta uveljavila s skrbnim in zavzetim delom. Odločili smo se, da podpremo integralnost znanj na področju strojništva zato, ker je po našem mnenju drobljenje znanj v sodobnem razumevanju sveta manj primerna. Pri posameznih številkah se bomo še posebej osredotočali na specifična področja, ki jih bomo predstavljali tako s sprotno uredniško politiko kot tudi z vabljenimi souredniki. Spoštovani kolegi znanstveniki, veseli bomo Vašega predloga za posebne tematske številke, ki bodo zagotavljale hitro in odmevno predstavljanje dosežkov naših kolegov na področju strojništva. Predstavite Vaše predloge odgovornemu uredniku, ki bo nato preveril predlog v posebnem recenzijskem postopku.

Tehnično se revija spreminja tako na naslovni strani kot tudi v osnovni zamisli. Osnovna revija ima najprej vse članke v angleščini. Nato pa so v ločenem delu predstavljeni povzetki vseh člankov in posebne novice za slovenske bralce v slovenščini. Celotno revijo bodo prejemali vsi redni naročniki v Sloveniji in tiste knjižnice po svetu, ki imajo državni status. Vsi ostali naročniki v tujini pa bodo dobili samo angleško verzijo vseh člankov brez priloge v slovenščini. Na ta način bomo po našem mnenju revijo približali vsem zainteresiranim bralcem v za njih primerni obliki. Tudi spletna stran je spremenjena in ima od sedaj naslov http://www.sv-jme.eu. Na tej spletni strani bodo dosegljivi vsi članki iz tekočih številk. S tem bomo omogočili predvsem mlajšim znanstvenikom, ki nimajo dostopa do kodiranih revij, pomembno prednost pri doseganju zadnjih objav v naši reviji. Avtorjem, ki čakajo na objave in želijo imeti čimprejšnjo potrditev objave, pa bomo na internetni strani potrdili objavo za en mesec vnaprej z vsemi bibliografskimi podatki.

Posebna novost bo slika na naslovnici, ki bo prikazovala značilne raziskovalne dosežke postopkov izvedenih v različnih laboratorijih. Na internetni strani bo za vsak postopek predstavljen izsek filma, ki bo omogočil bralcu internetne strani vpogled v posnetek določenega postopka. Na ta način bomo zagotovili aktualnost in specifično informacijo o postopkih, ki jih tiskani izvod revije ne more posredovati. Vljudno naprošamo avtorje, da v primeru specifičnih postopkov vključijo v predstavitev tudi možnost predstavitve na internetni strani.

Uredniški in svetovalni odbor bosta pridobila bolj aktivno vlogo. Polovico članov od tega je iz mednarodnega strokovno in znanstveno priznanega okolja. Vsem, ki ste sprejeli dolžnost člana uredniškega in svetovalnega odbora, ki bo skrbel za kakovostne prispevke in prvo izbiro prispevkov, se vnaprej zahvaljujem. Z Vašo pomočjo bo revija pridobivala na kakovosti, kar je naša skupna zaveza in velika želja.

Uredniku prof.Andru Alujeviču, njegovemu namestniku prof.Vincenc Butali in vsem članom uredniškega in svetovalnega odbora želim v imenu Izdajateljskega sveta in mojem osebnem imenu uspešno delo za naprej.

V Ljubljani, 20.2.2008

Prof.dr. Jože Duhovnik

Strojniški vestnik - Journal of Mechanical Engineering 54(2008)1, SI 3
UDK 627.84
Prejeto: 4.10.2006
Sprejeto: 19.12.2007

Analiza hidravličnih značilk varnostne zapornice v hidroelektrarni

Zlatko Rek[1,*] - Anton Bergant[2] - Miha Röthl - Primož Rodič[3] - Iztok Žun[1]
[1]Univerza v Ljubljani, Fakulteta za strojništvo
[2]Litostroj E.I.
[3]Inštitut za hidravlične raziskave

Varnostna zapornica je lahko vgrajena na vtoku v tunel, nizvodno od izravnalnika ali pa v sesalni cevi vodne turbine. Hidravlična oblika zapornice in značilke pretočnega sistema hidroelektrarne vplivajo na velikost obremenitev na zapornico. Pretočne razmere dolvodno od zapornice narekujejo potrebo po količini zraka, ki ga moramo dovesti v sistem. Numerična analiza hidravličnih značilk je izdelana za navpično tablasto zapornico pri različnih odprtjih zapornice. Analiza toka je izvršena s pomočjo standardnih numeričnih metod (metoda nadzornih prostornin). Rezultati izračuna so primerjani z rezultati meritev na hidravlično podobni zapornici v laboratoriju.

Ključne besede: hidroelektrarne, varnostne zapornice, hidravlične značilke, metode nadzornih prostornin

*Naslov odgovornega avtorja: Univerza v Ljubljani, Fakulteta za strojništvo, Aškerčeva 6, 1000 Ljubljana, zlatko.rek@fs.uni-lj.si

Strojniški vestnik - Journal of Mechanical Engineering 54(2008)1, SI 4
UDK 621.83.052
Prejeto: 10.7.2006
Sprejeto: 19.12.2007

Vrednotenje stanja zobniških gonil s pomočjo vibracij

Aleš Belšak* - Jože Flašker
Univerza v Mariboru, Fakulteta za strojništvo

Izkoristek najsodobnejših proizvodnih tehnologij in visoka stopnja stabilnosti proizvodnje brez nepredvidenih zaustavitev sta najpomembnejše faktorja, na katera imata pomemben vpliv predvsem nadzor stanja in ustrezno vzdrževanje mehanskih sistemov.

Ker se danes vedno bolj uporablja projektiranje strojev in naprav na dobo trajanja, je želja uporabnika, da je delovanje v predvideni dobi trajanja kakovostno in čim zanesljivejše ter da je zaustavitev čim manj. Tako s pomočjo spremljanja stanja ne ugotavljamo samo prisotnosti sprememb, ampak želimo napovedati vrsto in velikost poškodbe oz. napake, ki ogroža kvaliteto obratovanja v preostali življenjski dobi.

Ključne besede: zobniška gonila, odkrivanje napak, analize vibracij, analize verjetnosti, zanesljivost delovanja

*Naslov odgovornega avtorja: Univerza v Mariboru, Fakulteta za strojništvo, Smetanova 17, 2000 Maribor, ales.belsak@uni-mb.si

Strojniški vestnik - Journal of Mechanical Engineering 54(2008)1, SI 5
UDK 620.19
Prejeto: 28.6.2006
Sprejeto: 19.12.2007

Možnost detekcije različnih vrst napetostno-korozijskega pokanja na avstenitnih nerjavnih jeklih s sočasnim merjenjem akustične emisije in elektrokemijskega šuma

Žiga Bajt - Mirjam Leban - Jaka Kovač* - Andraž Legat
Zavod za gradbeništvo Slovenije

Prispevek opisuje možnost uporabe akustične emisije (AE) in elektrokemijskega šuma (EŠ) za zaznavo in ovrednotenje napetostno-korozijskega pokanja (NKP) na avstenitnem nerjavnem jeklu. Potek preskušanja pri stalni obremenitvi smo spremljali istočasno s tremi različnimi tehnikami: AE, EŠ in merjenjem raztezka vzorca. Z namenom povečati občutljivost na NKP je bilo jeklo toplotno obdelano. Različne vrste pokanja smo dosegli z uporabo dveh različnih elektrolitov in različnimi ravnmi natezne obremenitve. Medkristalno NKP je potekalo v vodni raztopini natrijevega tiosulfata pri obremenitvi manjši od meje plastičnosti, prekokristalno NKP pa je potekalo v vodni raztopini natrijevega tiocianata pri obremenitvi nad mejo plastičnosti. V primeru medkristalnega NKP nismo opazili sočasno izmerjenih povečanih dejavnosti AE, tranzientov EŠ in nezveznosti v raztezku. Razen posameznih opaženih prehodov EŠ, so bili signali veliko bolj gladki kot v primeru prekokristalnega NKP, kar je verjetno posledica bolj zvezne narave pojavov medkristalnega NKP. To je bil verjetno tudi razlog, da nismo uspeli zaznati sočasnih nezveznih značilnosti v merjenih signalih pri tem načinu NKP. Na drugi strani smo pri meritvah EŠ v drugi polovici testa opazili precejšnjo rast enosmerne sestavine toka, ki je časovno sovpadal s povečevanjem raztezka in deloma z večanjem dejavnosti AE. Predvidevali smo, da je ta premik toka v anodno smer posledica povečanega odtapljanja površine delovne elektrode zaradi rasti razpok. Na osnovi istočasne uporabe treh metod smo uspešno zaznali nekaj medkristalnih napetostno-korozijskih dogodkov. Zaznava je temeljila na sočasno izmerjenih povečanih dejavnostih AE, tranzientih EŠ in nezveznostih (skokih) v raztezku. Na osnovi časovne ločljivosti meritev smo sklepali, da so bili elektrokemijski pojavi posledica mehanskih pojavov med NKP. Na podlagi meritev smo sklepali, da je skupna uporabo EŠ in AE obetaven pristop za zaznavo in ovrednotenje NKP, potrebne pa so nadaljne raziskave in izboljšave merilnega sistema.

Ključne besede: napetostna korozija, elektrokemijski šum, akustične emisije, nerjavna jekla

*Naslov odgovornega avtorja: Zavod za gradbeništvo Slovenije, Dimičeva 12, 1000 Ljubljana, jaka.kovac@zag.si

Strojniški vestnik - Journal of Mechanical Engineering 54(2008)1, SI 6
UDK 658.5:669.712
Prejeto: 27.12.2006
Sprejeto: 28.9.2007

Model načrtovanja proizvodnje v livarni aluminija

Gordana Matičević[1,]* - Niko Majdandžić[1] - Tadija Lovrić[2]
[1]Univerza v Osijeku, Fakulteta za strojništvo, Hrvaška
[2]ININ d.o.o., Hrvaška

Znanih je več metod in strategij upravljanja proizvodnje, ki jih uspešno izvajamo v kovinski industriji in še posebej v avtomobilski in orodjarski industriji. Vendar je bilo objavljenih le malo raziskav s področja načrtovanja postopkov litja. Zato je glavni namen tega prispevka razvoj matematičnega modela načrtovanja livarskih opravil na podlagi zasnov MRP II (Manufacturing Resource Planning), JIT (Just in Time) in OPT (Optimized Production Technology). Razvojna strategija vključuje tudi pregled objavljenih prispevkov in vključitev razvitega matematičnega modela v livarno za preizkušanje modela z dejanskimi podatki. Predlagani model je uspešno vpet v sistem ERP (Enterprise Resource Planning) tovarne Aluminij d.d. v Mostarju. Sklepi, predstavljeni v tem prispevku, temeljijo na rezultatih preizkusov, izvedenih v tej livarni, zato so za potrditev rezultatov potrebne nadaljnje raziskave v drugih livarnah, na drugih proizvodnih področjih.

Ključne besede: proizvodnja aluminija, načrtovanje proizvodnje, matematični modeli, minimiranje zamud

*Naslov odgovornega avtorja: Univerza v Osijeku, Fakulteta za strojništvo v Slavonskem Brodu, Trg I. Brlić-Mažuranić 2, HR-35000 Slavonski Brod, Hrvaška, gordana.maticevic@sfsb.hr

Strojniški vestnik - Journal of Mechanical Engineering 54(2008)1, SI 7
UDK 658.5.012.7
Prejeto: 26.4.2006
Sprejeto: 19.12.2007

Določanje optimalnega nabora informacijskih terminalov za spremljanje proizvodnje v kosovnih industrijah

Jani Kleindienst[1] - Đani Jurićić[2,*]
[1]Kolektor Sinabit d.o.o. Elektronika
[2]Institut "Jožef Stefan"

Cilj avtomatiziranega zbiranja podatkov v kosovnih industrijah je zagotoviti čim bolj točne podatke o opravljenem delu y namenom doseganja učinkovitega in kakovostnega upravljanja proizvodnje. Podatki se nanašajo na čase, porabljene na posameznih opravilih delovnega naloga, število izdelanih kosov, količina izmeta in vzroki za izmet, vrste zastojev, njihovo trajanje in vzrok. Eden od načinov zbiranja podatkov iz proizvodnje vključuje njihovo beleženje preko informacijskih terminalov. Problem, ki se pri tem pojavlja je kako optimalno razporediti terminale tako, da so čakalni časi za vnos podatkov čim manjši. Prispevek obravnava pristop, ki sloni na optimizaciji naključne kriterijske funkcije, ki združuje stroške nabave terminalov in stroške zaradi čakalnih časov pri vnašanju proizvodnih podatkov. Ideja rešitve temelji na uporabi statistike dogodkov na proizvodni črti, ki je prevzeta iz zgodovine postopka. Prispevek podaja primer uporabe postopka na problemu optimalne izbire terminalov v konkretnem proizvodnem obratu.

Ključne besede: proizvodni sistemi, optimiranje, nadzor proizvodnje, krmiljenje proizvodnje

*Naslov odgovornega avtorja: Institut "Jožef Stefan", Odsek za sisteme in vodenje, Jamova cesta 39, 1000 Ljubljana, dani.juricic@ijs.si

Strojniški vestnik - Journal of Mechanical Engineering 54(2008)1, SI 8
UDK 621.9.04
Prejeto: 26.6.2006
Sprejeto: 28.9.2007

Nadzor rezalnih sil pri struženju z vstopnim kotom in geometrijsko obliko rezalnih ploščic

Toma Udiljak* - Stephan Škorić - Damir Ciglar
Univerza v Zagrebu, Fakulteta za strojništvo in gradnjo ladij, Hrvaška

Obdelovalnost lahko ocenimo z nizom kriterijev oz. obdelovalnih funkcij, poznavanje katerih je nujno za optimizacijo obdelovalnega postopka. Novi materiali rezalnih orodij in nove zasnove obdelovalnih orodij zagotavljajo nove možnosti in omogočajo količinske spremembe obdelovalnih funkcij. V tej raziskavi smo raziskali funkcijo rezalnih sil, kot eno izmed bistvenih obdelovalnih funkcij. Raziskavo smo opravili pri vzdolžnem struženju jekla 16MnCr5. Uporabili smo oplaščene karbidne ploščice za grobo in končno obdelavo z različnimi koti. Vstopne kote smo spreminjali s sistemom za vpenjanje orodja. Dobljeni rezultati so potrdili. da vstopni kot in geometrijska oblika ploščic zelo vplivata na rezalne sile, še posebej na potisno rezalno silo.

Ključne besede: struženje, rezalne sile, rezalne ploščice, geometrijska oblika ploščic

*Naslov odgovornega avtorja: Univerza v Zagrebu, Fakulteta za strojništvo in gradnjo ladij, Ivana Lučića 5, HR-10000 Zagreb, Hrvaška, toma.udiljak@fsb.hr

Strojniški vestnik - Journal of Mechanical Engineering 54(2008)1, SI 9
UDK 621.3.077.2
Prejeto: 18.12.2006
Sprejeto: 19.12.2007

Eksponentni sledilni nadzor elektro-pnevmatskega servo motorja

Dragan V. Lazić
Fakulteta za strojništvo, Srbija

Glede na osnovno pomembnost teorije sledenja tehničnih sistemov, je glavni namen tega prispevka nadaljnji razvoj teorije in uporabe sledenja, še posebej uporabne zasnove sledenja.

Prikazana je nova opredelitev uporabnega eksponentnega sledenja. Uporabno sledenje je določeno z izstopnim vektorjem, ki se razlikuje od predhodnih določitev, ki so bile dane z vektorjem izstopne napake. Določeno eksponentno sledenje je elementarno. Prikazani so novi kriteriji uporabnega eksponentnega sledenja. Na osnovi novih kriterijev je, z uporabo samoprilagodljivega načela, določen nadzorni algoritem uporabnega eksponentnega sledenja. Značilnost takega nadzornega sistema je sestavljena iz dveh povratnih virov: celotne negativne izstopne vrednosti in lokalne pozitivne nadzorne vrednosti. Taka sestava zagotavlja spajanje nadzora brez poznavanja notranje dinamike in brez meritev motilnih vrednosti.

Naprava, ki jo obravnavamo, je elektro-pnevmatski servo motor. Tak sistem pogosto uporabljamo kot končni nadzorni element samodejnega nadzornega sistema. Popravna naprava za omenjeno napravo je digitalni računalnik. Omenjene nadzorne sile obravnavane naprave rezultirajo v sledenje željenih izstopnih vrednosti z vnaprej določeno natančnostjo. V tem prispevku smo predstavili rezultate simulacije, dobljene z nadzornim algoritmom uporabnega sledenja na elektro-pnevmatskem servosistemu.

Rezultati so pokazali veliko kakovost samodejnega nadzora uporabnega eksponentnega sledenja. Vrsta nadzora zagotavlja spremembo izstopne vrednosti napake glede na določen eksponentni zakon.

Ključne besede: elektropnevmatični sistemi, servo motorji, nelinearni sistemi, samoprilagajanje

*Naslov odgovornega avtorja: Fakulteta za strojništvo, Oddelek za avtomatizacijo, Kraljice Marije 16, 11120 Beograd, Srbija, dragan.lazic@gmail.com

Strojniški vestnik - Journal of Mechanical Engineering 54(2008)1, SI 10
UDK 658.562.4:669.71
Prejeto: 19.12.2007
Sprejeto: 14.1.2008

Lasersko podprti optični nadzor visokotlačnih ulitkov iz aluminija

Valter Gruden[1] - Drago Bračun[2] - Janez Možina[2,*]
[1]Hidria-Rotomatika d.o.o.
[2]Univerza v Ljubljani, Fakulteta za strojništvo

Predstavljamo novo metodo nadzora površine visoko tlačnih ulitkov iz aluminija. Z njo želimo izboljšati dosedanjo prakso, pri kateri se ugotavlja prisotnost površinskih napak kot so dvoslojnosti, nezalitosti in hladni zvari zgolj vizualno. Osnova nove metode je laserska triangulacija. V prispevku opisujemo merilni sistem, postopek meritve, računalniško obdelavo oblaka izmerjenih točk s poudarkom na odkrivanju površinskih napak ter primerjavo delovanja nove metode z vizualnim pregledom.

Ključne besede: tlačno litje aluminija, kakovost površin, nadzor kakovosti, 3D meritve, merilni laserski sistemi

*Naslov odgovornega avtorja: Univerza v Ljubljani, Fakulteta za strojništvo, Aškerčeva 6, 1000 Ljubljana, janez.mozina@fs.uni-lj.si

Strokovna literatura

Ocena knjige

Aleksandar A. Rac
MAZIVA I PODMAZIVANJE MAŠINA
Zal.: Mašinski fakultet Beograd, 2007
317 strani, 115 slik, 123 tabel
format: 17 x 24,8 cm

Uporaba maziv je najučinkovitejši način reševanja triboloških problemov pri mehansko delujočih strojih in napravah, tehnoloških postopkov obdelave kovin pa tudi vrhunskih napravah kot so računalniki in druga elektronska oprema. Tako široko področje uporabe maziv je posledica močne odvisnosti zanesljivosti delovanja in obratovalne dobe omenjenih elementov in naprav od učinkovitosti mazanja gibajočih se delov. Pomen mazanja se kaže tudi v dejstvu, da preko 50 % vseh poškodb in odpovedi pri delu mehanskih sistemov nastane zaradi obrabe in je mazanje še vedno najbolj razširjen način za zmanjšanje trenja in posledično obrabe (odnašanja) materiala.

Številni vidiki neposredno povezani z mazivi in postopkom mazanja, vsakodnevno srečevanje s to problematiko številnih strokovnjakov v praksi ter večdesetletne iskušnje avtorja na tem področju, so tega vzpodbudili k sistematičnem pristopu pri obravnavi omenjene problematike in opredelitvi vsebine pričujoče knjige. Ta je zasnovana predvsem kot učbenik za študente strojništva (in drugih tehničnih fakultet na srbskem govornem področju), namenjena pa je tudi kot pripomoček inženirjem v praksi pri spoznavanju problematike mazanja ter iskanju določenih odgovorov.

Knjiga je razdeljena na 14 različno obsežnih poglavij, katerih vsebina je podana slikovno pregledno in strokovno prepričljivo. Osnovni pojmi, vloga, razvoj in poraba maziv, ki je istočasno tudi pokazatelj ekonomskega razvoja posamezne države, so podani v 1. poglavju. Osnovne teorije mazanja so opisane v 2. poglavju. Osrednji poglavji knjige sta 5 in 6, v katerih so obravnavana tekoča in poltekoča maziva ter njihove značilnosti. Močan poudarek avtor daje tehnični zakonodaji in standardom na področju mazanja, zato 9. poglavje zajema podrobno analizo metod za preizkušanje značilnosti maziv kot tudi ustrezne ISO standarde. Mazanje ležajev, zobniških dvojic, vodil in drugih elementov strojev je obravnavano v poglavjih 10 in 11. V poglavju 12 je posebej izpostavljena problematika sredstev za hlajenje in mazanje (SHM) pri obdelavi kovin. Sledita še poglavji o nadzoru in vzdrževanju maziv (poglavje 13) ter ponovni uporabi odpadnih olj (poglavje 14) kar, z izkazano skrbjo za trajnostni razvoj, zaokrožuje sistematičen pristop k problematiki maziv in postopka mazanja.

Na koncu knjige je podana obsežna literatura, razdeljena po posameznih poglavjih, ki zajema podroben pregled tematike do leta 2000. Glede na dejstvo, da je knjiga tiskana v letu 2007 pogrešamo novejše literaturne vire, po letu 2000. V dodatku I pa je podan še obsežen slovar strokovnih pojmov s tega področja.

Knjigo je avtor v osnovi predvidel kot učbenik za študente strojništva vendar jo, zaradi sistematičnosti in preglednosti obravnavane tematike, predlagamo tudi strokovnjakom v praksi za lažje spoznavanje in razumevanje problematike na področju maziv in postopkov mazanja.

Mirko Soković

Osebne vesti

Prešernove nagrade študentom Fakultete za strojništvo Univerze v Ljubljani

Uroš Trdan
Utrjevanje površin z laserskimi udarnim valovi
Mentor: prof. dr. Janez Grum

Uroš Trdan se je rodil 2. novembra 1980 v Ljubljani. Po končani Srednji šoli za elektrotehniko in računalništvo, se je v letu 1999 vpisal na Fakulteto za strojništvo v Ljubljani. Diplomiral je leta 2006 na proizvodnem strojništvu s temo "Utrjevanje površin z laserskimi udarnimi valovi" pod mentorstvom prof. dr. Gruma. Kandidat je že med študijem sodeloval na znanstvenem področju v okviru različnih projektov, katere rezultate je prikazal na slovenski ter hrvaški konferenci. Že kot študent se je priključil raziskavam, ki potekajo v okviru sodelovanja med laserskim centrom v Madridu, ki ga vodi prof. dr. Ocana ter prof. dr. Hillom z Univerze v Kaliforniji.

Površinsko udarno utrjevanje je namenjeno za najbolj zahtevne dinamično obremenjene strojne dele. Elasto-plastični premiki atomskih ravnin vzdolž delovanja laserskih udarnih valovanj vplivajo na zgoščevanje dislokacij v tankem površinskem sloju. Kandidat se je zelo temeljito seznanil s teoretičnim ozadjem utrjevanja, kot tudi z rezultatov rezultatov o utrjevanju površin na aluminijevih zlitinah, ki je bila tudi predmet njegove raziskave.

Kandidat Uroš Trdan je opravil raziskavo površin pred in po utrjevanju. Z merjenjem mikrotrdote ter zaostalih napetosti pa je pridobil osnovne podatke o vplivu izvedenega postopka utrjevanja. Z dodatnim makro in mikroskopskim pregledom površin na vzorcih v prečnem prerezu je ugotovil učinke utrditve, iz mikrostrukture pa vpliv zgoščevanja usedlin.

Posebnost njegovega dela je izjemno uspešno povezovanje teoretičnih spoznanj po literaturi z opravljenimi spremembami mikrotrdote in zaostalih napetosti v tankem površinskem sloju, ki ga puščajo udarni valovi po obdelavi.

Po diplomi se je v letu 2007 redno zaposlil kot asistent na Fakulteti za strojništvo v Ljubljani na Katedri za tehnologijo materialov. Kandidat je že predstavil rezultate svojih raziskav na 6. mednarodni konferenci na Madžarskem. Članek je v postopku objave v specializirani reviji Materials Science Forum s faktorjem vpliva.

Andrej Hostnik
Vpliv pogojev spremembe nadmorske višine na moč batnega in turbinskega motorja za pogon letal
Mentor: prof.dr. Ferdinand Trenc,
somentor: doc.dr. Tadej Kosel

Andrej Hostnik se je rodil v Ljubljani 5. marca 1975. V letu 1994 je z odliko končal Gimnazijo Ljubljana Šiška. Na Fakulteti za strojništvo v Ljubljani je leta 1997 diplomiral na višješolskem študiju; smer: letalstvo - B in se nato zaposlil v Slovenski vojski kot vojaški pilot na letalih tedanje 15. brigade. V šolskem letu 2006/2007 je na Katedri za letalstvo dokončal visokošolski strokovni študij. V času študija je bil v letu 1994/1995 proglašen za najboljšega študenta v 1. letniku in v letu 1996/1997 za drugega najboljšega študenta 5. semestra na višješolskem študiju. V letalski šoli sedaj opravlja delo poveljnika oddelka na letalih Pilatus Pc-9M Hudournik in kot inštruktor letenja poučuje v letalski šoli Slovenske vojske.

V predloženi raziskavi je bila predstavljena nova, izvirna, cenena in dokaj natančna metoda za ugotavljanje moči batnega in turbinskega motorja z notranjim zgorevanjem za pogon letal med poletom na različnih nadmorskih višinah, kar je v laboratorijskih pogojih nemogoče. Metoda temelji na aerodinamičnem preračunu; za določanje moči motorja potrebujemo upore letenja preizkušanega letala pri različnih hitrostih letala in izkoristek pogonskega vijaka pri različnih vrtilnih frekvencah. Eksperimentalno je bila določena zveza med koeficientom upora in resnično hitrostjo letala, izdelan približni polinom, preko katerega lahko določimo moč motorja in to za dve letali: Zlin-242L z batnim motorjem in turbovijačnega Pilatus Pc-9M Hudournik s potisnim turbinskim motorjem.

Pri drsnih letih je bil za pogone letal z batnim motorjem ter vijakom z nastavljivim korakom s pomočjo mazalnega mehanizma pojasnjen in dokazan sekundarni učinek avtorotacije vijaka na tlačilko za olje, ki omogoča, da lahko izničimo nezaželen učinek zaviranja vijaka v primeru odpovedi motorja ali pa pri zaviranju letala. V okviru raziskave je bila podana možnost uporabe

omenjenega učinka v smislu predpisanega priporočila, ki povečuje varnost poleta.

Peter Dolenec
Vplivni parametri na porazdelitev vtoka zraka v prostor
Mentor: izr.prof.dr. Vincenc Butala

Peter Dolenec, rojen 29. marca 1982 v Ljubljani, seje po uspešno opravljeni maturi na Gimnaziji Bežigrad v Ljubljani leta 2001 vpisal na Univerzo v Ljubljani, Fakulteto za strojništvo in uspešno končal študij na smeri Energetsko in procesno strojništvo. Decembra 2006 je prejel priznanje Fakultete za strojništvo, kot eden izmed petih najboljših študentov 5. letnika v študijskem letu 2005/06. Nagrajenec Peter Dolenec je univerzitetni študijski program končal v 5. letih in 30. dnevih s povprečno oceno vseh izpitov in vaj v petih letih študija 8,973, s povprečno oceno 3., 4., in 5. letnika 9,33 in z končno oceno študija odlično 10.

Nagrado Fakultete za strojništvo prejme za delo, s katerim je kandidiral za univerzitetno Prešernovo nagrado za leto 2007, z naslovom: "Vplivni parametri na porazdelitev vtoka zraka v prostor", ki ga je izdelal pod mentorstvom izr.prof.dr. Vincenca Butala. V delu so analitično analizirani parametri, ki vplivajo na porazdelitev in na dometno razdaljo curka vtoka zraka v prostore z različno obliko. Proučena sta znana pristopa analize teh parametrov: študij na modelu in računalniška simulacija. Prvič je izdelan predlog metodologije za načrtovanje in ocenjevanje kakovostne porazdelitve vtoka zraka v prostor ob upoštevanju temperaturnega in hitrostnega polja ter polja koncentracij primesi. Metodologija je preizkušena na dveh primerih: učilnice in telovadnice.

Doktorat, magisteriji in diplome

DOKTORAT

Na Fakulteti za strojništvo Univerze v Ljubljani je z uspehom zagovarjal svojo doktorsko disertacijo:

dne *27. decembra 2007*: **Aleš Gorkič**, z naslovom: "Optodinamska karakterizacija in nadzor laserskih obdelovalnih procesov z večvrstnimi laserskimi bliski" (mentorja: prof. dr. Janez Možina in prof. dr. Janez Diaci).

S tem je navedeni kandidat dosegel akademsko stopnjo doktorja znanosti.

MAGISTERIJI

Na Fakulteti za strojništvo Univerze v Ljubljani so z uspehom zagovarjali svoja magistrska dela:

dne *11. decembra 2007*: **Jure Petkovšek**, z naslovom: "Prenos toplote pri mehurčkastem vrenju na tankih grelnikih" (mentor: prof. dr. Iztok Golobič) in **Damir Dolenc**, z naslovom: "Simulator obratovanja Kaplanovega in Francisovega turbinskega agregata" (mentorja: prof. dr. Alojz Sluga in doc. dr. Anton Bergant);

dne *13. decembra 2007*: **Edvin Boškin**, z naslovom: "Energetska analiza procesa za proizvodnjo anhidrita ftalne kisline" (mentorja: prof. dr. Janez Oman in doc. dr. Andrej Senegačnik).

S tem so navedeni kandidati dosegli akademsko stopnjo magistra znanosti.

DIPLOMIRALI SO

Na Fakulteti za strojništvo Univerze v Ljubljani so pridobili naziv univerzitetni diplomirani inženir strojništva:

dne *27. decembra 2007*: Dejan AVGUŠTIN, Primož GORTNAR, Boštjan KREUTZ, Lovro SAMBOL, Gregor SLAK, Blaž VOLKAR;

dne *28. decembra 2007*: Marko BLAŽKO, Andrej ČEBULAR, David LADIĆ, Boštjan ROJKO, Iztok RUTAR.

Na Fakulteti za strojništvo Univerze v Mariboru so pridobili naziv univerzitetni diplomirani inženir strojništva:

dne *20. decembra 2007*: Zoran JANKOVIĆ, Robert KURNIK.

*

Na Fakulteti za strojništvo Univerze v Ljubljani so pridobili naziv diplomirani inženir strojništva:

dne *6. decembra 2007*: Marko BIZJAK, Dušan KUŠTRIN, Blaž SLATINŠEK, Rok VRHOVNIK;

dne *7. decembra 2007*: Klemen CORN, Matjaž GOLOREJ, Miha KUNAVER, Tadej MUZNIK, Domen ZUPANČIČ;

dne *27. decembra 2007*: Vladimir BAHČ, Peter BENČINA, Marko BLAZNIK, Aleša BOŠNJAK, Mirsad CVRK, Rok DRAŠLER, Uroš ERŽEN, Zdenko FAJFAR, Jure FERBAR, Jaka FILIPIČ, Matej GOMBOC, Jurij JERANT, Marko KAFERLE, Andrej KAVRE, Gregor KLEČ, Boris KOROŠEC, Grega KRČ, Ivan KRIŽNIČ, Saša MALERIČ, Rok MARKOVIČ, Primož MERLAK, Rok MRAK, Milan MUREN, Joež OBRSTAR, Jure PREMELČ, Nejc RAJZER, Klemen REMŠKAR, Rok STAKNE, Luka ŠKRLEC, Andrej VALJAVEC;

dne *28. decembra 2007*: Blaž BERČON, Bogdan LESKOVEC, Uroš MEDIĆ, Tina NEMANIČ, Dejan VRBNJAK, Andrej ŽIBREHT.

Na Fakulteti za strojništvo Univerze v Mariboru so pridobili naziv diplomirani inženir strojništva:

dne *6. decembra 2007*: Bogdan ZDEŠAR;

dne *20. decembra 2007*: Jožef KANCLER, Boris RAJTER.